Pathophysiological Effects of *Brachyspira* Species on Ion Transport Within the Porcine Colon Resulting in Diarrheal Disease

A Thesis Submitted to the College of Graduate and Postdoctoral Studies

In Partial Fulfillment of the Requirements

For the Degree of Doctor of Philosophy

In the Department of Veterinary Biomedical Sciences

University of Saskatchewan

Saskatoon

By

Cole Brett Enns

Permission to Use

In presenting this thesis/dissertation in partial fulfillment of the requirements for a Postgraduate degree from the University of Saskatchewan, I agree that the Libraries of this University may make it freely available for inspection. I further agree that permission for copying of this thesis/dissertation in any manner, in whole or in part, for scholarly purposes may be granted by the professor or professors who supervised my thesis/dissertation work or, in their absence, by the Head of the Department or the Dean of the College in which my thesis work was done. It is understood that any copying or publication or use of this thesis/dissertation or parts thereof for financial gain shall not be allowed without my written permission. It is also understood that due recognition shall be given to me and to the University of Saskatchewan in any scholarly use which may be made of any material in my thesis/dissertation.

Requests for permission to copy or to make other uses of materials in this thesis/dissertation in whole or part should be addressed to:

Head of the Department of Veterinary Biomedical Sciences

Western College of Veterinary Medicine, 52 Campus Drive

University of Saskatchewan

Saskatoon, Saskatchewan S7N 5B4 Canada

OR

Dean

College of Graduate and Postdoctoral Studies

University of Saskatchewan

116 Thorvaldson Building, 110 Science Place

Saskatoon, Saskatchewan S7N 5C9 Canada

Abstract

Swine dysentery, a production limiting diarrhea in swine, is responsible for profound economic loss annually. *Brachyspira hyodysenteriae* is the etiological agent responsible for colonization of the colon and development of classical swine dysentery. Like *Brachyspira hyodysenteriae*, *Brachyspira hampsonii* causes mucohemorragic diarrhea which is indistinguishable from swine dysentery.

Classical swine dysentery has been characterized as a malabsorptive diarrhea in which Na^+ and Cl^- absorption is abolished in diarrheic pigs. However, characterization of the transporters responsible for these alterations in ion transport have not been studied. Thus, this thesis focuses on the pathophysiological mechanisms involved in altering the colonic mucin environment and the alterations in ion transport responsible for the development of diarrheal disease.

Both secretory and absorptive responses were characterized in the colon of experimentally challenged pigs infected with *Brachyspira hyodysenteriae* or *Brachyspira hampsonii*. Anion secretion was assessed in Ussing chambers by measuring short-circuit current following agonist addition. Additionally, ^{22}Na and ^{36}Cl radiolabelled isotope fluxes in Ussing chambers were used to assess changes in unidirectional and net ion transport. ^{3}H-mannitol radiolabelled isotope fluxes were also used to assess barrier function. Changes in ion channel and transporter mRNA and protein expression in the colon of diseased pigs was assessed by RT-qPCR and western blot. To determine the role of cytokines on modulation of ion channel and transporter function RT-qPCR was used to assess gene transcripts throughout the porcine colon. Finally, to

provide a mechanism for the alterations in ion transport, Caco-2 monolayers were exposed to both cytokines and a *Brachyspira hampsonii* lysate.

Anion secretion along with Na^+ and Cl^- absorption was significantly reduced in the colon of diarrheic pigs infected with *Brachyspira hyodysenteriae* and *Brachyspira hampsonii*, with no change in epithelial barrier function. This response was attributed to a decrease in channel and transporter mRNA and protein. The only cytokine significantly up-regulated throughout the colon of diseased pigs out of the 12 cytokines examined was IL-1α. lL-1α was responsible for the decrease in the anion exchanger DRA mRNA but, not chloride channel CFTR or the cation exchanger NHE3 mRNA expression as indicated by Caco-2 monolayers exposed to human recombinant IL-1α for 24 hours. Interestingly, Caco-2 monolayers exposed to a *Brachyspira hamspsonii* lysate had significantly reduced mRNA expression of both CFTR and NHE3 after 48 hours of exposure accompanied by a significant increase in IL-1α expression.

I conclude, that although the observed decrease in anion secretion would not contribute to diarrheal development, it would begin to explain some of the pathophysiological changes in mucin rheological properties observed within the colon. These changes in the colonic mucin environment benefit *Brachyspira* species allowing for greater growth and colonization. On the other hand, the significant decrease in Na^+ and Cl^- absorption in the colon of diarrheic pigs due to loss of NHE and DRA mRNA and protein define the pathophysiological mechanism by which this malabsorptive diarrhea develops. These changes in ion transport are attributed to both the host's cytokine response and direct effects of *Brachyspira* species.

Acknowledgments

I would like to thank Dr. Matthew Loewen for his support and guidance throughout my Ph.D. program

I would like to thank my lab members Brandon, Van, Marina, Alyssa, and Khanh for their support and help during my program. You guys have made this journey a fun one.

I would like to thank my committee members, Dr. Andrew Van Kessel, Dr. Don Hamilton, Dr. George Forsyth, and Dr. Daniel MacPhee for taking the time to mentor and provide support throughout the course of my project.

I would like to thank my family for all their love and support throughout the duration of my Ph.D. this feat would not have been achievable without you guys.

Finally, I would like to thank my fiancé Megan. Your love, patience, and support have been critical in achieving this goal. I am ever grateful and am excited to see where life takes us!

Table of Contents

Page

List of Tables

List of Figures

List of Abbreviations

ANO-	-	Anoctamin
ATP	-	Adenosine triphosphate
ATP1A1	-	Na^+-K^+ ATPase
BEST-	-	Bestrophin
BK	-	Big potassium
BME	-	β-mercaptoethanol
BSA	-	Bovine serum albumin
Ca^{2+}	-	Calcium ion
CaCC	-	Calcium-activated chloride channel
Caco-2	-	Caucasian colon adenocarcinoma
cAMP	-	Cyclic adenosine monophosphate
cDNA	-	complementary deoxyribonucleic acid
CF	-	Cystic fibrosis
CFTR	-	Cystic fibrosis transmembrane conductance regulator
CFU	-	Colony forming units
cGMP	-	Cyclic guanosine monophosphate
Cl^-	-	Chloride ion
CLCA-	-	Chloride channel accessory protein
CLD	-	Congenital chloride diarrhea
C_T	-	Cycle threshold
DMEM	-	Dulbecco's modified eagle medium
DRA	-	Downregulated in adenoma
ENaC	-	Epithelial sodium channel
FBS	-	Fetal bovine serum
GAPDH	-	Glyceraldehyde 3-phosphate dehydrogenase
HIV	-	Human immunodeficiency virus
HPLC	-	High-performance liquid chromatography

IBD	-	Inflammatory bowel disease
IBMX	-	3-isobutyl-1-methylxanthine
I_{sc}	-	Short-circuit current
IFN-	-	Interferon
IL-	-	Interleukin
J_{ms}	-	Mucosal to serosal flux
J_{sm}	-	Serosal to mucosal flux
J_{net}	-	Net flux
K^+	-	Potassium ion
KCL	-	Potassium chloride
KCNE3	-	Potassium voltage-gated channel subfamily E member 3
KCNN4	-	Potassium calcium-activated channel subfamily N member 4
KCNQ1	-	Potassium voltage-gated channel subfamily Q member 1
LPS	-	Lipopolysaccharide
MUC-	-	Mucin
mV	-	millivolt
mRNA	-	Messenger ribonucleic acid
Na^+	-	Sodium ion
NHE-	-	Sodium/hydrogen exchanger
NHERF-	-	Na^+/H^+ exchanger regulatory factor
NKCC1	-	Na^+-K^+-$2Cl^-$ co-transporter 1
nox	-	nicotinamide adenine dinucleotide oxidase
PAMP	-	Pathogen-associated molecular patterns
PAT-1	-	Putative anion transporter-1
PBS	-	Phosphate buffered saline
PGE	-	Prostaglandin E
PKA	-	Protein kinase A
PKC	-	Protein kinase C

PRRs	-	Pattern-recognition receptors
PTGS-	-	Prostaglandin-endoperoxide synthase
RT-qPCR	-	Reverse transcriptase - quantitative polymerase chain reaction
SGK1	-	Serum and glucocorticoid-regulated kinase 1
SGLT-	-	Sodium-glucose co-transporter
SLC26A3	-	Solute carrier family 26 member 3
Spp.	-	Species
TEER	-	Transepithelial electrical resistance
TGF-	-	Transforming growth factor
TLR	-	Toll-like receptor
TMEM16A	-	Transmembrane member 16A
TNF-α	-	Tumor necrosis factor

Chapter 1 - Introduction

1.1 Rationale

Enteric pathogens infecting pigs, resulting in diarrheal disease causes substantial economic loss in swine producing countries each year. *Brachyspira hyodysenteriae* the etiological agent of swine dysentery results in the formation of diarrheal disease accompanied by mucus induction and what is thought to be fecal blood (290). Like *B. hyodysenteriae*, emergent *Brachyspira hampsonii* causes clinical symptoms indistinguishable from *B. hyodysenteriae* (49). Disease associated with *Brachyspira* spp. results in low mortality but, high morbidity, resulting in poor feed conversion and stunted growth (68). These two pathogens are of significant importance to the North American swine industry as cases of *Brachyspira* colitis are on the rise due to restrictions regarding antibiotic use.

The pathophysiological mechanisms involved in the colon of pigs infected with these two *Brachyspira* spp. are not well characterized. Previous studies attempting to characterize ion transport in the colon of diseased pigs have been limited to *B. hyodysenteriae* with no studies assessing *B. hampsonii*. Diarrhea caused by *B. hyodysenteriae* has been characterized as being malabsorptive in nature with no increase in luminal anion secretion (13, 277). Decreased absorption of both Na^+ and Cl^- was observed in the colon of diseased pigs and attributed to be the cause of diarrheal development (13). However, due to assumptions made and techniques used by the previous authors regarding the ionic flux of these ions, these previous studies could be erroneous. Furthermore, the changes in ion channels and transporters required to carry this decreased absorptive response have not been characterized.

In addition to the development of diarrhea, mucus induction is another clinical sign associated with the pathogenesis of both *B. hyodysenteriae* and *B. hampsonii* (49, 121, 266). Recent studies assessing changes in mucin expression in the colon of *B. hyodysenteriae* diseased pigs has revealed elevated production of gel-forming mucins MUC2 and MUC5AC (251). Other studies have shown that *B. hyodysenteriae* is attracted to mucins suggesting that these changes are beneficial to the pathogen (161, 207, 223, 251). Anion secretion is required for proper release of mucins from goblet cells and heavily influences mucin rheological properties (98, 115, 148, 151, 253). Although anionic secretion has been previously suggested to be unaffected during *B. hyodysenteriae* infection, these findings seem unlikely due to the presence of severe inflammation throughout the colon of diseased pigs (277). Therefore, the changes in mucin production must be paired with changes in anion channel function and expression, which has not been characterized in the colon of swine infected with either pathogen.

Together the scope of this thesis is to identify and characterize the cellular mechanisms supporting the altered colonic mucin environment and development of diarrhea. Identifying and understanding the pathophysiological mechanisms involved in the porcine colon during diarrheal episodes provides new targets for subunit vaccine development. Furthermore, this research provides new insight into potential pathophysiological mechanisms involved in human intestinal spirochetosis.

1.2 Objectives

1. To characterize the electrogenic anionic secretory response in three segments of the porcine colon in healthy and *Brachyspira* infected pigs
2. To characterize electroneutral Na^+ absorption in the apex colon of diarrheic pigs infected with *Brachyspira* spp.
3. To characterize electroneutral Cl^- absorption in the apex colon of diarrheic pigs infected with *Brachyspira* spp.
4. To determine if *Brachyspira* spp. cause altered paracellular movement of solutes in the porcine colon

1.3 Hypotheses

1. *Brachyspira* spp. decrease electrogenic anion secretion throughout the porcine colon resulting in altered mucin rheological properties favoring spirochete colonization.
2. *Brachyspira* spp. decrease electroneutral Na^+ absorption in the porcine colon contributing to the development of diarrheal disease.
3. Decreased electroneutral Cl^- absorption in the porcine colon in diseased pigs contributes to the diarrheal disease
4. Tight junction permeability is not different from control in the colon of *Brachyspira* diseased pigs

Chapter 2 – Literature Review

2.1 *Brachyspira* species

Brachyspira are large gram-negative, anaerobic but oxygen tolerant spirochete bacteria belonging to the phylum *Spirochaetes* (118). These bacteria are characterized by their coiled morphology and unique movement patterns caused by the 14-18 periplasmic flagella associated with each cell (53, 233). Some *Brachyspira* species have been associated with diarrheal disease, which has been shown to affect a wide range of hosts, including humans, swine, and small rodents (49, 77, 121, 146). Some of these pathogenic strains infect specific animal host's, while others exhibit widespread host pathogenicity.

2.1.1 *Brachyspira species in swine*

Swine dysentery, also commonly known as bloody scours, is an infectious disease that causes mucohaemorrhagic diarrhea in pigs during the grower and finisher phases of production (290). The etiological agent of swine dysentery in the 1970s was named *Treponema hyodysenteriae* which was modified to *Serpula,* and then *Serpulina* and has since been renamed and is known as *Brachyspira hyodysenteriae* today (121, 233, 289, 291). The cecum and colon are the primary sites of inflammation and lesions caused by swine dysentery (8). The first appearance of swine dysentery dates back to 1921 in the Midwestern United States (75). However, swine dysentery became a significant problem during the 1950's and 1960's in many swine raising countries. By the early 1970's, it was estimated that 38% of swine herds in the United States were infected with swine dysentery and cost the American swine industry $200 million annually (122). The occurrence of swine dysentery disappeared during the 1980's, and

1990's due to the use of antimicrobials and management practices but remerged in North America in 2007 and has since been a difficult disease to eradicate from swine herds around the world (117, 208, 209).

In October 2009, grower pigs with clinical signs identical to those of swine dysentery were observed in two commercial swine barns in Saskatchewan. Analysis of samples submitted to the University of Saskatchewan did not identify the known causative agent of swine dysentery, *Brachyspira hyodysenteriae* (266). However, through the use of polymerase chain reaction (PCR) targeting the *Brachyspira* NADH oxidase (*nox*) gene, it was determined that the amplicon matched the clade II of the recently described *Brachyspira hampsonii* (49, 263, 266). Based on analysis of *nox* gene sequences *Brachyspira hampsonii* was clustered into two distinct clades I and II (49). Clades I and II were subsequently referred to as *Brachyspira hampsonii* strain 30599 and *Brachyspira hampsonii* strain 30446, respectively (266); however, today genetic analysis of *B. hampsonii* isolates using multilocus sequence typing has determined there are 4 distinct genetic groups, replacing the old clade designations (208). Currently, *Brachyspira hampsonii* continues to circulate throughout swine herds worldwide (49, 198, 262).

Other *Brachyspira* species that have recently emerged and are of interest due to the lack of evidence in their ability to produce clinical disease in pigs include *Brachyspira murdochii*, *Brachyspira suanatina*, and the zoonotic *Brachyspira pilosicoli*.

2.1.2 *Brachyspira species in humans*

Brachyspira infections in humans is referred to as human intestinal spirochetosis and like their swine counterparts colonize the colon of their host. The two etiological agents associated with human intestinal spirochetosis are *Brachyspira aalborgi* and *Brachyspira pilosicoli* (136, 304). Infection with these two bacteria results in diarrheal disease associated with mucus induction (206, 261, 307). Traditionally, human spirochetes have been largely believed to be non-invasive like their swine counterparts, however, spirochetes have been observed within human epithelial cells and subepithelial macrophages, suggesting that the pathogenesis between *Brachyspira* species that infect humans and swine may differ (101, 102).

The prevalence of human intestinal spirochetosis is relatively low in countries with a high standard of living while the incidence of the disease is common in poorer areas (307). In well developed countries, two specific people groups are at the greatest risk of intestinal spirochetosis; first being homosexual males and second being peoples infected with human immunodeficiency virus (HIV) (307). Although speculative, the increased infection in homosexual men is likely due to the fact that human intestinal spirochetosis is likely sexually transmitted, while those with HIV are more susceptible to infection due to the fact that they are immunocompromised (173, 294).

In both swine and humans, the pathophysiological mechanisms involved in the pathogenesis and development of diarrheal disease by *Brachyspira* spp. remain poorly understood. However, in order to explore the pathologies associated with these bacteria the basic physiology of the colon must be explored.

2.2 The colonic epithelium

The transport of solutes, electrolytes, and water in the colon is controlled by a highly polarized layer of epithelium covering the lumen. This epithelial layer consists of four major cell types including columnar cells, goblet cells, enterochromaffin cells, and tuft cells which are continually shed and rapidly renewed (20, 55, 103). These individual cells are organized into crypts. Near the base of the colonic crypts, new cells arise from stem cells, with all cell types migrating from the bottom of the crypts to the top where these cells undergo apoptosis after 4-5 days and are immediately replaced (51).

These four cell types that make up the epithelium have a wide variety of functions responsible for maintaining homeostasis within the gastrointestinal tract. Columnar cells are responsible for the majority of ion transport, with epithelial cells within the colonic crypts having high anionic secretory activity while cells on the villus tips have an absorptive function (129, 171). Goblet cells are responsible for secreting mucins which together are responsible for creating and maintaining the complex framework of the protective mucus overlaying the colonic epithelium (287). This mucus layer provides the first line of defense against bacterial pathogens and toxins that pose a threat to the colonic epithelium. Enterochromaffin cells are a type of enteroendocrine cell that function as chemosensors responsible for the majority of the body's serotonin production having a regulatory effect on gastrointestinal motility and secretion (25, 104, 203). Like enterochromaffin cells, tuft cells are thought to be chemosensory cells, however, at the current time, the exact role of these cells is unknown (219). Paneth cells, unlike the other cell types, do no migrate toward the villus tips, instead, they remain interspersed among the stem cell populations located in the bottom of crypts.

Together these cell types work in conjunction with one another maintaining electrolyte and fluid homeostasis and protecting the host from enteric pathogens and environmental toxins.

2.3 Epithelial transport

The vast majority of epithelial transport occurs through active transport of ions through columnar cells in the gastrointestinal tract creating the driving force for fluid transport. Under basal conditions, the colon has an absorptive function with Na^+ and Cl^- being absorbed and K^+ and HCO_3^- being secreted (32). These processes of absorption and secretion are carried out by specific ion channels and transporters that will be explained in depth (Figure 1.1).

2.3.1 *Absorption*

The bulk transport of Na^+ and Cl^- in the colonic epithelium is due to electroneutral absorption by luminal Na^+/H^+ exchanger (NHE) isoforms NHE2 and NHE3 and Cl^-/HCO_3^- exchanger SLC26A3 also known as downregulated in adenoma (DRA) (4, 43, 135, 181). Both NHE3 and DRA are critical in maintaining electrolyte, and fluid homeostasis as knockout of these genes results in diarrheal development (280, 327). The remaining absorption is electrogenic and is due to absorption through a luminal epithelial sodium channel (ENaC), and transcellular/paracellular absorption of Cl^- (246).

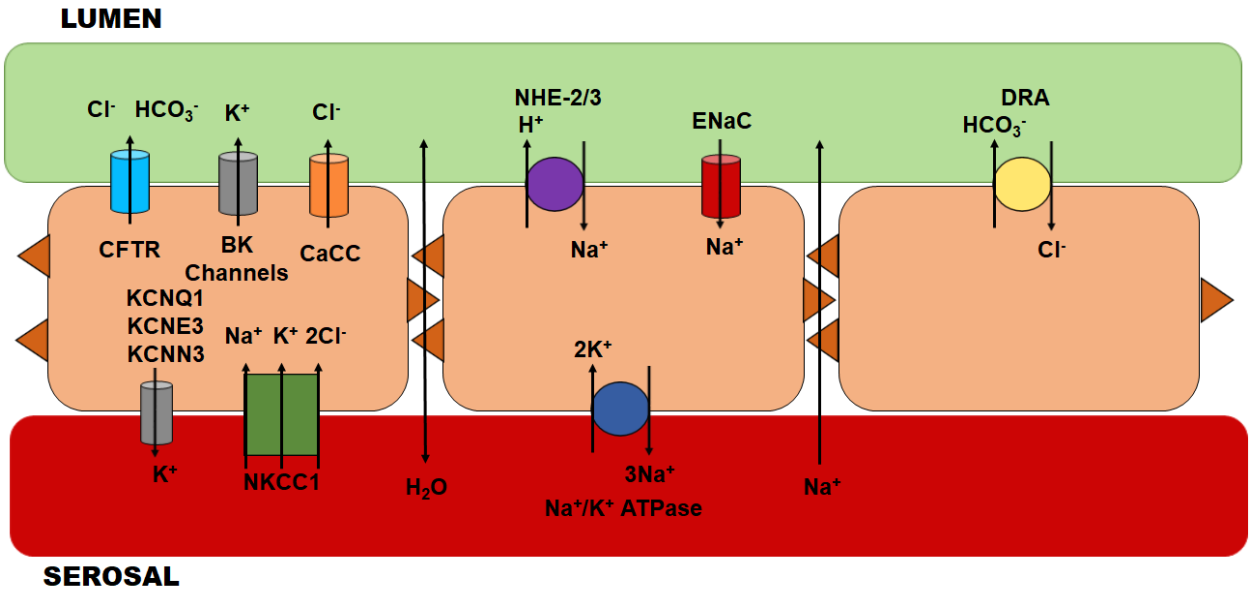

Figure 1.1. Overview of ion transport processes within the mammalian colon.

This schematic outlines the major ion channels and transporters involved in ion transport within the epithelium of the mammalian colon. The far-left cell depicts a secretory epithelial cell found within the crypt responsible for anion and potassium secretion. The middle and far-right cells depict absorptive cells responsible for the absorption of Na^+ and Cl^-. All transporters are found in a single columnar transporting cell and are separated for clarity. CFTR = cystic fibrosis transmembrane conductance regulator. BK channels = big potassium channels. CaCC = calcium-activated chloride channels. KCNQ1 = potassium voltage-gated channel subfamily Q member 1. KCNE3 = potassium voltage-gated channel subfamily E member 3. KCNN4 = potassium calcium-activated channel subfamily N member 4. NKCC1 = Na^+-K^+-$2Cl^-$ co-transporter 1. NHE = Na^+/H^+ exchanger. ENaC = epithelial sodium channel. DRA = downregulated in adenoma. Na^+/K^+ ATPase = sodium-potassium ATPase.

As both electroneutral and electrogenic absorptive processes are ATP-independent and are unable to transport Na^+ against its electrochemical gradient, the ATP-dependent Na^+/K^+ ATPase pump is required to maintain a negative membrane potential. Na^+/K^+ ATPase works by utilizing ATP to actively transport 3 Na^+ out of the epithelial cell while allowing the entry of 2 K^+ (33, 155, 170). As a result of this process, the Na^+ concentration within the cell remains low compared to the extracellular fluid, and cellular membrane voltage is negative, which creates the driving force for luminal Na^+ absorption (181). To maintain the driving force generated by the Na^+/K^+ ATPase, K^+ ions are removed from the cell through apical and basolateral K^+ channels (273). Regional differences in electroneutral and electrogenic Na^+ absorption have been described with electroneutral transport being the predominant route of absorption in the proximal colon while electrogenic absorption is the primary mode of Na^+ transport in the distal colon (63, 246, 255). However, during diarrheal episodes resulting in chronic stimulation by mineralocorticoids, ENaC expression has been observed throughout the colon and ileum to help mitigate electrolyte and fluid loss (279, 324).

2.3.2 *Secretion*

Epithelial secretion refers to the luminal movement of Cl^-, HCO_3^- and K^+ as well as basolateral transport of K^+. Like the absorptive process, secretion is achieved by active transport of Na^+ and K^+ via Na^+/K^+ ATPase. The subsequent efflux of K^+ through apical and basolateral K^+ channels causes hyperpolarization of the cellular membrane driving Cl^- and HCO_3^- secretion through apical anion channels. Due to the low intracellular concentrations of Na^+ and negative membrane potential established by Na^+/K^+ ATPase, Cl^- concentrations are restored by the basolateral Na^+-K^+-$2Cl^-$

cotransporter (NKCC1) (116). Epithelial secretion within the gastrointestinal tract is responsible for clearance of enteric pathogens and is important for mucin secretion and rheological properties (253). Disturbances in epithelial secretion can result in the development of diarrhea, pathogen colonization, and altered mucin environment.

The cystic fibrosis transmembrane conductance regulator (CFTR) is the predominant luminal Cl^- and HCO_3^- secretory channel in the colonic epithelium (110). CFTR is mainly activated by protein kinase A (PKA), but also by other second messenger pathways, including protein kinase C (PKC), Ca^{2+}/calmodulin-dependent kinase, cGMP dependent kinase depending on the initial stimulus (52, 56, 145, 152, 160, 295, 310, 317). Elevated cAMP or Ca^{2+} concentrations activates either cAMP or Ca^{2+}-activated K^+ channels, hyperpolarizing the cell resulting in subsequent opening of CFTR due to phosphorylation of the channel (56, 193). CFTR activation by second messengers cAMP and Ca^{2+} inhibits both electroneutral Na^+ absorption through the Na^+/H^+ exchanger NHE3 and electrogenic Na^+ absorption through ENaC, resulting in net secretion of the epithelium (62, 113).

Besides CFTR, apical Cl^- secretion is achieved via calcium-activated chloride channels (CaCC) located on the apical surface of enterocytes in the gastrointestinal tract (124). As their name suggests, CaCCs are activated by elevated intracellular concentrations of Ca^+ produced by stimulation of G-protein coupled muscarinic receptors by acetylcholine. Three families of CaCCs are expressed within the colon including CLCAs, Anoctamins and Bestrophins. Anoctamin 1 (ANO1) also known as TMEM16A is the primary CaCC present in the gastrointestinal tract responsible for luminal Cl^- secretion (235, 236). The importance of TMEM16A in the gastrointestinal

tract has been debated, with one study suggesting that loss of TMEM16A only minimally affects total Cl^- currents, while another study suggests that TMEM16A is not only required for Ca^{2+}, activated Cl^- secretion but also CFTR mediated Cl^- transport (26, 222).

A large proportion of the driving force for the secretory process is a result of K^+ secretion hyperpolarizing the epithelial cell and increasing the electrochemical driving force for Cl^- efflux. Apical K^+ secretion from within the cell to the lumen of the colon is primarily due to BK channels (KCNMA1 and 4) also called Maxi-K due to their large conductance of K^+ through cell membranes (272). BK channels are activated by membrane depolarization and elevated concentrations of Ca^{2+} due to the fact that they contain a voltage-sensor and binding site for Ca^{2+} (69).

K^+ channels facilitate K^+ secretion from within the cell primarily to the basolateral membrane however, a splice variant of KCNN4, KCNN4c is located on the apical membrane and responsible for apical K^+ transport (21, 23). Like anion secretion, K^+ secretion occurs by activation of K^+ channels by second messengers cAMP or Ca^{2+}. KCNQ1 and KCNE3 are activated by elevated cAMP concentrations aiding in hyperpolarization of the epithelial cell driving apical Cl^- efflux (278). Increases in Ca^{2+} activate KCNN4 causing the basolateral and apical exit of K^+. KCNN4 appears to be essential for driving Cl^- secretion as KCNN4 null mice had complete loss of agonist-induced Ca^{2+} activated Cl^- secretion in their distal colon and small intestine (89).

2.4 The colonic mucus layer

The first layer of defense to pathogens within the gastrointestinal tract is a complex mucus layer overlying the gastrointestinal epithelium (169). This mucus layer is

made of highly glycosylated proteins known as mucins. In the colon, two types of mucins are expressed, secreted gel-forming mucins (MUC2) secreted by goblet cells and transmembrane mucins (MUC3, 12, 13, 17) (147, 149). The colonic mucus layer is composed of two layers consisting of an inner adherent layer and an unattached outer layer consisting mainly of the secreted gel-forming mucin MUC2 (147). The outer mucus layer is inhabited by commensal bacteria while the inner mucus layer is impenetrable to bacteria, preventing pathogens from gaining access to the mucosal surface (147). Underlying the inner mucus layer is the glycocalyx consisting of transmembrane mucins anchored to the mucosal surface of enterocytes forming a barrier which is thought to have similar properties as the secreted mucus layers (149).

Anionic secretion, specifically HCO_3^- secretion through CFTR has been shown to heavily influence the properties of secreted mucins such as MUC2 (98, 114, 115, 151, 253). Gel-forming mucins are stored at a low pH in a high Ca^{2+} concentration environment within goblet cells and upon secretion require Ca^{2+} chelation. Ca^{2+} chelation of mucins occurs by binding of HCO_3^- subsequently allowing electrostatic forces to unfold and expand, increasing mucin volume by more than 1000-fold (148, 253). Cl^- secretion has also been shown to interact with Ca^{2+} and alters mucin rheological properties related to viscosity (90). If apical anion secretion is not present gel-forming mucins aggregate and accumulate trapping bacteria and debris resulting in mucosal damage (98, 114, 253).

Secretion of mucus throughout the gastrointestinal tract not only acts as a protective barrier but also helps to lubricate and flush pathogens distally as a means of preventing enteric infection (148). Alterations in the mucus layer overlying the colonic

epithelium has been shown in numerous enteric infections (39, 115, 143, 251). Paradoxically, some of these infections such as those caused by *Brachyspira hyodysenteriae* and *Brachyspira hamposonii* elevated mucus production resulting in mucus disorganization and de novo synthesis of MUC5AC and increased production of MUC2 thought to aid in bacterial colonization (251, 323). Combining what is known *in vivo* with assays performed *in vitro*, *B. hyodysenteriae* infections alter the colonic mucin environment by up-regulation of IL-17A, increased goblet cell differentiation by up-regulation of forkhead box protein A3 (FOXA3) and SAM pointed domain-containing ETS transcription factor (SPDEF), and by unidentified bacterial components released by neutrophil elastase that increase mucin production through the MAPK3/ERK1 pathways (252). Other infections such as those caused by *Clostridium difficile* and enterohemorrhagic *Escherichia coli* results in a reduction of this protective barrier through reduced mucin secretion or destruction of the existing mucus layer (39, 142). Thus, modification of the mucus layer overlying the colonic epithelium contributes to the pathogenesis of many enteric pathogens.

2.5 Innate immunity in the colonic mucosa

As previously discussed, the mucus layer overlying the colonic epithelium acts as the first barrier to invading pathogens preventing mucosal damage. However, some pathogens secrete toxins or gain direct access to the underlying epithelium resulting in the initiation of an immune response. The first line of the innate immune system is to use a range of sensors known as pattern-recognition receptors (PRRs) located on the surface of both immune and non-immune cells that sense pathogen-associated molecular patterns (PAMPs) (6, 211, 241). PAMPs are molecules found on the surface

of many microorganisms that do not exist on mammalian cells (211). These include lipopolysaccharide (LPS) on the surface of Gram-negative bacteria, lipoteichoic acids on Gram-positive bacteria, as well as peptidoglycan and flagellum from many bacterial species (5). The main PRRs that detect pathogens in the colon are Toll-like receptors (TLRs) expressed on the surface of macrophages, dendritic cell, neutrophils, and epithelial cells (6, 184). Recognition of PAMPs by their respective TLR causes activation of NF-κβ and MAPK signaling pathways resulting in the secretion of pro-inflammatory cytokines (76).

2.6 Cytokine modulation of ion channels

Epithelial and immune cells secrete a large number of cytokines, in response to PAMPs that act as a bridge for communication between other immune cells and the adaptive immune system, while having strong regulatory effects on ion channel function. Several proinflammatory and regulatory cytokines have been shown to have excitatory and/or inhibitory effects on ion secretion, absorption, and intestinal barrier function (234). A number of cytokines have been identified in the blood and colon of pigs suffering from diarrheal disease caused by *Brachyspira hyodysenteriae*. Blood cytokine profiles of diarrheic pigs identified IL-1β to increase during the onset of diarrhea, and TNF-α expression increased at peak dysentery while IFN-γ was not detected after inoculation (176). Colonic samples revealed a slightly different cytokine profile with up-regulation of IL-1β, IL-6, IL-8, and IL-17A in the mid-section or apex colon of diseased pigs (252). Interestingly, porcine colonic explants exposed to live *B. hyodysenteriae* had elevated expression of IL-1α after 8hrs of exposure with no change in IL-8, IFN-γ, or TNF-α (322). Many of these cytokines identified cause modification of ion channel and

transporter function and are capable of contributing to the development of diarrheal disease and modification of the colonic mucin environment aiding in spirochete colonization.

2.6.1 *Effect of cytokines on anion secretion*

Many studies have assessed the effect of cytokine regulation on anionic secretion through CFTR and CaCCs in colonic derived cell lines. Proinflammatory and anti-inflammatory cytokines are produced by two types of T lymphocytes that express CD4 and CD8 on their cell surfaces (27). T lymphocytes expressing CD4 produce a large proportion of cytokines which are further classified into two distinct groups known as Th1 and Th2 cytokines, with Th1 cytokines primarily being proinflammatory and Th2 being anti-inflammatory/regulatory (27). The cytokine profile in the blood and colon of diarrheic pigs infected with *B. hyodysenteriae* has identified TNF-α, IL-1α, IL-1β, IL-6, IL-8, and IL-17A the cytokines involved in the pathogenesis of the disease (176, 322). This section will focus on these cytokines and what is known regarding their regulation of ion transport.

Th1 proinflammatory cytokine TNF-α has been studied extensively as it is produced by inflammatory cells populating the epithelial surface in patients suffering from cystic fibrosis (CF) and inflammatory bowel disease (IBD), both of which are diseases caused by altered anion transport (17, 156, 210, 215). Secreted by activated macrophages, TNF-α has been shown to down-regulate CFTR mRNA expression in human colorectal HT-29 cells after only 4hrs of exposure (220). Interestingly, CFTR mRNA expression was decreased as a result of TNF-α reducing the half-life of CFTR mRNA transcripts rather than suppressing the rate of transcription (220). Another study

assessing the synergistic effects of TNF-α and IFN-γ on Cl^- secretion determined that cAMP and calcium-activated short-circuit currents were significantly reduced, supported by a reduction in CFTR protein expression after 48hrs of exposure in human colorectal T84 cells (87). In another study, however, TNF-α caused elevated cAMP-activated anionic secretion through CFTR but not CaCCs in submucosal glands in porcine trachea and primary bronchus (18).

Another proinflammatory cytokine, IL-1β has been noted to be of importance in the pathogenesis of cystic fibrosis and inflammatory bowel disease (204, 298). IL-1β has been shown to have a biphasic effect CFTR mRNA expression in T84 cells (44). The effects of IL-1β on CFTR expression were determined to be dose dependent as cytokine concentrations between 0.25-0.5 ng/ml had a stimulatory effect while concentrations >1.00 ng/ml were inhibitory (44). Like TNF-α, IL-1β also induced cAMP-activated secretion via CFTR in porcine airway submucosal glands (18). NF-κβ has been implicated in elevating CFTR expression after exposure to IL-1β in T84 and Calu-3 cells by causing an increase in CFTR gene promoter activity (45).

Much less is known regarding the effects of IL-6, IL-8, and IL-17A on anionic secretion. One study observed that IL-8 was responsible for a decrease in β_2-adrenergic induced Cl^- secretion in rat and human alveolar epithelial type II cells by a decrease in CFTR activity and biosynthesis (265). Another study found that IL-17A elevated forskolin-stimulated HCO_3^- secretion through CFTR in human bronchial epithelial cells (HBE) by an undetermined mechanism (175). At the current time, there are no studies assessing the role of IL-6 on anion secretion.

IL-1α is of particular interest as this cytokine was significantly upregulated in colonic explants exposed to live *Brachyspira hyodysenteriae* (322). IL-1α has previously been shown to cause an increase in short-circuit current (I_{sc}) in rabbit ileum within 30-minutes of exposure to 5ng/ml (50, 58). Furthermore, myofibroblast cells preincubated with IL-1α significantly elevated I_{sc} in acutely juxtaposed T84 monolayers (131). However, the increase in I_{sc} in all cases was attributed to elevated expression of PTGS1 and PTGS2 resulting in elevated production of PGE_2 rather than an increase in channel expression.

2.6.2 *Effect of cytokines on electroneutral Na^+ absorption*

Loss of electroneutral Na^+ absorption in the gastrointestinal tract is a major contributor to the development of diarrheal disease (280, 335). TNF-α has been shown to repress NHE3 mRNA and protein expression through phosphorylation of Sp1 and Sp3 transcription factors by a cAMP-dependent protein kinase in human colorectal C2BBe1 cells (9). Additionally, TNF-α also down-regulated NHE2 mRNA and protein expression through activation of NF-κβ in C2BBe1 cells (10). Suppression of these two NHE isoforms by TNF-α was further supported by significant impairment of electroneutral Na^+ absorption in C2BBe1 cells (9, 10).

IL-1β has also been shown to inhibit NHE function in the gastrointestinal tract. A recent study has shown that IL-1β strongly reduces mRNA and protein expression of Na^+/H^+ exchanger regulatory factor 3 (NHERF3) in human colorectal Caco-2BBE cells (194). Reduced expression of NHERF3 has been identified in the inflamed intestine of both ulcerative colitis patients and murine colitis models (186, 330). The absence of NHERF3 leads to dysfunction of NHE3 however, it is not a result of decreased mRNA or

protein expression but rather an increase in protein turnover due to reduced membrane retention time (59, 130). Other studies have shown that mice lacking the Na^+/H^+ exchanger regulatory factor 1 (NHERF1) and Na^+/H^+ exchanger regulatory factor 2 (NHERF2) have reduced NHE3 activity and transporter abundance on the brush border membrane of jejunum and colon while mRNA levels remain unchanged (40, 54).

Unlike the effects of TNF-α and IL-1β, IL-17A has been shown to elevate NHE3 protein expression in cultured human kidney (HK-2) cells after 72hrs of exposure (230). This increase in NHE3 protein was attributed to increased expression and phosphorylation of serum and glucocorticoid regulated kinase 1 (SGK1) stimulated by IL-17A addition (230). Although these studies were performed in kidney-derived cells, it is possible that similar effects occur in gastrointestinal epithelia.

The role of IL-1α on modifying NHE isoform expression and function has not been well studied. Previous studies have found that basolateral stimulation of rabbit ileum with human IL-1α decreases both Na^+ and Cl^- absorption while stimulating Cl^- secretion (58). These effects were mirrored closely when rabbit ileal samples were stimulated with PGE_1 which resulted in net Cl^- secretion, however, when ileal samples were first treated with IL-1α and subsequently exposed to PGE_1 the magnitude of change in net flux and electrical properties was reduced (58). These findings suggested that the effects of IL-1α and PGE_1 are not additive in nature, suggesting a common pathway (58). Additionally, in another study assessing enterocyte-subepithelial myofibroblast interaction exposure of human colon 18Co or P2JF cells preincubated with IL-1α grown acutely juxtaposed to T84 cells significantly elevated basal I_{sc} (131). This effect was attributed to upregulation of PTGS1 and PTGS2 expression in 18Co and

P2JF cell lines and production of PGE_2 (131). Both PGE_1 and PGE_2 bind to prostanoid receptors EP_2 and EP_4 which results in the synthesis of cAMP (72).Thus, these previous studies suggest that IL-1α inhibits Na^+ absorption by elevation of cAMP instead of modulating Na^+ transporter gene expression.

2.6.3 *Effect of cytokines on electroneutral Cl^- absorption*

SLC26A3 also known as downregulated in adenoma (DRA) is a Cl^-/HCO_3^- exchanger that has been implicated as the major route of electroneutral Cl^- absorption in the colon (270). Loss of DRA has been determined to be a major contributor to the development of diarrhea in patients suffering from congenital chloride diarrhea (CLD) and IBD (162, 321, 327). Furthermore, knockout of DRA in mice resulted in diarrheal development (157).

Studies assessing cytokine modulation of DRA function and expression are limited however, some have reported inhibitory effects. TNF-α decreases DRA mRNA and protein expression in Caco-2, HT-29 cells as well as crypt derived ileal enteroids from mice (178). Additionally, mice injected with TNF-α had significantly decreased DRA mRNA and protein expression in their ileum and colon (178). These effects were attributed to TNF-α activation of NF-κβ decreasing DRA promoter activity resulting in decreased gene and protein expression (178).

Like TNF-α, IL-1β has been shown to decrease DRA mRNA expression in Caco-2 after 24hrs of exposure suggesting that IL-1β inhibits DRA gene transcription (328). Interestingly, DRA expression was not altered in Caco-2 cells exposed to IL-6 for 24hrs (328).

2.7 Mechanisms of bacterial-induced diarrhea in the gastrointestinal tract

At the current time, five general mechanisms are responsible for the development of diarrheal disease in the gastrointestinal tract (133). These mechanisms are as follows 1: elevated anionic secretion of Cl^- and HCO_3^- into the lumen. 2: reduced electroneutral Na^+ absorption via NHE3. 3: reduced Cl^- absorption via DRA. 4: increased paracellular permeability through disruption of tight junctions. 5: reduced Na^+ and glucose absorption via SGLT1 (133) (Figure 1.2).

Enteric bacterial pathogens alter ion transport in the gastrointestinal tract by two main modes of action through direct regulation of ion transport and/or barrier function or indirectly through cytokines, neuropeptides or effacement of absorptive villi (133). This section focuses on known pathophysiological mechanisms employed by enteric bacterial pathogens resulting in diarrheal development in both humans and livestock.

2.7.1 *Human enteric pathogens*

A number of bacterial enteric pathogens that cause diarrhea in humans have been well characterized. Although these bacteria are not a concern in food animal medicine, it is possible that in the future they may be. This section will focus on the pathophysiological mechanisms of *Vibrio cholera*, *Clostridium difficile* and *Shigella* species.

2.7.1.1 *Vibrio cholerae*

Vibrio cholerae is an enteric pathogen that causes severe diarrhea in areas of the world where people that do not have access to clean drinking water. Through ingestion, *V. cholerae* colonizes in the host's small intestine where it releases toxins. *V. cholerae* has several toxins that are released, one of which is cholera toxin (CT).

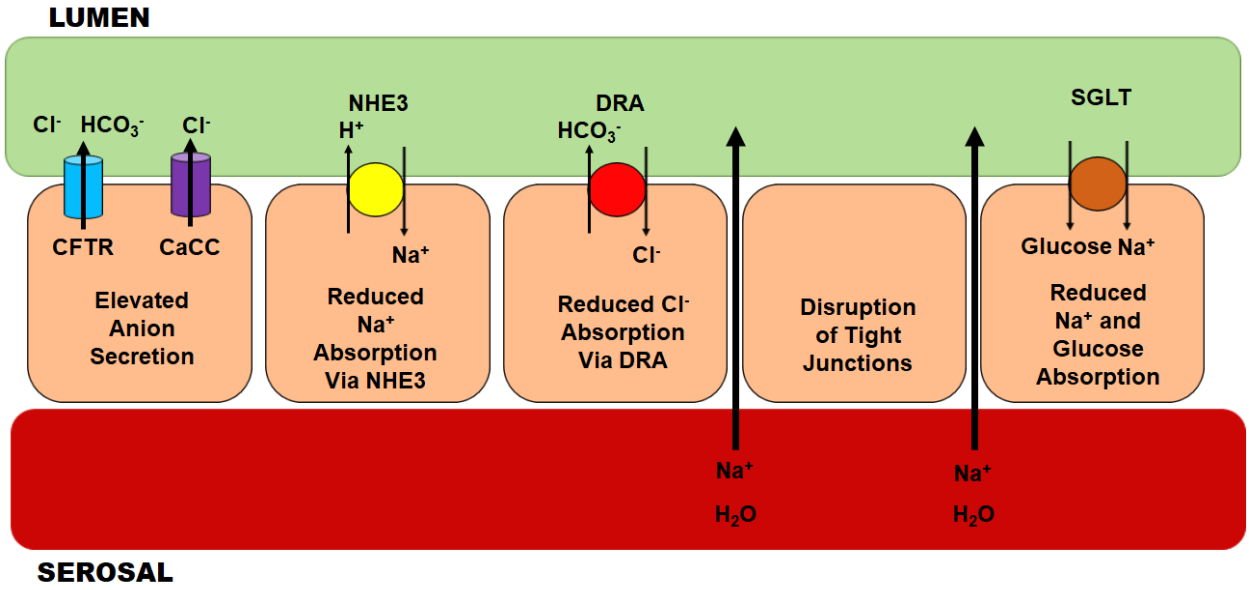

Figure 1.2. Alterations in ion transport known to cause diarrhea.

Cellular mechanisms known to cause diarrhea within the gastrointestinal tract. CFTR = cystic fibrosis transmembrane conductance regulator. CaCC = calcium-activated chloride channels. NHE3 = Na^+/H^+ exchanger isoform 3. DRA = downregulated in adenoma. SGLT = sodium/glucose co-transporter.

CT initially binds to the GM1 ganglioside receptor on the mucosal surface of enterocytes in the small intestine (134). CT is made of an A subunit and five B subunits in which the A subunit is bound pentameric ring of B subunits, where the B subunits are responsible for delivery of the A subunit into the cell through the GM1 receptor (46, 134).

The A subunit increases cAMP production by ADP-ribosylating a GTPase, which is responsible for regulating adenylate cyclase (56). The production of cAMP activates PKA, phosphorylating CFTR, resulting in anion secretion (56). Elevated cAMP driven secretion results in inhibition of electroneutral Na^+ absorption through NHE2 and NHE3 contributing to the development of diarrhea (113, 292).

In addition to CT, *V. cholera*e releases three additional toxins that manipulate ion channel transport further supporting the secretory diarrheal phenotype. Among these toxins is accessory cholera toxin (ACE), which activates Ca^{2+}-dependent anion secretion, however, cAMP and cGMP mediated anion secretion was unaffected (306). NAG-stable toxin increases cGMP production by activating guanylyl cyclase, thus leading to phosphorylation of CFTR by cGMP-dependent protein kinase (PKG) (244, 316). *V. cholerae* cytolysin (VCC) is the final toxin that creates anion permeable pores in epithelial cells creating large vacuoles, in addition to having cytolytic effects on red blood cells (174).

In addition to the three toxins that modulate ion transport, *V. cholerae* produces three toxins that affect barrier function by causing the breakdown of tight junction proteins contributing to diarrheal development. One of these toxins is hemagglutinin/protease or HA/P which is an extracellular protease that cleaves the tight junction protein occludin, resulting in re-arrangement of zonula occluden-1 (ZO-1)

around cell-to-cell boundaries (326). RTX (repeats in toxin), another *V. cholerae* toxin, causes loss of barrier function decreasing transepithelial resistance (TER) by cross-linking actin monomers into oligomers (93, 177). The final barrier function altering toxin is Zot, which is biologically inactive until it is cleaved into a 12kDa peptide by a *V. cholerae* specific protease (309). This peptide causes loss of barrier function by binding to an apical receptor called zonulin which is expressed on the surface of epithelial cells in the small intestine and is responsible for the disassembly of tight junctions (319). A smaller six amino acid peptide derived from Zot named AT-1002 has also been shown to decrease transepithelial resistance due to redistribution of ZO-1 away from cell to cell tight junction boundaries (109). Collectively *V. cholerae* releases three toxins that result in secretion and malabsorption of electrolytes in conjunction with three toxins that alter barrier function resulting in severe, life-threatening diarrhea.

V. cholerae induces changes in the small intestinal mucin environment by causing mucus hypersecretion that peaks and then subsides (227). Ileal loops in rabbits exposed to CT had rapid mucus secretion that lasted only 3-5 hours after toxin exposure leading to goblet cell depletion (185). CT and ACE result in elevated anion secretion in response to increased levels of cAMP and Ca^{2+} which both acutely regulate mucin secretion in gastrointestinal and airway epithelium by activating PKA and PKC (2, 38, 70). This depletion of mucus is likely beneficial to *V. cholerae* as it must penetrate the mucus layer overlaying the epithelium to bind the GM1 ganglioside receptors (134). At the current time, there are no *in vivo* or *in vitro* studies assessing specific changes in mucin composition following *V. cholerae* infection.

2.7.1.2 *Clostridium difficile*

C. difficile is a dynamic pathogen that takes advantage of a host that has been exposed to a broad-spectrum antibiotic suppressing the commensal microbial population (315). Its inability to outcompete other bacteria species keeps it at bay and normally is found in the gastrointestinal accounting for 2-3% of the microbial population (315). The pathogenic process of *C. difficile* begins with colonization of the colon followed by the release of two exotoxins, Toxin A and B (TcdA and TcdB), as well as an additional toxin produced by some strains of *C. difficile* named binary toxin (CDT) (240). Before being internalized, TcdA binds to glycoprotein gp96 expressed on the apical surface of colonocytes (218).

Conversely, TcdB binds to apically expressed chondroitin sulfate proteoglycan 4 (CSPG4) and poliovirus receptor-like 3 (PVRL3) (182, 333). Together these two toxins disrupt the cytoskeletal structure and barrier function by glycosylating the small GTPase protein Rho (302). Furthermore, the binary toxin (CDT) an actin-specific ADP ribosyltrantransferase produced by some *C. difficile* strains exacerbates the effects of TcdA and TcdB by causing disorganization of the cytoskeleton leading to an even more severe diarrhea (7, 19).

Studies have shown that TcdA has a direct effect on ion transport and barrier function. Purified TcdA has been shown to cause accumulation of Na^+, Cl^-, K^+ and total protein in rabbit colon (190). Additionally, Ussing chamber studies using guinea pig ileum have demonstrated that TcdA induces significant changes in paracellular permeability and decreases electrogenic Na^+ absorption through ENaC while inducing a Cl^- secretory response (212). Furthermore, TcdA alone and in conjunction with TcdB

has been shown to decrease Downregulated in Adenoma (DRA) protein levels but not mRNA both *in vivo* and *in vitro* (66). Although TcdA has been considered the primary cause of the pathogenesis caused by *C. difficile*, one study has shown that TcdB causes inhibition of the critical NHE3 isoform by facilitating protein internalization, thus contributing to diarrheal disease (125). These findings would suggest that TcdA in conjunction with TcdB are responsible for the pathogenesis caused by *C. difficile* infections.

C. difficile induced diarrhea is contributed to by severe inflammation and the release of neuropeptides. TcdA and TcdB cause an inflammatory response resulting in tissue damage and fluid exudation (133). Cytokine profiles of patients suffering from *C, difficile* infections show upregulation of IL-1β, IL-6, IL-8, IL-17A, and IL-16 (331). TcdA and TcdB cause the release of proinflammatory cytokines TNF-α and the release of IL-1β and IL-6 by direct activation of monocytes (88). Upregulation of these cytokines as described previously have strong regulatory effects on ion transport within the gastrointestinal tract and likely directly contribute to diarrheal development.

In addition to causing the release of proinflammatory cytokines, *C. difficile* also causes activation of enteric nerves causing the release of neuropeptides; Substance P (SP), calcitonin gene-related peptide (CGRP) and neurotensin which have been shown to induce Cl^- secretion (47, 158, 245). Together these mechanisms contribute to the pathophysiology of *C. difficile* infections resulting in diarrheal disease.

C. difficile has been shown by many groups to bind to mucins both *in vivo* and *in vitro* and is thought to facilitate the delivery of toxins to the epithelium (80, 84, 128). However, little information is known regarding the changes that occur to the mucin

environment within the colon of humans. To date, only one study has examined changes in mucin properties in colonic biopsies and fecal samples (79). Interestingly, patients suffering from *C. difficile* infections had reduced levels of the secreted mucin, MUC2 in both their stool and tissue with no change in the cell-surface mucin, MUC1 (79). The hypothesis is that a decrease in MUC2 allows for greater binding of *C. difficile* to surface mucins (79). Mucin galactose residues are exposed in patients suffering from *C. difficile* and potentially are the receptor required for TcdA binding subsequently driving colonization and pathogenesis of the disease (79).

2.7.1.3 *Shigella species*

There are four *Shigella* species that cause diarrheal disease in humans which include *S. sonnei*, *S. flexneri*, *S. dysenteriae*, and *S. boydii* (133, 191, 226). *S. sonnei and S. flexneri* are the two most common species responsible for diarrheal disease in developed countries (1). *S. dysenteriae* and *S. boydii* infections are rare but, *S. dysenteriae* induces diarrhea that is the most severe of all four *Shigella* spp. due to its production of Shiga toxin which can cause hemolytic uremic syndrome (133).

The mechanism that *Shigella* species utilize to gain access into epithelial cells is multipart and involves uptake by epithelial cells by utilizing a type III bacterial secretion system (T3SS) (166). *Shigella* species first move across M cells in the colonic epithelial layer and translocate the basolateral membrane (243). Afterward, the bacteria attach to the basolateral surface of epithelial cells and through the T3SS, forms a pore in the cellular membrane (34, 312). Delivery of T3SS effector proteins results in actin remodeling and polymerization resulting in uptake of the bacterium (166). The presence

of actin tails on *Shigella* species allows for cell to cell movement, increasing the ability of the bacteria to colonize the intestinal epithelium (247).

Shigella species cause an inflammatory diarrhea by causing an initial release of IL-1β after destroying macrophages when emerging from M-cells (275, 329). The inflammation is then significantly increased due to the presence of free bacteria on the basolateral side of the epithelial cells, which allows access to Toll-like receptors.

These bacteria have evolved to evade the host's immune system by a series of mechanisms. One of these mechanisms is the alteration in LPS acetylation which reduces TLR4 activation allowing for free bacteria to evade detection (46). Additionally, *Shigella* species inject a number of effector proteins that alter the host's immune system that modulates the host's diarrheal response. These proteins include OspF, OspG, and IpaH (133). OspF targets MAP kinase signaling by inhibiting ERK1/2, p38, and JNK (187). These kinases control the production of proinflammatory cytokines including IL-1, IL-6, and TNF-α. Furthermore, MAP kinases are also targeted by IpaH which is a ubiquitin ligase (264). IpaH ubiquitinates Ste7, a MAPKK which causes degradation of the protein, consequently, MAP kinase signaling is inhibited preventing further production of proinflammatory cytokines. In contrast, OspG causes interference with ubiquitination of phospho-IκBα, preventing its degradation (167). Under normal conditions phosphorylation of Iκβα causes its degradation allowing for NFκβ translocation and transcriptional activation (24). Inhibition of NFκB activity subsequently inhibits further synthesis of cytokines (167).

Shigella species cause loss of absorptive function by actively destroying the epithelial cells and compromising barrier function within the GI tract contributing to

diarrheal disease. Tight junction proteins claudin-1, ZO-1, ZO-2, and occludin are negatively impacted during *Shigella* infections, however, a specific toxin that causes the breakdown of these proteins has not yet been identified (267). In addition to altered barrier function, *Shigella* species have been shown to increase intracellular calcium concentrations, stimulating Cl^- secretion while inhibiting NHE3 activity (73, 168).

Like other human enteric pathogens *Shigella* species, specifically *S. boydii* and *S. sonnei* have been shown to bind to human colonic mucins (254). Interestingly, these two *Shigella* species did not bind rat colonic mucin or human/rat small intestinal mucins suggesting the presence of a specific binding site on human colonic mucins required for colonization (254). In another study, *S. flexneri* was shown to induce significant changes in mucus rheological properties and composition in the human colon-derived cell line HT29-MTX (288). In infected monolayers, the mucus layer overlying the HT29-MTX cells was dense and tightly bound to the epithelial cells and mostly made of MUC5AC, which is not normally expressed in the colon *in vivo* (229, 288). It is thought that changing the mucus structure to a denser more tightly bound layer likely facilitates access to the colonic epithelial surface allowing for greater colonization (288).

As I have discussed earlier anion secretion is critical for proper secretion and expansion of gel-forming mucins like MUC5AC (98, 253). However, *Shigella* species do not appear to inhibit cAMP or Ca^{2+} anion secretion; rather they elevated intracellular Ca^{2+} concentrations driving Cl^- secretion (73). Ca^{2+} however, affects intestinal mucin rheological properties, in which mucins become smaller and denser as Ca^{2+} concentrations increase (90). Elevation of intracellular Ca^{2+} likely explains the tightly

bound dense mucus observed in HT29-MTX cells infected with *S. flexneri*, thus, allowing for greater colonization and subsequent infection.

2.7.2 *Production animal enteric pathogens*

Severe economic losses are endured each year due to enteric pathogens that cause high morbidity and mortality in production animals across the globe. Infections of the gastrointestinal tract are associated with increased cost of production due to the use of antimicrobials, decreased feed conversion and mortality. Production animals refer to animals raised for human consumption and include beef and dairy cattle, swine, and poultry. This section will focus on the pathophysiological mechanisms of bacteria that cause diarrhea in production animals as well as humans and will include *E. coli*, *Salmonella*, and *Brachyspira*.

2.7.2.1 *Escherichia coli*

E. coli is a facultative anaerobe that makes up a small part of the microbial population within the gastrointestinal tract of healthy individuals (154). There are, however, five species of *E. coli* that have obtained pathogenic attributes that are responsible for severe, life-threatening diarrhea. These pathogenic *E. coli* strains include enteropathogenic *E. coli* (EPEC), enterohemorrhagic *E. coli* (EHEC), enterotoxigenic E. coli (ETEC), enteroaggregative *E. coli* (EAEC), enteroinvasive *E. coli* and diffusely adherent *E. coli* (DAEC). Collectively, these *E. coli* strains are of interest to both human and production animal medicine. This section will focus on enterotoxigenic *E. coli* (ETEC) as it is major *E. coli* strain involved in enteric colibacillosis in swine (196).

ETEC induced diarrhea is characterized as a secretory diarrhea due to the high loss of ions and water in the small intestine during infection. ETEC secretes two

essential toxins known as heat-stable (ST) and heat-labile (LT) enterotoxins which are the main contributors to the development of diarrheal disease (300). ST is a peptide consisting of 18-19 amino acids while LT is a heterohexameric protein consisting of an A subunit and five smaller B subunits (3, 106, 284). The receptor for ST is guanylyl cyclase C (GC-C) which is expressed on the surface of intestinal epithelial cells, while LT like cholera toxin, binds to the monosialoganglioside GM1 receptor on the surface of epithelial cells (83, 140, 213). Binding of the heat-labile toxin results in luminal anion secretion by elevating cAMP production resulting in activation of PKA, subsequently phosphorylating CFTR (256). In contrast, binding of heat-stable toxin also causes activation of CFTR, however, this occurs through elevating levels of cGMP by stimulating guanylate cyclase causing translocation of the CFTR protein to the surface of the apical membrane (91, 108). Together these two enterotoxins cause net secretion of Cl^- and $HCO3^-$, and water into the lumen of the jejunum while inhibiting electroneutral Na^+ absorption via cAMP inhibition of NHE isoforms (339, 340).

ETEC is responsible for promoting major changes to the mucus environment within the small intestinal. The mucus layer overlying the small intestine is unlike that of the colon in which the mucus layer is less dense and loosely attached (150). ETEC heat labile enterotoxin has been shown to induce MUC2 expression resulting in elevated mucin secretion which aids in colonization (179). ETEC takes advantage of this change in the mucus environment by secreting EtpA, an adhesin that facilitates mucin attachment (179). The present data suggests that EtpA allows for binding to both secreted mucins such as MUC2, as well as transmembrane mucins like MUC3 (179) Interestingly, ETEC also secretes YghJ, a metalloprotease and EatA, a secreted serine

protease that both degrade intestinal mucins allowing for greater access to the surface of small intestinal enterocytes and transmembrane mucins (180, 195). By modifying the mucin environment in the small intestine, ETEC effectively gains access to the surface epithelium allowing for binding of GM1 receptors facilitating diarrheal development.

2.7.2.2 *Salmonella species*

Salmonella species remain one of the most diverse bacteria with over 2600 different serotypes (313). Some of these species are host specific while others are host-adaptive and cause disease in a variety of animals as well as humans. Food production animals such as cattle, swine, and poultry can all be infected by *Salmonella* species resulting in production limiting diarrhea, systemic infections, and in some cases death (22, 141, 285). *Salmonella* shedding by infected animals occurs through contact with saliva, skin, and feces subsequently, infecting other animals and posing a threat to human health by consumption of contaminated meat and animal handling (78). Contamination of carcasses occurs at slaughterhouses where cross-contamination between healthy animals and animals that are shedding *Salmonella* can occur (14).

Salmonella species are gram-negative bacteria that cause inflammation induced diarrhea in humans and animals by colonizing in the ileum, cecum, and colon. All *Salmonella* share the ability to invade their host through uptake by both phagocytic and nonphagocytic intestinal cells by secreting effector proteins (313). This invasion mechanism is due to *Salmonella's* ability to use a type III protein secretory system which encodes for T3SS1 and T3SS2 proteins required to enter M-cells, epithelial cells, and dendritic cells (41, 60, 86). Among the T3SS1 effector proteins SopE, SipA, SopE2, and SopB have been best characterized. *Salmonella* strains that express SipA or SopE

exclusively provoke inflammation of the mucosa while SopE2 and SopB do not cause inflammation unless accompanied by SipA or SopE (119, 338).

Further studies suggest that effector protein SopE in *S. typhimurium* depends on Rho GTPases and caspase- 1 to elicit a proinflammatory response *in vivo* (214). SopE and SopE2 activate Rho GTPases, which triggers actin-mediated host cell invasion (120). Hence, Rho GTPase is thought to act as a signal that triggers caspase-1 releasing IL-1 and IL-18 causing inflammation of the gastrointestinal mucosa (159). Once the pathogen invades the host cell, expression of SopE and T3SS1 desists (120). This means that these effector proteins are of critical importance for the invasion of gastrointestinal epithelial cells but not for later stages of the infection.

T2 proteins have been characterized to aid *Salmonella* species in survival once the epithelial cells have been invaded. These effector proteins have been shown to cause inhibition of various aspects of endocytic trafficking, including fusion between lysosomes and *Salmonella*-containing vacuoles (SCVs) (308). Additionally, T2 proteins aid in the avoidance of NADPH oxidase-dependent destruction by macrophages, and interference with the localization of inducible nitric oxide synthase (iNOS) to the SCV (48, 97, 311). Together these effector proteins cause substantial physiological changes resulting in the development of diarrhea.

Infection of cell lines with *Salmonella* has been shown to cause chemokine and cytokine secretion and upregulation of prostaglandin-endoperoxide synthase 2 (PTGS2) formerly known as cyclooxygenase 2 (Cox-2) (30, 37). It has been previously shown that *S. typhimurium* infection of human intestinal xenographs increases basal, as well as Ca^{2+} and cAMP-stimulated ion transport resulting in secretion of Cl^- and $HCO3^-$ into the

lumen (30). PTGS2 inhibitors reversed this secretory response along with suppressing PGE_2 secretion (30). Furthermore, another study demonstrated that the release of prostaglandins PGE_2 and $PGF_{2\alpha}$ in HT-29 infected cells with *S. dublin* was able to elicit Cl^- secretion in naive T84 cells *in vitro* (257).

Infection of HT-29/cl.19 cells with *Salmonella* increased total and membrane abundance of CFTR and Na^+-K^+-$2Cl^-$ co-transporter (NKCC1) in a manner dependent on PTGS2 (257). Cl^- secretion is dependent on NKCC1 to replenish Cl^- within the cell through the basolateral membrane. It has been suggested that *Salmonella* infections may cause increased synthesis of NKCC1 allowing for increased Cl^- secretion (257). These findings suggest that *Salmonella* induces secretory diarrhea dependent on the upregulation of PTGS2 and prostanoid synthesis.

Although *Salmonella* invades gastrointestinal cells, barrier function is unaffected by *S. typhimurium* infections unlike other bacterial pathogens such as *V*. cholerae (105, 319, 326). The use of gut loop clearance studies using C^{14} labeled mannitol on rhesus monkeys and rabbits infected with *S*. *typhimurium* revealed that barrier function was not disrupted in the jejunum, ileum or colon (105). These findings suggest that invasion by *Salmonella* species does not alter tight junction permeability, consequently having no additive contribution to diarrhea.

Alternatively, studies using a variety of cell lines such as MDCK, Caco-2, and T84 cells have observed decreased TER and decreases in expression of tight junction proteins after infection with *Salmonella* (85, 172, 296). *In vitro* experiments examining specific tight junction proteins have displayed a reduction in ZO-1 and occludin expression after only 2 hours of infection in T84 cells (172). A subsequent study found

that claudin-1 expression was decreased during T84 cell infection with *S. typhimurium* (189). These studies suggest that disruption of tight junctions resulting in impaired barrier function may contribute to diarrheal development during *Salmonella* infections.

Studies assessing changes in the mucin environment of the small intestine following *Salmonella* infection appear to be limited to the serovar *S. typhimurium* and are conflicting in their reports (15, 336). One study observed a decrease in goblet cell abundance and altered mucin composition in the ileum of mice infected with *S. typhimurium* (15). In contrast, another study found that wild-type mice infected with *S. typhimurium* had elevated expression and production of MUC2 which was important in limiting colonization, as $MUC2^{-/-}$ mice had a significantly greater bacterial load (336). However, another study has provided evidence that *S. typhimurium* binds to a neutral mucin termed Mucus-Rs and is thought to be the initial binding site in the small intestine (314). At the current time, it is unclear whether changes in the mucin environment benefit the pathogen or the host, as it appears that both may potentially benefit. More research is needed in this area to determine the role of mucins in the pathogenesis of *Samonella* species.

2.7.2.3 *Brachyspira species*

Little is known regarding the pathophysiological mechanisms involved during *Brachyspira* infections resulting in diarrheal disease. The colon is the primary site of bacterial colonization resulting in inflammation and the formation of lesions. Diarrhea ensues accompanied by large amounts of mucus and some fecal blood.

Studies assessing the alterations in electrolyte and solute transport in the colon by *Brachyspira* has been limited to the swine isolate *Brachyspira hyodysenteriae*. *B.*

hyodysenteriae has been described to cause malabsorptive diarrhea in which Na^+ and Cl^- absorption is abolished in diarrheic animals (13). These conclusions were made based on experiments performed in infused isolated colonic loops in anesthetized control and diseased pigs (13, 277). However, pilot experiments on isolated colonic loops in healthy pigs utilizing radiolabelled ^{22}Na and ^{36}Cl were used to demonstrate linear changes in radiolabelled flux which led the authors to use a simplified version of the Berger and Steele equation (13, 28, 277). When diarrheic animals were assessed, total volume and concentration of non-isotope Na^+ and Cl^- was used to indirectly calculate lumen to blood and blood to lumen fluxes (13, 277). Thus, the authors state that non-linear changes in ion flux would result in erroneous results.

Luminal Cl^- secretion appears not to contribute to diarrheal development during *B. hyodysenteriae* infections, as diarrheic pigs had no change in blood to lumen Cl^- flux when compared to controls (277). Furthermore, agonist-induced net HCO_3^- secretion by 40mM theophylline was abolished in diarrheic pigs (277). Basal values of cAMP and cGMP were not elevated in *B. hyodysenteriae* diseased pigs (277). These findings suggest that diarrhea caused by *B. hyodysenteriae* is unlike that of many other enteric pathogens such as *V. cholerae* and enterotoxigenic *E*. *coli* which induce diarrhea primarily by cyclic nucleotide-activated anion secretion (91, 108, 244, 256, 316).

A key defining feature of *Brachyspira* infections in both swine and humans is the massive induction of fecal mucus accompanying diarrhea (49, 121, 127, 206, 266). The altered colonic mucus environment along with *Brachyspira*'s affinity for mucins has been studied in depth. *Brachyspira hyodysenteriae* and the zoonotic spirochete *Brachyspira pilosicoli* have been shown to be attracted to mucin concentrations of 6-8% which

closely mirrors the viscosity of the mucus layer overlying the colonic epithelium (223). Furthermore, *B. hyodysenteriae* has been shown to have a strong chemotactic response towards porcine mucin components serine and fucose while, also binding to mucin carbohydrate structures (161, 207, 251). These findings have suggested that the mucin layer overlaying the colonic epithelium is pertinent for spirochete colonization and growth. Other studies have focused on the alterations in mucin production within the colon during *Brachyspira* infections.

Two groups have determined that both *B. hyodysenteriae* and *B. hampsonii* significantly alter the mucin environment in the colon of diarrheic pigs (251, 323). Under normal physiological conditions, the mucus layer covering the colonic epithelium is primarily composed of the secreted gel-forming mucin MUC2 (147, 149). *B. hyodysenteriae* infections resulted in elevated production of MUC2, while both *B. hyodysenteriae* and *B. hampsonii* caused *de novo* synthesis of MUC5AC, a gel-forming mucin usually produced in the gastric mucosa and not in the colon (229, 251, 323). Furthermore, the mucus layer in the colon of diarrheic pigs became disorganized compared to control pigs (251, 323). In *B. hyodysenteriae* infections the changes in mucin production were attributed to three mechanisms, the first being the ability of IL-17A to induce mucus secretion in HT29 MTX-E12 cells, the second being exposure of live *B. hyodysenteriae* to neutrophil elastase which resulted in mucus secretion dependent on MAPK3/ERK1 pathways, and lastly elevated goblet cell hyperplasia (251, 252).

Interestingly, the combined effects of IL-1β, IL-6, IL-8, IL-17A and neutrophil elastase did not induce mucus secretion. These findings suggest that the degradation of

membrane proteins on the surface of *B. hyodysenteriae* by neutrophil elastase results in the release of toxins that alter transcriptional processes. These changes in the mucin environment have been suggested to create a niche for *Brachyspira* elevating the number of mucin binding sites for the bacterium, promoting growth and colonization (251).

Chapter 3 – Decreased Electrogenic Anionic Secretory Response in the Porcine Colon Following *in vivo* Challenge with *Brachyspira hyodysenteriae* and *Brachyspira hampsonii* would Support an Altered Mucin Environment

Cole B. Enns[1], John C.S. Harding[2], Matthew E. Loewen[1b]

1. Department of Veterinary Biomedical Sciences, 2. Department of Large Animal Clinical Sciences, Western College of Veterinary Medicine, University of Saskatchewan. 52 Campus Drive. Saskatoon, Saskatchewan, Canada S7N 5B4

Author Contributions

C.E., J.H., and M.L. conceived and designed research; C.E., J.H., and M.L. performed experiments; C.E. analyzed data; C.E. and M.L. interpreted results of experiments; C.E. prepared figures; C.E. and M.L. drafted manuscript; C.E., J.H., and M.L. edited and revised manuscript; C.E., J.H., and M.L. approved final version of manuscript.

*This manuscript has been accepted for publication, but, has not yet been published.

*See Appendix for Descriptive Materials & Methods.

Brachyspira spp. cause diarrheal disease in multiple animal species by colonization of the colon, resulting in colitis, mucus induction and disrupted ion transport. Unique to spirochete pathogenesis is the immense production of mucus resulting in a niche mucin environment favoring spirochete colonization. Mucin rheological properties are heavily influenced by anionic secretion and loss of secretory function has been implicated in diseases such as cystic fibrosis. Here, the effects on the agonist-induced electrogenic anionic secretory response by infectious colonic spirochete bacteria *Brachyspira hyodysenteriae* and *Brachyspira hampsonii* was assessed in pigs. Proximal, apex and distal sections of colon were assessed in Ussing chambers. Activation of secretion via isoproterenol, carbachol, and forskolin / IBMX demonstrated a significantly decreased change in short-circuit current (I_{sc}) in *Brachyspira*-infected pigs in all sections. Tissue resistances did not account for this difference; rather, it was attributed to a decrease in anionic secretion as indicated by a decrease in bumetanide inhibitable I_{sc}. RT-qPCR analyses and western blot determined the major anionic channels of the epithelium were down-regulated in diarrheic pigs paired with altered mucin gene expression. Cytokines were not responsible for the down-regulation of anion channel gene transcripts. Only IL-1α was upregulated in all segments but, was without effect on CFTR mRNA expression in Caco-2 monolayers. However, a whole cell *Brachyspira hampsonii* lysate significantly reduced CFTR mRNA expression in Caco-2 monolayers. Together, these findings indicate that these two *Brachyspira* spp. cause a decreased anionic secretory response in the porcine colon supporting the altered mucin environment favoring spirochete colonization.

3.1 Introduction

Mucoid diarrheal disease associated with altered colonic fluid and electrolyte movement following intestinal spirochete infection is observed in several species (307). In humans, *Brachyspira aalborgi* and *Brachyspira pilosicoli* are generally associated with colonic inflammation accompanied by mucoid diarrhea (206, 307). In swine, *Brachyspira hyodysenteriae* and emergent *Brachyspira hampsonii* cause severe colonic inflammation and mucoid diarrhea (49, 121, 266). All of these bacteria share a commonality that sets them apart from other pathogens in that colonization of the colon results in elevated mucus production and mucus thickening while many other pathogens decrease or deplete the mucus layer overlying the epithelium (142, 225, 252).

Normally, mucus production in the gastrointestinal tract acts as the first barrier of defense to invading pathogens (205). This net-like mucus barricade is comprised primarily of secreted mucin MUC2 by goblet cells in the small intestine and colon (148, 205). *Brachyspira hyodysenteriae* infections alter the mucin environment in the porcine colon by increasing the expression and synthesis of MUC2 and MUC5AC (49, 121, 206, 251, 266). *Brachyspira hyodysenteriae* has been shown to have a strong chemotactic response to mucins, suggesting that the altered mucin environment is beneficial for colonization (223, 251).

The mucin environment is heavily influenced by epithelial ion transport, specifically the transport of anions (98, 115, 151, 253). Specifically, mucins require HCO_3^- and Cl^- to interact with Ca^{2+} for proper unfolding and rheological properties after secretion by goblet cells (90, 148, 253). If these anions are not present, mucins aggregate and accumulate, trapping debris and bacteria resulting in tissue damage (90,

98, 114, 253). CFTR appears to be critical in proper secretion and expansion of mucins as indicated by the cystic fibrosis Δ508 and *Citrobacter rodentium* mouse models (114, 115, 253). At the current time, no studies have assessed the anionic secretory response during *Brachyspira* infections that would contribute to a niche mucin environment beneficial for spirochete colonization.

Initial studies concluded that *Brachyspira hyodysenteriae* abolishes the absorptive capacity of the porcine colon, without affecting the secretory blood to lumen movement of Cl^- (13, 277). The observation of unchanged blood to lumen anionic movement seems unlikely due to the nature of the inflammatory response noted in the colon, elevated blood cytokine profiles of diarrheic pigs, and porcine colonic explants exposed to live *Brachyspira hyodysenteriae* (176, 252, 322). Numerous *in vitro* studies have shown that intestinal epithelial cells exposed to the pro-inflammatory cytokines, TNF-α and IFN-γ, have reduced protein expression of CFTR and calcium-activated chloride channels, while IL-4 and IL-13 have the opposite effect, elevating the expression of apical chloride channels (67, 87, 95, 96, 132, 258). IL-1β has a dose-dependent effect on CFTR, in which low concentrations elevate CFTR mRNA and protein expression while high concentrations have inhibitory effects (44).

Here the electrogenic anion secretory response in the proximal, apex and distal segments of the porcine colon was assessed in Ussing chambers to determine its contribution to mucin thickening and disorganization, aiding in spirochete colonization and growth. Ussing chamber short-circuit (I_{sc}) electrogenic secretory response describes the apical movement of Cl^-, HCO_3^-, and K^+ as well as basolateral transport of K^+. However, the movement of Cl^- and HCO_3^- through the basolateral membrane of the

polarized epithelial cell via NKCC1 and exiting through apical Cl^- channels, generates the majority of the electrogenic response. All three segments of the colon were assessed because regional differences in anion secretion in rat and human colon have been previously reported (228, 237). This study presents the first strong evidence for a decreased anionic secretory response in the colon of diarrheic pigs following agonist addition and inhibition of anion conductance in Ussing chambers. These findings, combined with significant decreases in anion channel mRNA and protein expression, support the reduced secretory phenotype, contributing to thickening, disorganization, and reduced clearance of mucus, benefitting *Brachyspira* pathophysiology. Furthermore, the decrease in the anionic secretory response appears not to be a result of the host cytokine response, rather a direct effect of the bacteria or toxin in which ion channel transcriptional and translational process are inhibited.

3.2 Materials & Methods

3.2.1 *Animals*

Fifty-four 6-8 week-old purebred Yorkshire barrows were housed in pairs with 12 pigs per room and provided antibiotic-free diet and water *ad libitum*. Treatment groups were each housed in separate BSL2 animal care rooms. Pigs were acclimated to their new environment for 7 days before inoculation with either *Brachyspira hyodysenteriae* strain G44 (kindly provided by Boehringer-Ingelheim Vet Medica, St. Joseph, MO; n=17), *Brachyspira hampsonii* strain 30446 (n=16), or a mock inoculum of sterile liquid culture media (n=18). The number of pigs in each group differed slightly because inoculated pigs that did not develop diarrhea were not used. Feeders were removed

from pens 12 hours prior to inoculation, but water was not. Inoculation was conducted by passing a stomach tube and flushing 30ml of 10^8-10^9 cells/ml inoculum into the stomach of a pig, followed by sterile PBS as previously described (266). Pigs were then assessed daily for clinical signs of disease, and fecal consistency-scores were recorded twice daily to accurately determine the onset and severity of diarrhea. *Brachyspira hyodysenteriae* and *Brachyspira hampsonii* strain 30446 pigs developed diarrhea within 3-7 days after inoculation and were euthanized 24 hours after onset of dysentery. Control pigs remained healthy (non-diarrheic) and were euthanized on an age-matched basis with inoculated pigs euthanized the same day. This research was designed and conducted in accordance with the Canadian Council for Animal Care and approved by the University of Saskatchewan Committee on Animal Care and Supply (Protocol #20130034).

3.2.2 *Electrogenic Ussing chamber studies*

After euthanasia, 17-18 cm segments of proximal (2.5 cm distal from the cecum), apex of the spiral colon (midpoint between the cecum and sigmoid colon) and distal (sigmoid colon) colon were collected and washed with Krebs buffer (pH 7.4) containing (in mM) 113 NaCl, 5 KCl, 1.6 Na_2HPO_4, 0.3 $NaH_2PO_4 \bullet H_2O$, 25 $NaHCO_3$, 1.1 $MgCl_2 \bullet 6H_2O$, 2.2 $CaCl_2 \bullet 2H_2O$ and 10 glucose, and chilled to 4ºC. Samples were immediately transported to the lab in Krebs buffer gassed with 95% O_2 -5% CO_2 where the serosa (visceral peritoneum) and longitudinal and circular muscle layers of the colonic wall were removed with forceps (stripped) from all segments leaving only the mucosa and submucosal rudiments as previously described (61). Pieces of stripped mucosa (2-4 tissue replicates of each segment per pig) were then placed on $1cm^2$

tissue Ussing chamber inserts and inserted into the Ussing chamber (Physiologic Instruments, San Diego, CA). Each reservoir was independently gassed with 95% O_2-5%CO_2. A heated circulating water bath maintained the buffer in the Ussing chamber at 37ºC. Transepithelial potential differences were short-circuited to 0 mV with a voltage clamp using Ag-AgCl electrodes and 3M KCL agar bridges (Physiologic Instruments, San Diego, CA) on apical and basolateral sides as previously described (61).

Tissues were allowed to equilibrate for twenty minutes before the addition of any drugs. A 1mV pulse every 30 seconds was used to determine the resistance and tissue viability from the resulting current. After the equilibration period, 10µM of the adrenergic agonist isoproterenol (I6504; Sigma Aldrich) was added to the basolateral side of the chamber to increase cAMP physiologically and stimulate cAMP-activated channels, such as CFTR. After steady state was reached, 0.1mM of carbachol (C4382; Sigma Aldrich) was added to the basolateral side of the chamber. This cholinergic agonist increases intracellular Ca^{2+} activating calcium-activated channels. After steady state was reached, 10µM forskolin (F6886; Sigma Aldrich) and 1mM of 1M 3-isobutyl-1-methylxanthine (IBMX) (I5879; Sigma Aldrich) were added to the apical and basolateral sides of the Ussing chamber causing a massive irreversible and sustained elevation in cAMP to fully activate cAMP-activated secretion. Finally, after steady state was reached 0.1mM bumetanide (B3023; Sigma Aldrich) was added to the basolateral side of the Ussing chamber to inhibit the basolateral Na^+-K^+-$2Cl^-$ co-transporter 1 (NKCC1).

3.2.3 *RT-qPCR analysis of cytokine, ion channel, and transporter mRNA expression*

Mucosal samples collected at the time of euthanasia and subsequently stored in RNAlater® (AM7021; Ambion®) at -80˚C were homogenized in 1ml of TRIzol reagent (15596018; Life Technologies) and RNA extracted according to the manufacturer's protocol. A standard of <500ng/µl was used as exclusion criteria for RNA samples.

cDNA was created from mRNA using the GoScript Reverse Transcription system (A5001; Promega). cDNA was diluted in RNase-free water and frozen at -80˚C. Gene expression was assessed by RT-qPCR using GoTaq qPCR Master Mix (A6002; Promega) and Stratagene Mx5000P real-time qPCR machines according to the manufacture's protocol. The average C_T (cycle threshold) value was used to calculate the fold difference of each gene using the ΔΔCt calculation method. Porcine primers were designed for GAPDH, CFTR, TMEM16A, ANO6, ANO9, ANO10, BEST2, BEST4, CLCA1, CLCA4, NKCC1, IL-1α, IL-1β, IL-6, IL-8, IL-10, IL-17A, IL-18, TNF-α, IFN-γ, TGF-β1, TGF-β2, TGF-β3. MUC1, MUC2, MUC4, and MUC5AC (Table 3.1). Porcine GAPDH was used as the reference gene for analyses. Human primers were designed for GAPDH, CFTR, NKCC1, IL-1α, IL-1β, and PTGS2 (Table 3.2). Human GAPDH was used as the reference gene for analyses.

3.2.4 *Western blot analysis of TMEM16A*

Protein was extracted from control and diseased colonic tissues from the proximal, apex and distal sections of the colon using the ProteoExtract transmembrane protein kit (71772-3; Novagen®) according to the manufacturer's protocol. Samples were boiled in 2x denaturing buffer (20% glycerol, 4% SDS, 125 mM Tris pH 6.8, 0.3

Table 3.1. Porcine primer sequences for RT-qPCR

Gene Name	Forward (5'-3')	Reverse (5'-3')
GAPDH	ACA TCA AGA AGG TGG TGA AGC AGG	TGA GCT TGA CGA AGT GGT CGT TGA
CFTR	ACA CTT CAC AGC AGC TCA AAC AGC	TGG AAC CAG CGT AGT GTT GAC AGA
TMEM16A	AGA GGA CGA CAT GTA CCA AAG CCA	AGG CTC GTG ATG CCG TAT TTA CCA
ANO6	AGG AAT AGC GAT TCT GGC TGT GGT	TTT CCC TGC CTC TGA AGT CAG CAA
ANO9	TGG ATG CCA TCA AGA TGG TCA GGT	ACT CAG ATG TGA AGG CGA TGA CCA
ANO10	CAG CCG CCT TTG CTG TGC TAA ATA	GCA TTC ACT TGC GGT GAC ATT CCA
BEST2	ATA CAG CTA TTT CCT GGC CTG CCT	AGT TGG TCT CAA AGT CGT CGT CGT
BEST4	TTC TAT GCT GGC TGG CTC AAG GT	TGG TTG GTT TCG AAG TCG TCG TCA
CLCA1	ATC TCC GAA GCA CAT GGG AAG TGA	AGT TTG CCT GCT TGA TTC AGT CGC
CLCA4	TGG GAT TCG AAG AGC GTT TGA GGT	TCA GCA CTT GGT CCC AGA GCA ATA
NKCC1	GCT CCA AAT TCA CGC CCA GCT TTA	ATG AGC CAT CGC TGA TAC TTG GCT
IL-1α	ACG AAC CCG TGT TGC TGA AG	TTG GAT GGG CGG CTG ATT TG
IL-1β	CTC CAG CCA GTC TTC ATT GTT CAG	GTT GTC ACC GTA GTT AGC CAT CAC
IL-6	CCA ATC TGG GTT CAA TCA GGA GAC	CAG CCT CGA CAT TTC CCT TAT TGC
IL-8	ATA CGC ATT CCA CAC CTT TCC ACC	TCT GTA CAA CCT TCT GCA CCC ACT
IL-10	AAG ACG TAA TGC CGA AGG CAG AGA	TGC TAA AGG CAC TCT TCA CCT CCT
IL-17A	CTG CAG TAC ATC AGG AGA AA	GCT GAG GGA AGT TCT TGT
IL-18	GGA CAT CAA GCC GTG TTT	GTT ACT GCC AGA CCT CTA GT
TNF-α	ACG CTC TTC TGC CTA CTG CAC TTC	TCC CTC GGC TTT GAC ATT GGC TAC
IFN-γ	ATG GTA GCT CTG GGA AAC TG	TCT GGC CTT GGA ACA TAG TC
TGF-β1	TGA GCA TCT TGG ACC TTA TC	GTT ACC ACT GAG CCA CAA
TGF-B2	CGC GAT TTG CAG GTA TTG	GGT TGG ACT GTT GTG ACT
TGF-B3	GTG GGA AAT TAA CCC TCT CT	CAG GAG AGG AAA CCC ATA AT
MUC1	CCA CAA CCT GAA GAC ACA GT	GCT GAG CAG AGG AAG GAA AT
MUC2	CTT CTA GAT GGG TGT GTC TC	GTG GTA GTT GGT GGT GTA
MUC4	TCT GGG ATG ATG CTG ATT TCT C	CCC ACA CTA GCT GGT TGT ATT
MUC5AC	CAG TCC ATC ATT GTC GAG TAC C	CAC CAC CTC GTT GTT GAA GA

Table 3.2. Human primer sequences for RT-qPCR

Gene Name	Forward (5'-3')	Reverse (5'-3')
GAPDH	CAA GGT CAT CCA TGA CAA CTT TG	GGG CCA TCC ACA GTC TTC TG
CFTR	TCC TCC AAA CCT CAC AGC AAC TCA	AAG GCA CGA AGT GTC CAT AGT CCT
NKCC1	CAT TAA CTG GTG GGC TGC ATT GCT	TCA CGT GGT CTT CCA CTC CAG AAA
IL-1α	TAC CTC ACG GCT GCT GCA TTAC	GGT CTT CAT CTT GGG CAG TCAC
IL-1β	GCT GAT GGC CCT AAA CAG ATG	TGT AGT GGT GGT CGG AGA TTC
PTGS2	GAA GCC TTC TCT AAC CTC TC	GGA TCA GGG ATG AAC TTT CT

mM bromophenol blue) containing 20% β-mercaptoethanol (BME; M6250; Sigma-Aldrich) for five minutes and analyzed by 10% SDS-PAGE (286).

For western blot analysis, proteins were transferred onto PVDF membrane (RPN303LFP; GE Healthcare Life Sciences) at 0.2mA for 4 hours at 4ºC with transfer buffer (25mM Tris, 192mM glycine, 20% methanol) (286). Membranes were blocked for an hour at room temperature with a 10% RapidBlock™ (M325-AMRESCO®) blocking solution and subsequently probed overnight at 4˚C with primary antibodies anti-TMEM16A (QC13356-42173; AVIVA Biosciences) and anti-β-Actin (C-4; sc-47778; Santa Cruz Biotechnology) in PBST. Membranes were then incubated for 1 hour at room temperature with secondary antibodies Alexa Fluor 488 Goat anti-Rabbit IgG antibody (A-11008; Thermo Fisher Scientific) and ECL Plex Goat anti-Mouse IgG-Cy5 antibody (PA45009; Amersham Biosciences) in PBST. Proteins were subsiquently detected and analyzed using Typhoon Trio and ImageQuant TL System (63005583; GE Healthcare Life Sciences).

3.2.5 *Cell culture*

The Caco-2 cell line derived from human colorectal adenocarcinoma (HTB-37; ATCC, Manassas, VA) was cultured in Dulbecco's modified Eagle medium (DMEM) (10-0130CM, Corning, Manassas, VA) containing 10% heat-inactivated fetal bovine serum (Gibco, Burlington, ONT, Canada), 1% penicillin-streptomycin (15140-122; Life Technologies), and 1% MEM non-essential amino acids (Gibco, Grand Island, NY) at 37˚C in a humidified atmosphere with 5% CO_2. Cells were plated on polyester Transwell® permeable supports (0.4µm pores, 24 mm in diameter, Corning) and

cultured under standard conditions until confluency. Cells were maintained for 10 days after confluency was achieved before being used in downstream experiments.

3.2.6 *Exposure of Caco-2 monolayers to recombinant human IL-1α*

To determine if the single pro-inflammatory cytokine that was significantly upregulated throughout the colon of diarrheic pigs infected with *Brachyspira hyodysenteriae* and *Brachyspira hampsonii* strain 30446 was responsible for the decrease in CFTR mRNA expression *in vivo*, polarized Caco-2 monolayers were exposed to human recombinant IL-1α (I2778; Sigma Aldrich). Polarized Caco-2 monolayers were subsequently probed for changes in CFTR mRNA expression by RT-qPCR. Both apical and basolateral surfaces were exposed to IL-1α at concentrations of 10, 100 and 500 ng/ml for 24hrs. The Caco-2 cell line was chosen as no porcine colon-derived cell lines are commercially available. To ensure that IL-1α had a biological effect on Caco-2 monolayers, qPCR primers were developed for prostaglandin-endoperoxide synthase 2 (PTGS2) which has been previously shown to become up-regulated in multiple cell types after IL-1α exposure (58, 131, 259).

3.2.7 *Caco-2 monolayer exposure to Brachyspira hampsonii lysate*

To determine if *Brachyspira* has a direct effect on modulating ion channel expression I wanted to determine if a whole cell *Brachyspira* lysate was capable of down-regulating CFTR mRNA expression in Caco-2 cells. The *Brachyspira hampsonii* strain 30446 lysate was prepared by centrifuging 50ml of culture broth containing actively motile spirochete bacteria (10^8/ml) at 10,000 X *g* for 40 min, after which the supernatant was poured off (224). Bacterial pellets were resuspended in phosphate buffered saline (Gibco; 10010-023, Life Technologies) and vortexed until the pellet

completely dissolved. This material was subsequently disrupted by sonication (Sonics & Materials Inc., Danbury, CT, USA) at 50% duty for 120 s at 4˚C (224). Lysate total protein concentrations were determined using BCA protein assay (ThermoFisher; Rockford, IL) using bovine serum albumin (BSA) as a standard according to the manufacture's protocol. Polarized Caco-2 monolayers were exposed apically to the whole cell *Brachyspira hampsonii* lysate (0.005-50µg/ml) in PBS or a PBS control for 48hrs. 50µg/ml of total bacterial protein was determined to be ~10^8 CFU/ml and considered a pathophysiological concentration.

3.2.8 *Statistical analysis*

Data was normally distributed (Shapiro-Wilk test; $P > 0.05$) and are expressed as mean $\pm$ standard error of the mean (SEM). Change in I_{sc} between diseased and control colon were analyzed using nested ANOVA (tissue replicates within pig) and Tukey post-hoc. Each colonic segment (proximal, apex, distal) were analyzed independently. Differences between tissue resistances and initial potential differences for diseased and control segments of colon were similarly analyzed using nested ANOVA. One-way ANOVA with Tukey post-hoc was used to assess log transformed (log10) fold changes for *in vivo* data obtained by RT-qPCR. Fold changes obtained by RT-qPCR for *in vitro* data was analyzed by Student's *t*-test. Western blot analysis was analyzed with Student's *t*-test (control vs. *Brachyspira* species in two separate analyses). Significance was set *a priori* at $P < 0.05$.

3.3 Results

3.3.1 *Brachyspira hyodysenteriae and Brachyspira hampsonii strain 30446 significantly reduces cAMP and calcium-activated short-circuit current in the porcine colon.*

Electrogenic anionic secretion was assessed in Ussing chambers via activation of apical Cl^- channels and inhibition of basolateral NKCC1 in control and diseased colon tissues. Tissues from diarrheic pigs had a significantly decreased ($P < 0.001$) cAMP-activated I_{sc} in response to β-adrenergic stimulation of adenylyl cyclase via isoproterenol when compared to control in all three segments of the colon, (Figures 3.1A, 3.2A, 3.3A) suggesting a decrease in anionic transport through CFTR. Isoproterenol activates CFTR when it binds the adrenergic receptor dissociating the G-coupled protein into an α and β-subunit. The β-subunit binds with adenylate cyclase converting ATP into cAMP which binds to the regulatory subunits of protein kinase A (PKA), thereby phosphorylating and activating CFTR increasing the I_{sc}. Additionally, calcium-activated I_{sc} was severely reduced throughout the colon ($P < 0.001$) by cholinergic activation by carbachol when compared to control (Figure 3.1B, 3.2B, 3.3B). Carbachol binds to muscarinic acetylcholine receptors resulting in an intracellular influx of Ca^{2+} causing activation of calcium-activated ion channels.

Further activation of cAMP by forskolin/IBMX resulted in a significant decrease ($P < 0.001$) in cAMP-induced I_{sc} throughout the colon when compared to control (Figures 3.1C, 3.2C, 3.3C). Forskolin acts directly on adenylyl cyclase resulting in elevated levels

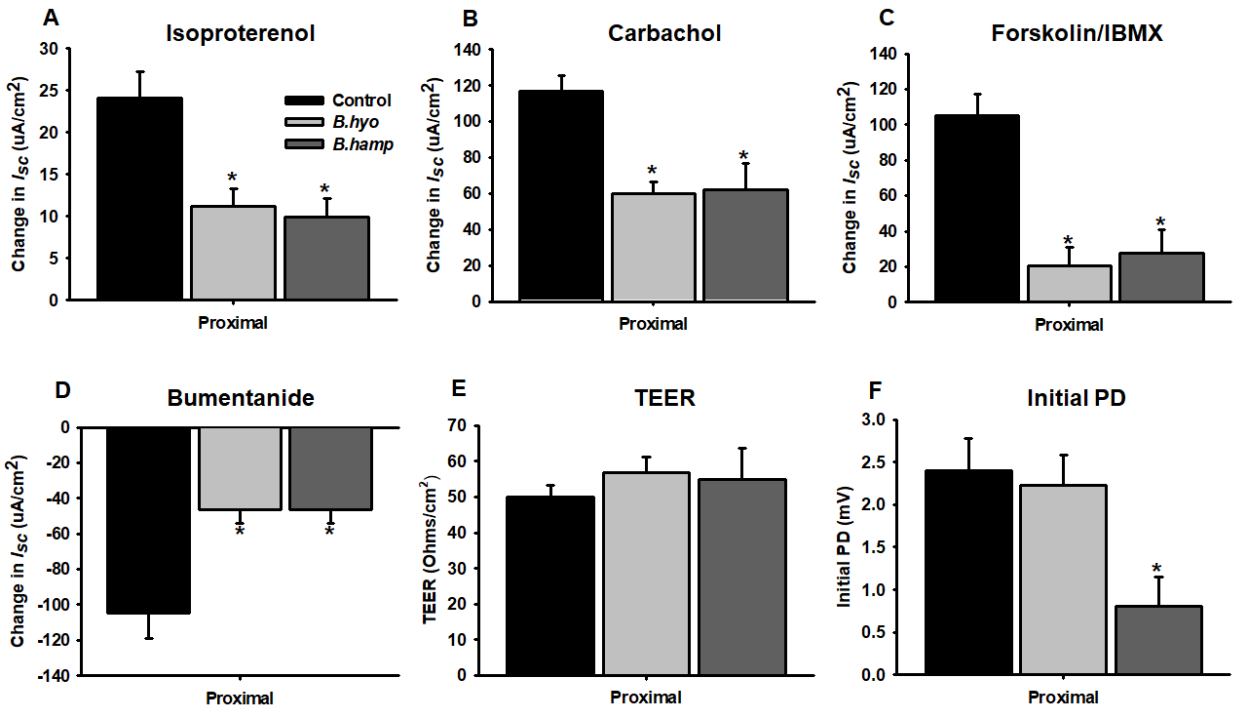

Figure 3.1. *Brachyspira hyodysenteriae* and *Brachyspira hampsonii* strain 30446 decrease anionic short-circuit current in the proximal segment of the porcine colon.

Change in I_{SC} in response to the addition of ion channel activators (isoproterenol; A, carbachol; B, forskolin/IBMX; C) and Na^+-K^+-$2Cl^-$ 1 inhibitor (bumetanide; D) in the proximal segment of control and diseased porcine colon. Transepithelial electrical resistance (TEER) (E) of control and diseased porcine colon after twenty minutes of equilibration. Initial potential difference (F) of diseased and control proximal colon after twenty minutes of equilibration. I_{SC} = short-circuit current; Data presented as mean ± SEM, analyzed using nested ANOVA and Tukey Post Hoc. * = $P < 0.001$ (n=18 ctrl, n=17 *B. hyodysenteriae,* n=16 *B. hampsonii* strain 30446).

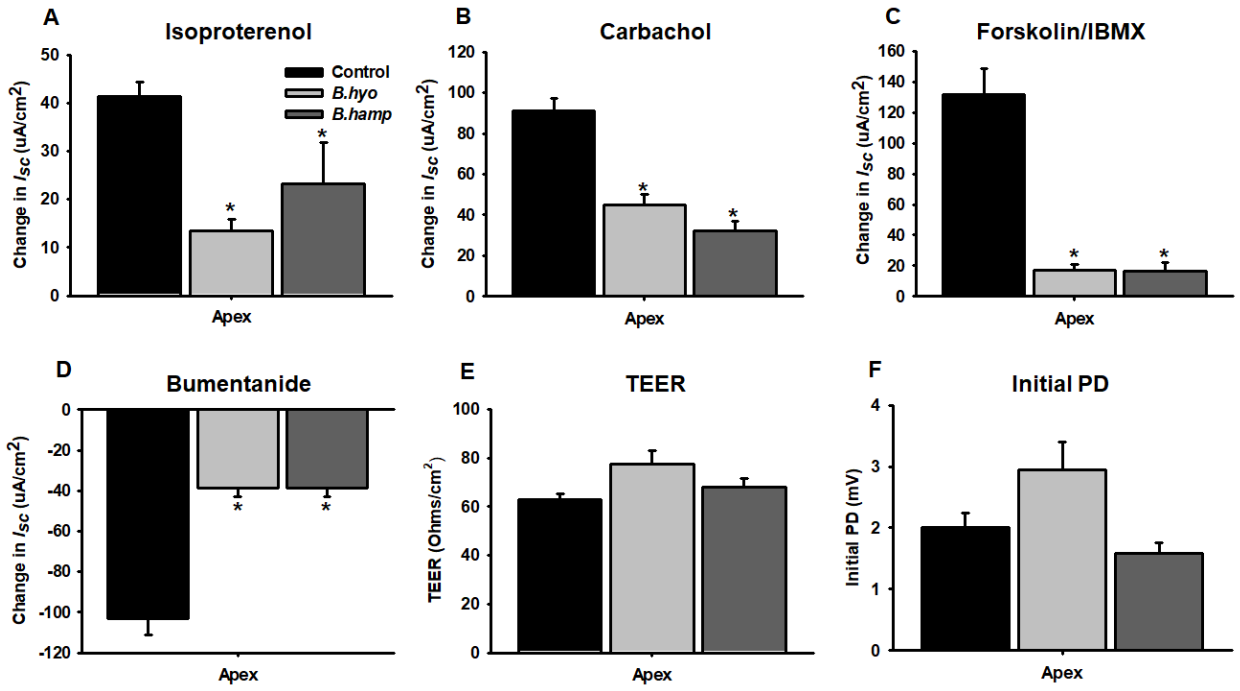

Figure 3.2. *Brachyspira hyodysenteriae* and *Brachyspira hampsonii* strain 30446 decrease anionic short-circuit current in the apex segment of the porcine colon.

Change in I_{sc} in response to the addition of ion channel activators (isoproterenol; A, carbachol; B, forskolin/IBMX; C) and Na^+-K^+-$2Cl^-$ 1 inhibitor (bumetanide; D) in the apex segment of control and diseased porcine colon. Transepithelial electrical resistance (TEER) (E) of control and diseased porcine colon after twenty minutes of equilibration. Initial potential difference (F) of diseased and control apex colon after twenty minutes of equilibration. I_{sc} = short-circuit current; Data presented as mean $\pm$ SEM, analyzed using nested ANOVA and Tukey Post Hoc. * = $P < 0.001$ (n=18 ctrl, n=17 *B. hyodysenteriae,* n=16 *B. hampsonii* strain 30446).

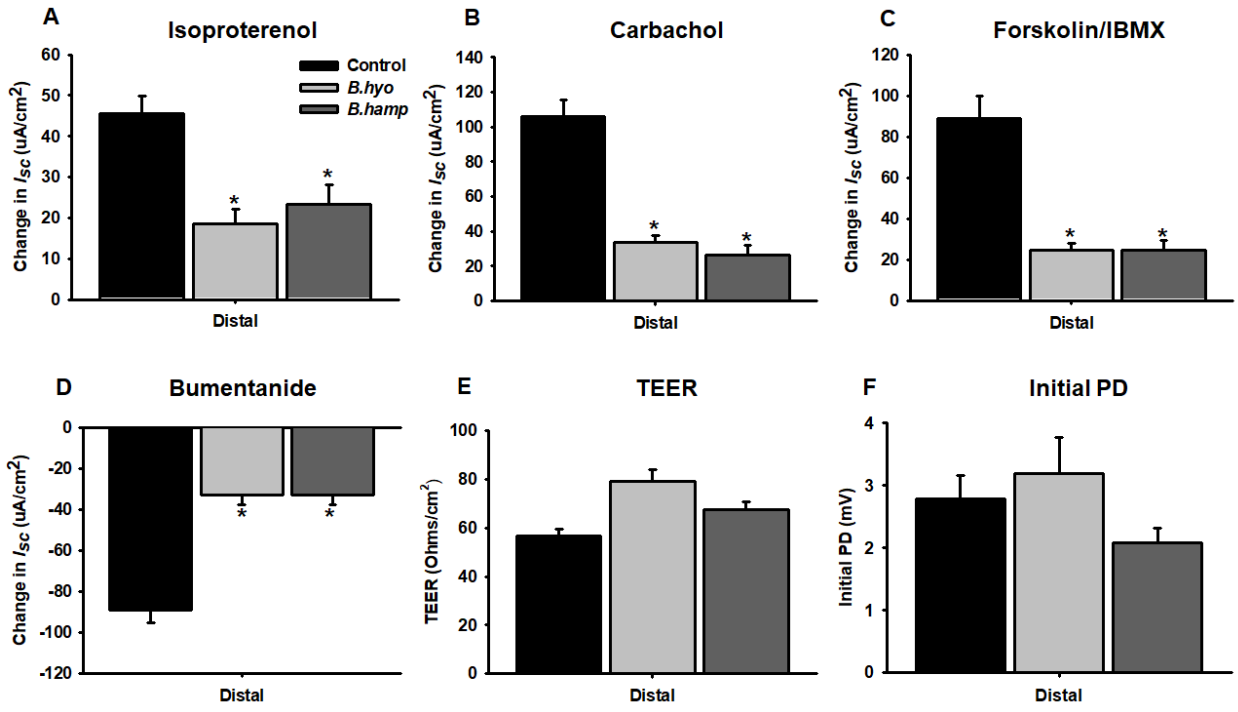

Figure 3.3. *Brachyspira hyodysenteriae* and *Brachyspira hampsonii* strain 30446 decrease anionic short-circuit current in the distal segment of the porcine colon.

Change in I_{sc} in response to the addition of ion channel activators (isoproterenol; A, carbachol; B, forskolin/IBMX; C) and Na^+-K^+-$2Cl^-$ 1 inhibitor (bumetanide; D) in the distal segment of control and diseased porcine colon. Transepithelial electrical resistance (E) of control and diseased porcine colon after twenty minutes of equilibration. Initial potential difference (F) of diseased and control distal colon after twenty minutes of equilibration. I_{sc} = short-circuit current; Data presented as mean $\pm$ SEM, analyzed using nested ANOVA and Tukey Post Hoc. * = $P < 0.001$ (n=18 ctrl, n=17 *B. hyodysenteriae,* n=16 *B. hampsonii* strain 30446).

of cAMP, thereby activating PKA and causing phosphorylation of CFTR. IBMX is a phosphodiesterase inhibitor which inhibits the degradation of cAMP. Inhibition of NKCC1 with bumetanide, blocking the anionic component of the I_{sc} resulted in less of a decrease in I_{sc} in diseased tissues compared to control ($P < 0.001$) (Figure 3.1D, 3.2D, 3.3D). This difference in bumetanide inhibition, which prevents basolateral to apical anionic movement, confirms the impact that these two *Brachyspira* species have on decreasing anionic secretion (experimental representative traces in Figure 3.4A-I).

Differences in electrogenic secretion was not attributed to differences in tissue resistance. Tissue resistances were measured for all colonic segments in diseased and control tissues by Ussing chamber (Figure 3.1E, 3.2E, 3.3E). No significant difference between infected and control tissues were noted, suggesting that these two *Brachyspira* species do not alter the integrity of the colonic mucosa as indicated by the decrease in I_{sc}. Finally, *Brachyspira* infected tissues have been previously reported to have lower cAMP levels (277), potentially resulting in lower initial resting potential difference (PD). I found no difference in PD, except in the proximal segment of diarrheic pigs infected with *Brachyspira hampsonii* strain 30446 (Figure 3.1F, 3.2F, 3.3F). Thus, changes in initial resting PD do not account for changes found in the agonist-induced I_{sc}.

3.3.2 *RT-qPCR analyses of Cl^- channels and NKCC1*

Gene expression was assessed by RT-qPCR for the major chloride channels and transporters in the colonic epithelium to determine the mechanism(s) behind the decrease in anionic secretion. mRNA expression of CFTR, the major cAMP-activated chloride channel in the gut epithelium, was significantly down-regulated in the proximal

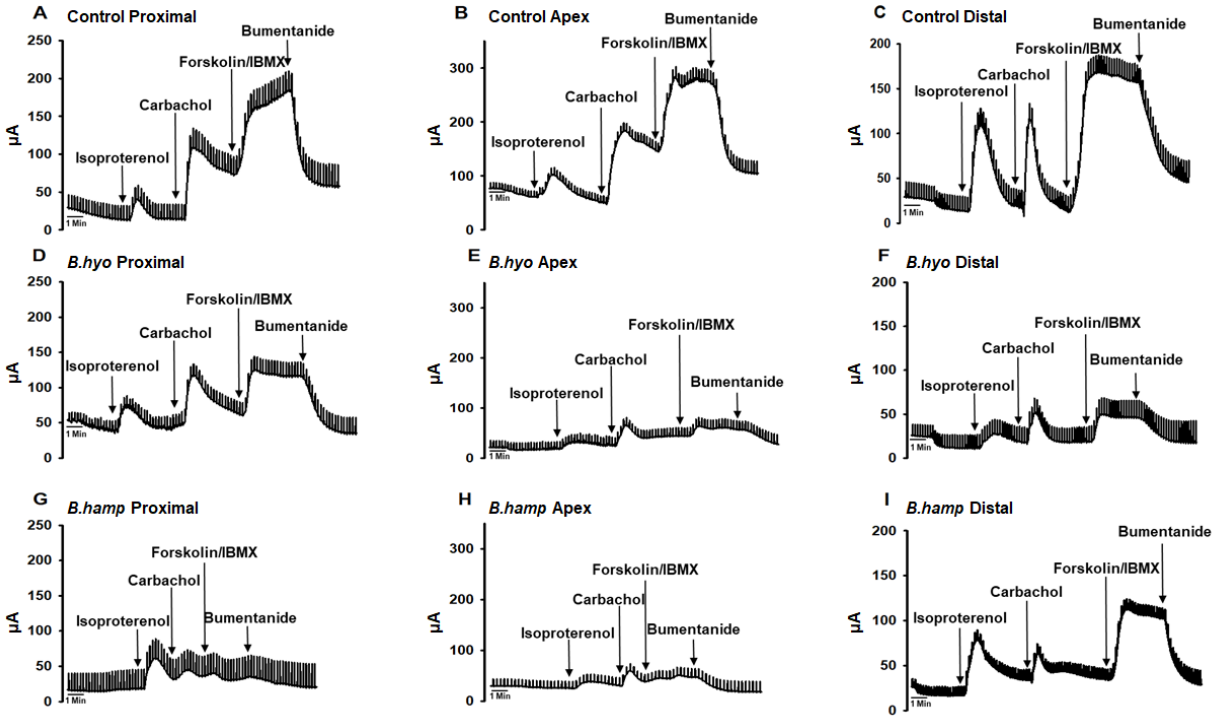

Figure 3.4. Representative I_{sc} traces of control, *Brachyspira hyodysenteriae*, and *Brachyspira hampsonii* strain 30446 infected colonic segments.

Experimental I_{sc} traces representing cellular responses to activating and inhibiting drugs in the proximal, apex and distal segments of control pigs (A-C), *Brachyspira hyodysenteriae* (D-F) and *Brachyspira hampsonii* strain 30446 (G-I) respectively.

and apex colonic segments of both *Brachyspira hyodysenteriae* ($P < 0.05$) and *Brachyspira hampsonii* strain 30446 ($P < 0.05$) diseased pigs (Table 3.3).

Furthermore, members of the calcium-activated Cl^- channel families, anoctamin and bestrophin were similarly down-regulated ($P < 0.05$) throughout the colon of diarrheal pigs (Table 3.3). The exceptions to this phenomenon were BEST2 and TMEM16A. BEST2 mRNA expression was significantly elevated in all three segments of the colon for both *Brachyspira* species ($P < 0.05$) (Table 3.3). BEST2 is found on the basolateral membrane of goblet cells and is highly permeable to basolateral entry of HCO_3^- which would contribute to an increase, rather than a decrease in I_{sc} (332). TMEM16A mRNA expression, however, was not significantly different from control in any segment of the porcine colon in diarrheic pigs (Table 3.3). Thus, changes in TMEM16A gene expression could not account for all electrophysiological observations.

Porcine CLCA1 was significantly down-regulated in the apex and distal segments of diarrheic pigs ($P < 0.05$), while CLCA4 was significantly down-regulated in all three segments of colon infected with *Brachyspira* species ($P < 0.05$) (Table 3.3). This is an unexpected observation because these gene products are usually increased during epithelial inflammatory processes and seem to modulate both inflammatory responses and epithelial ion channel activity (57). Both human and porcine CLCA1 increase whole cell CaCC activity (112, 192), while human CLCA1 increases TMEM16A in a paracrine manner (269, 334).

Additionally, there was a significant decrease in the expression of basolateral ion transporter NKCC1 in the apex of diarrheic pigs infected with *Brachyspira hyodysenteriae* ($P < 0.05$) (Table 3.3). This decrease in NKCC1 mRNA expression was

Table 3.3 Fold changes in ion channel and transporter mRNA expression in the porcine colon.*

	Segment of Porcine Colon								
	Proximal			Apex			Distal		
Ion Channel	Ctrl	*B. hyo*	*B. hamp*	Ctrl	*B. hyo*	*B. hamp*	Ctrl	*B. hyo*	*B. hamp*
CFTR	1.42^{a} ± 0.61	**0.43^{b} ± 0.06**	**0.42^{b} ± 0.07**	1.02^{a} ± 0.09	**0.24^{b} ± 0.05**	**0.40^{b} ± 0.06**	1.37^{a} ± 0.27	0.70^{a} ± 0.09	0.83^{a} ± 0.14
TMEM16A	1.61^{a} ± 0.72	0.97^{a} ± 0.46	0.91^{a} ± 0.22	1.41^{a} ± 0.57	0.64^{a} ± 0.21	0.52^{a} ± 0.12	1.09^{a} ± 0.22	0.65^{a} ± 0.23	0.61^{a} ± 0.13
ANO6	1.04^{a} ± 0.12	1.08^{a} ± 0.18	0.74^{a} ± 0.09	1.04^{a} ± 0.14	0.59^{a} ± 0.11	**0.51^{b} ± 0.11**	1.19^{a} ± 0.25	0.72^{a} ± 0.18	0.92^{a} ± 0.18
ANO9	1.71^{a} ± 0.50	**0.51^{b} ± 0.19**	**0.52^{b} ± 0.11**	1.18^{a} ± 0.23	**0.45^{b} ± 0.12**	**0.22^{b} ± 0.07**	1.58^{a} ± 0.61	**0.55^{b} ± 0.15**	**0.30^{b} ± 0.06**
ANO10	1.09^{a} ± 0.18	0.75^{a} ± 0.15	0.78^{a} ± 0.06	1.10^{a} ± 0.19	**0.42^{b} ± 0.11**	**0.45^{b} ± 0.05**	1.07^{a} ± 0.18	**0.43^{b} ± 0.02**	**0.47^{b} ± 0.10**
BEST2	1.30^{a} ± 0.45	**68.85^{b} ± 26.2**	**68.32^{b} ± 19.09**	1.94^{a} ± 1.07	**29.02^{b} ± 8.55**	**31.85^{b} ± 20.82**	1.67^{a} ± 0.66	**8.04^{b} ± 2.41**	**5.33^{b} ± 1.54**
BEST4	1.21^{a} ± 0.27	**0.40^{b} ± 0.06**	0.82^{a} ± 0.11	1.16^{a} ± 0.30	**0.46^{b} ± 0.10**	**0.38^{b} ± 0.07**	1.07^{a} ± 0.17	**0.34^{b} ± 0.07**	**0.29^{b} ± 0.08**
CLCA1	1.13^{a} ± 0.28	0.49^{a} ± 0.08	1.27^{a} ± 0.45	1.08^{a} ± 0.19	**0.29^{b} ± 0.10**	**0.24^{b} ± 0.05**	1.09^{a} ± 0.17	**0.45^{b} ± 0.09**	**0.23^{b} ± 0.03**
CLCA4	1.49^{a} ± 0.46	**0.06^{b} ± 0.03**	**0.04^{b} ± 0.01**	1.67^{a} ± 0.86	**0.04^{b} ± 0.03**	**0.01^{b} ± 0.01**	1.18^{a} ± 0.28	**0.14^{b} ± 0.05**	**0.05^{b} ± 0.03**
NKCC1	2.51^{a} ± 1.57	0.66^{a} ± 0.12	1.00^{a} ± 0.22	1.08^{a} ± 0.19	**0.36^{b} ± 0.14**	0.65^{a} ± 0.17	1.06^{a} ± 0.14	0.62^{a} ± 0.13	0.57^{a} ± 0.16

*Fold changes in ion channel mRNA expression in three segments (proximal, apex, distal) of the colon in control, *Brachyspira hyodysenteriae*, and *Brachyspira hampsonii* diseased pigs. Data presented as mean ± SEM of fold difference in gene expression measured by RT-qPCR. For each gene marked with a different superscript differ by at least $P<0.05$ compared to control in each segment in each segment. CFTR = cystic fibrosis transmembrane conductance regulator; TMEM16A = anoctamin 1; ANO6 = anoctamin 6; ANO9 = anoctamin 9; ANO10 = anoctamin 10; BEST2 = bestrophin 2; BEST4 = bestrophin 4; CLCA1 = chloride channel accessory 1; CLCA4 = chloride channel accessory 4; NKCC1 = Na^{+}-K^{+}-$2Cl^{-}$ co-transporter 1. Significantly different values are marked in bold. (n=12 ctrl, n=12 *B. hyodysenteriae,* n=12 *B. hampsonii* strain 30446).

not significantly different than control in the proximal or distal segments of *Brachyspira hyodysenteriae* infected pigs or in any of the colonic segments of pigs infected with *Brachyspira hampsonii*. This finding suggests that NKCC1 is not entirely responsible for the decrease in apical anion conductance. The decreased inhibition of I_{sc} by bumetanide throughout the colon of diarrheic pigs is likely due to decreased anion conductance through CFTR and calcium-activated Cl- channels resulting in a reduced secretory response.

3.3.3 *Western blot analysis of TMEM16A*

Western blot was performed to elucidate the mechanism of the paradoxical unchanged TMEM16A mRNA expression and the decreased calcium-activated I_{sc}. TMEM16A channel protein was significantly decreased in the proximal ($P < 0.001$) ($P < 0.001$), apex ($P = 0.011$) ($P < 0.001$) and distal ($P < 0.001$) ($P < 0.001$) segments of diarrheic pigs infected with *Brachyspira hyodysenteriae* and *Brachyspira hampsonii* strain 30446, respectively, when compared to controls (Figure 3.5 A, B). This decrease in TMEM16A protein throughout the colon of diarrheic animals correlates with the decrease in calcium-activated I_{sc} observed after the addition of carbachol. This finding suggests that *Brachyspira* spp. may be able to cause post-translational modification of TMEM16A protein resulting in its degradation.

3.3.4 *RT-qPCR analyses of colonic mucin mRNA expression*

Mucin gene transcripts were examined in the proximal, apex and distal segments of the porcine colon of pigs infected with *Brachyspira hyodysenteriae* and *Brachyspira*

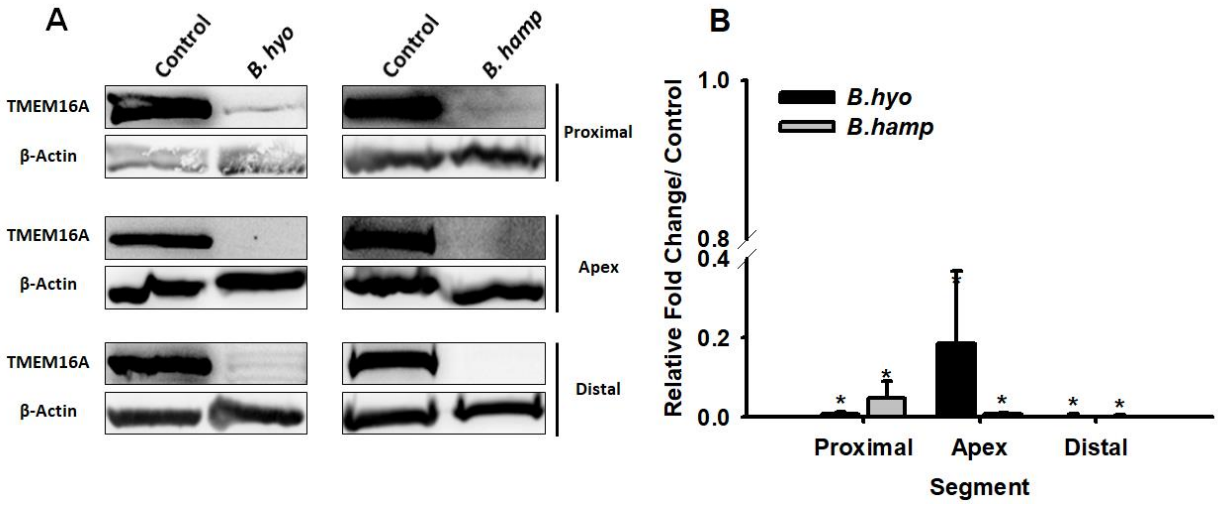

Figure 3.5. *Brachyspira hyodysenteriae* and *Brachyspira hampsonii* strain 30446 significantly reduce TMEM16A protein expression in the porcine colon.

Western blot (A) and densitometry (B) of TMEM16A (~93 kDa) compared to β-actin (~43 kDa) reference for *Brachyspira hyodysenteriae* and *Brachyspira hampsonii* strain 30446 infected proximal, apex and distal segments of porcine colon relative to control within segment. TMEM16A = anoctamin 1, β-actin = beta-actin. Data presented as mean ± SEM, analyzed using Student's *t*-test. * = $P < 0.05$ (n=3 ctrl, n=3 *B. hyodysenteriae,* n=3 *B. hampsonii* strain 30446).

hampsonii strain 30446. Previous research has shown that diarrheic pigs infected with *Brachyspira hyodysenteriae* had a significant increase in MUC2 and MUC5AC expression in the mid-section of the porcine colon (251). My findings partially agree with these findings in which I found that MUC5AC mRNA expression was significantly up-regulated ($P < 0.05$) in all three segments of colon in both *Brachyspira hyodysenteriae* and *Brachyspira hampsonii* infected pigs (Table 3.4). However, I found that MUC2 expression in the colon of diarrheic pigs was not significantly different than control animals (Table 3.4). Likewise, MUC4 expression throughout the colon was not significantly different from control while MUC1 mRNA expression was significantly down-regulated ($P < 0.05$) in all three colonic segments of diarrheic pigs (Table 3.4). My findings support the previous report that *Brachyspira hyodysenteriae* and now *Brachyspira hampsonii* strain 30446 infections alter mucin gene transcription to develop a favorable mucin environment in the host's colon, aiding in bacterial colonization and growth.

3.3.5 *RT-qPCR analyses of regulatory colonic cytokine mRNA expression*

Regulatory cytokines known to modulate ion channel function were assessed in pigs infected with both *Brachyspira* species. IL-10, a potent inhibitor of immune-mediated inflammation, was not significantly different in diarrheic pigs when compared to control except for the distal segment of pigs infected with *Brachyspira hampsonii* which was significantly down-regulated ($P < 0.05$) (Table 3.5). TGF-β1 functionally down-regulates CFTR and TMEM16A mRNA and protein expression resulting in impaired Cl^- and HCO_3^- secretion (137, 293). TGF-β1 and TGF-β2 were significantly down-regulated in the distal colon ($P < 0.05$) of diarrheic pigs while expression in the

Table 3.4. Fold changes in mucin mRNA expression in the porcine colon.*

	Segment of Porcine Colon								
	Proximal			Apex			Distal		
Mucin	Ctrl	*B. hyo*	*B. hamp*	Ctrl	*B. hyo*	*B. hamp*	Ctrl	*B. hyo*	*B. hamp*
MUC1	$1.23^{a} \pm 0.25$	**$0.30^{b} \pm 0.06$**	**$0.24^{b} \pm 0.07$**	$1.02^{a} \pm 0.09$	**$0.20^{b} \pm 0.05$**	**$0.08^{b} \pm 0.01$**	$1.18^{a} \pm 0.28$	**$0.25^{b} \pm 0.07$**	**$0.15^{b} \pm 0.14$**
MUC2	$1.21^{a} \pm 0.33$	$1.97^{a} \pm 0.61$	$2.78^{a} \pm 1.01$	$1.53^{a} \pm 0.63$	$0.72^{a} \pm 0.13$	$2.77^{a} \pm 0.56$	$1.35^{a} \pm 0.36$	$0.94^{a} \pm 0.44$	$0.70^{a} \pm 0.28$
MUC4	$1.70^{a} \pm 0.81$	$1.64^{a} \pm 0.58$	$3.93^{a} \pm 0.44$	$1.24^{a} \pm 0.43$	$0.61^{a} \pm 0.13$	$1.72^{a} \pm 0.25$	$1.02^{a} \pm 0.09$	**$0.27^{b} \pm 0.10$**	$1.55^{a} \pm 0.69$
MUC5AC	$1.15^{a} \pm 0.55$	**$90.29^{b} \pm 27.86$**	**$40.89^{b} \pm 5.74$**	$1.93^{a} \pm 0.91$	**$39.34^{b} \pm 11.79$**	**$17.78^{b} \pm 3.02$**	$1.31^{a} \pm 0.46$	**$11.80^{b} \pm 4.36$**	**$12.18^{b} \pm 2.22$**

*Fold changes in mucin gene mRNA expression in three segments (proximal, apex, distal) of the colon in control, *Brachyspira hyodysenteriae*, and *Brachyspira hampsonii* diseased pigs. Data presented as mean ± SEM of fold difference in gene expression measured by RT-qPCR. For each gene marked with a different superscript differ by at least $P<0.05$ compared to control in each segment. MUC1 = mucin 1; MUC2 = mucin 2; MUC4 = mucin 4; MUC5AC = mucin 5AC Significantly different values are marked in bold. (n=12 ctrl, n=12 *B. hyodysenteriae,* n=12 *B. hampsonii* strain 30446).

Table 3.5. Fold changes in regulatory cytokine mRNA expression in the porcine colon.*

	Segment of Porcine Colon								
	Proximal			Apex			Distal		
Cytokine	**Ctrl**	***B. hyo***	***B. hamp***	**Ctrl**	***B. hyo***	***B. hamp***	**Ctrl**	***B. hyo***	***B. hamp***
IL-10	$1.05^{a} \pm 0.16$	$0.74^{a} \pm 0.20$	$1.17^{a} \pm 0.42$	$1.52^{a} \pm 0.47$	$1.30^{a} \pm 0.74$	$0.40^{a} \pm 0.10$	$1.07^{a} \pm 0.16$	$0.67^{a} \pm 0.25$	**$0.30^{b} \pm 0.03$**
TGF-β1	$1.38^{a} \pm 0.48$	$0.43^{a} \pm 0.05$	$2.78^{a} \pm 1.01$	$1.10^{a} \pm 0.21$	$0.96^{a} \pm 0.11$	$2.77^{a} \pm 0.56$	$1.01^{a} \pm 0.07$	**$0.50^{b} \pm 0.07$**	$0.70^{a} \pm 0.28$
TGF-β2	$1.98^{a} \pm 0.89$	$0.35^{a} \pm 0.06$	$0.28^{a} \pm 0.07$	$1.13^{a} \pm 0.27$	$0.60^{a} \pm 0.25$	$0.44^{a} \pm 0.18$	$1.38^{a} \pm 0.42$	$0.44^{a} \pm 0.09$	**$0.27^{b} \pm 0.04$**
TGF-β3	$1.38^{a} \pm 0.55$	**$0.15^{b} \pm 0.03$**	**$0.23^{b} \pm 0.07$**	$1.09^{a} \pm 0.2$	**$0.29^{b} \pm 0.07$**	**$0.27^{b} \pm 0.05$**	$1.41^{a} \pm 0.45$	**$0.35^{b} \pm 0.06$**	**$0.29^{b} \pm 0.06$**

*Fold changes in regulatory cytokine mRNA expression in three segments (proximal, apex, distal) of the colon in control, *Brachyspira hyodysenteriae*, and *Brachyspira hampsonii* diseased pigs. Data presented as mean ± SEM of fold difference in gene expression measured by RT-qPCR. For each gene marked with a different superscript differ by at least $P<0.05$ compared to control in each segment. TGF-β1 = transforming growth factor β1; TGF-β2 = transforming growth factor β2; TGF-β3 = transforming growth factor β3; IL-10 = interleukin 10. Significantly different values are marked in bold. (n=12 ctrl, n=12 *B. hyodysenteriae,* n=12 *B. hampsonii* strain 30446).

proximal and apex segments was not significantly different from control (Table 3.5). TGF-β3 was significantly down-regulated in all three segments of colon in diarrheic pigs infected with *Brachyspira* spp. ($P < 0.05$) (Table 3.5). Based on these findings it appears that regulatory cytokines are not responsible for the decrease in the anionic secretory response.

3.3.6 *RT-qPCR analyses of pro-inflammatory colonic cytokine mRNA expression*

A possible mechanism that may explain the decrease in cAMP and calcium-activated I_{sc} is elevated gene expression of pro-inflammatory cytokines, which are known to modulate ion channel and transporter function (67, 132, 258). My RT-qPCR results indicate that there was a significant increase in IL-1α expression in all three colonic segments ($P < 0.05$), and significantly elevated IL-1β expression in the distal segments of pigs infected with both *Brachyspira* species ($P < 0.05$) (Table 3.6). However, TNF-α was significantly down-regulated ($P < 0.05$) throughout the colon of diarrheic pigs, while IFN-γ mRNA expression remained unchanged except for the apex segment of pigs infected with *Brachyspira hampsonii* which had significantly decreased expression ($P < 0.05$) (Table 3.6).

IL-6 expression was significantly up-regulated in the proximal segment ($P < 0.05$) of diarrheic pigs infected with *Brachyspira hampsonii*, while IL-8 expression was significantly up-regulated in the apex ($P < 0.05$) and distal ($P < 0.05$) segments of these same animals (Table 3.6). IL-18 mRNA expression was significantly up-regulated in the proximal and apex ($P < 0.05$) segments of *Brachyspira hampsonii* disease pigs and only the apex ($P < 0.05$) segment of *Brachyspira hyodysenteriae* diseased pigs (Table 3.6).

Table 3.6. Fold changes in pro-inflammatory cytokine mRNA expression in the porcine colon.*

	Segment of Porcine Colon								
	Proximal			Apex			Distal		
Cytokine	Ctrl	*B. hyo*	*B. hamp*	Ctrl	*B. hyo*	*B. hamp*	Ctrl	*B. hyo*	*B. hamp*
IL-1α	$1.13^{a} \pm 0.26$	**$13.56^{b} \pm 4.35$**	**$21.17^{b} \pm 5.58$**	$1.15^{a} \pm 0.26$	**$13.37^{b} \pm 2.68$**	**$18.11^{b} \pm 4.19$**	$1.22^{a} \pm 0.40$	**$22.78^{b} \pm 10.07$**	**$9.59^{b} \pm 3.03$**
IL-1β	$1.58^{a} \pm 0.54$	$3.17^{a} \pm 0.90$	$3.89^{a} \pm 1.56$	$1.21^{a} \pm 0.28$	$3.16^{a} \pm 0.75$	$5.25^{a} \pm 1.37$	$1.20^{a} \pm 0.22$	**$7.34^{b} \pm 2.72$**	**$7.36^{b} \pm 0.13$**
IL-6	$1.04^{a} \pm 0.50$	$2.75^{a} \pm 0.65$	**$4.58^{b} \pm 1.24$**	$1.37^{a} \pm 0.40$	$3.77^{a} \pm 1.44$	$2.67^{a} \pm 0.98$	$1.56^{a} \pm 0.73$	$2.11^{a} \pm 0.72$	$8.36^{a} \pm 4.52$
IL-8	$1.46^{a} \pm 0.47$	$2.91^{a} \pm 1.34$	$4.17^{a} \pm 1.42$	$1.30^{a} \pm 0.44$	$2.84^{a} \pm 0.62$	**$5.78^{b} \pm 1.66$**	$1.14^{a} \pm 0.29$	$1.81^{a} \pm 0.42$	**$5.23^{b} \pm 2.01$**
IL-17A	$1.20^{a} \pm 0.30$	$9.17^{a} \pm 4.78$	$1.72^{a} \pm 0.88$	$1.29^{a} \pm 0.36$	**$6.62^{b} \pm 2.10$**	$2.49^{a} \pm 1.37$	$1.68^{a} \pm 0.64$	$4.19^{a} \pm 0.89$	$9.33^{a} \pm 5.59$
IL-18	$1.08^{a} \pm 0.22$	$3.41^{a} \pm 1.42$	**$16.34^{b} \pm 8.29$**	$1.04^{a} \pm 0.14$	$1.75^{a} \pm 0.43$	**$6.59^{b} \pm 2.78$**	$0.83^{a} \pm 0.08$	$1.44^{a} \pm 0.33$	$3.77^{a} \pm 2.09$
TNF-α	$1.21^{a} \pm 0.35$	**$0.27^{b} \pm 0.06$**	$0.84^{a} \pm 0.36$	$1.03^{a} \pm 0.12$	**$0.47^{b} \pm 0.14$**	**$0.35^{b} \pm 0.08$**	$1.08^{a} \pm 0.17$	**$0.41^{b} \pm 0.09$**	**$0.28^{b} \pm 0.06$**
IFN-γ	$1.64^{a} \pm 0.59$	$1.53^{a} \pm 0.60$	$0.52^{a} \pm 0.27$	$1.05^{a} \pm 0.14$	$0.41^{a} \pm 0.18$	**$0.32^{b} \pm 0.14$**	$1.85^{a} \pm 0.90$	$1.40^{a} \pm 0.49$	$0.47^{a} \pm 0.30$

*Fold changes in pro-inflammatory cytokine mRNA expression in three segments (proximal, apex, distal) of the colon in control, *Brachyspira hyodysenteriae*, and *Brachyspira hampsonii* diseased pigs. Data presented as mean ± SEM of fold difference in gene expression measured by RT-qPCR. For each gene marked with a different superscript differ by at least $P<0.05$ compared to control in each segment. IL-1α = interleukin 1 alpha; IL-1β = interleukin 1β; IL-6 = interleukin 6; IL-8 = interleukin 8; IL-17A = interleukin 17A; IL-18 = interleukin 18; TNF-α = tumor necrosis factor α; IFN-γ = interferon γ. Significantly different values are marked in bold. (n=12 ctrl, n=12 *B. hyodysenteriae,* n=12 *B. hampsonii* strain 30446).

Furthermore, IL-17A expression was determined to be significantly up-regulated only in the apex ($P < 0.05$) of pigs infected with *Brachyspira hyodysenteriae* (Table 3.6).

The present findings partially agree with those of Kruse et al. who examined blood cytokine profiles of pigs infected with *Brachyspira hyodysenteriae* (176). IL-1β was found to increase at the onset of diarrhea, while TNF-α was detected after inoculation with a peak occurring during the diarrheal period (176). Additionally, IFN-γ was not detected at any time after inoculation (176). Cytokine mRNA profiles of colonic samples from diarrheic pigs infected with *Brachyspira hyodysenteriae* had elevated levels of IL-1β, IL-6, IL-8, and IL-17A, however, this study only examined the mid-section of the porcine colon which is not representative of the entire colon (252). Furthermore, porcine colonic explants exposed to live *Brachyspira hyodysenteriae* for 8 hours had a significant increase in IL-1α mRNA expression while IL-8, IFN-γ and TNF-α's expression was unchanged compared to control (322). My findings, however, revealed that only IL-1α was upregulated throughout the porcine colon in diarrheic animals.

3.3.7 *IL-1α does not decrease CFTR mRNA expression in polarized Caco-2 monolayers*

To investigate whether the up-regulation of IL-1α mRNA expression throughout the colon of diarrheic pigs was responsible for the decreased expression of CFTR mRNA and reduced cAMP I_{sc}, polarized Caco-2 monolayers were exposed to varying concentrations (10, 100 and 500ng/ml) of human recombinant IL-1α for 24hrs. RT-qPCR revealed that IL-1α had no effect on modulating CFTR gene expression at any concentration when compared to control (Table 3.7). To ensure that IL-1α was

biologically active in my model, PTGS2 mRNA expression was assessed as IL-1α exposure results in elevated expression in several cell types (58, 131, 259). I found that all monolayers independent of IL-1α concentration had a significant 2-fold increase in PTGS2 mRNA expression ($P < 0.05$) (Table 3.7).

3.3.8 *Brachyspira hampsonii lysate decreases CFTR mRNA expression while increasing IL-1α expression in polarized Caco-2 monolayers*

To determine if a *Brachyspira* lysate was capable of directly altering CFTR mRNA expression, polarized Caco-2 monolayers were exposed to varying concentrations of lysate (0.005-50µg/ml) for 48hrs. My results revealed that lysate concentrations of 5 and 50µg/ml was capable of significantly down-regulating CFTR expression ($P = 0.008$) ($P = 0.003$) (Figure 3.6A) while NKCC1 (Figure 3.6B) was not significantly different from control. Additionally, lysate exposure resulted in a significant increase in IL-1α mRNA expression at a lysate concentration 50µg/ml ($P = 0.003$) (Figure 3.7A). IL-1β however, was not significantly different from control at any lysate concentration (Figure 3.7B).

Table 3.7. Fold changes in CFTR and PTGS2 mRNA expression in polarized Caco-2 cell monolayers after 24hr exposure to IL-1α.*

	Concentration of recombinant human IL-1α			
Gene Name	**Control**	**10ng/ml**	**100ng/ml**	**500ng/ml**
CFTR	$1.00^{a} \pm 0.02$	$1.09^{a} \pm 0.13$	$1.38^{a} \pm 0.03$	$1.11^{a} \pm 0.20$
PTGS2	$1.00^{a} \pm 0.07$	**$2.22^{b} \pm 0.23$**	**$2.41^{b} \pm 0.29$**	**$2.21^{b} \pm 0.21$**

*Fold changes in CFTR and PTGS2 mRNA expression in polarized Caco-2 monolayers exposed to human recombinant IL-1α for 24hrs. Data presented as mean ± SEM of fold difference in gene expression measured by RT-qPCR. For each gene marked with a different superscript differ by at least $P<0.05$ compared to control. CFTR = cystic fibrosis transmembrane conductance regulator; PTGS2 = prostaglandin-endoperoxide synthase 2. Significantly different values are marked in bold. (n=6).

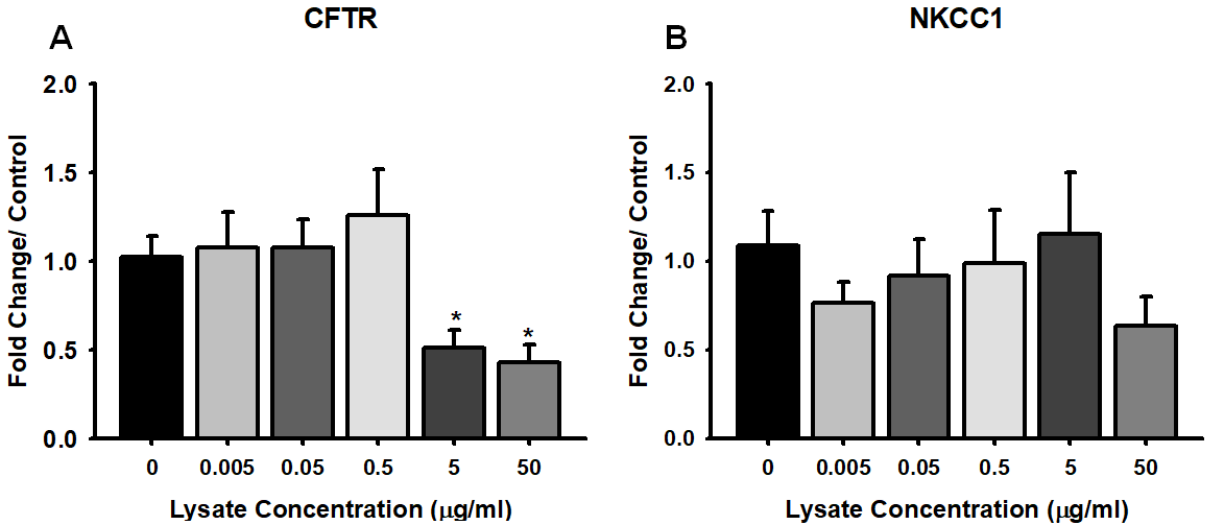

Figure 3.6: *Brachyspira hampsonii* strain 30446 lysate down-regulates CFTR mRNA expression after 48hrs with no effect on NKCC1 mRNA in Caco-2 monolayers.

Fold change in CFTR and NKCC1 mRNA expression compared to control as measured by RT-qPCR after exposure to a *Brachyspira hampsonii* strain 30446 whole cell lysate at five concentrations (0.005-50μg/ml) for a period of 48 hours. CFTR = cystic fibrosis transmembrane conductance Regulator, NKCC1 = Na^{+}-K^{+}-$2Cl^{-}$ 1 co-transporter. Data presented as mean ± SEM, analyzed using one-way ANOVA. * = $P < 0.05$. (n=6).

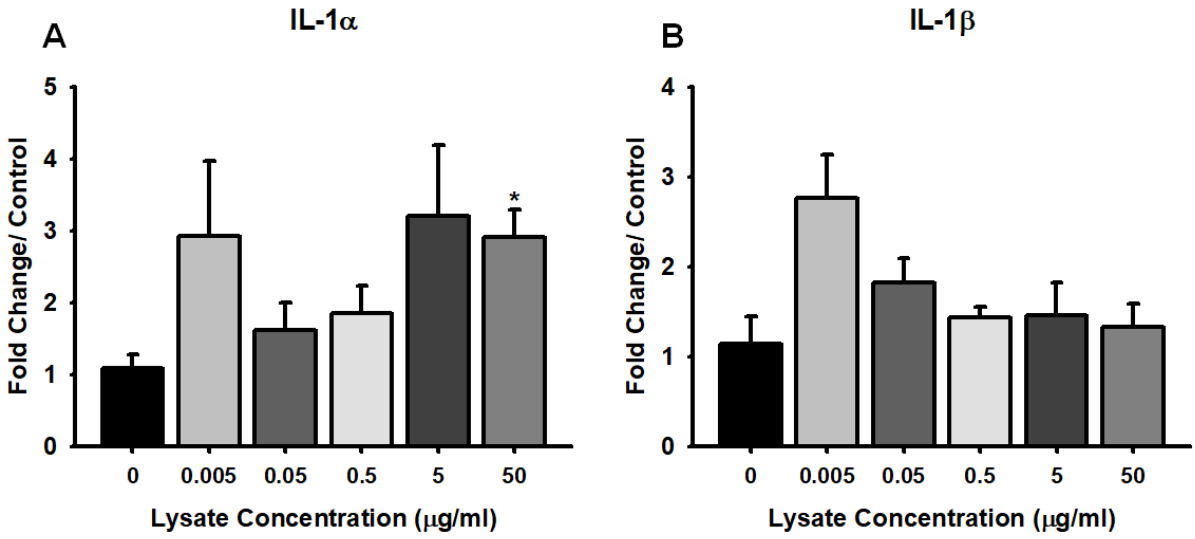

Figure 3.7: *Brachyspira hampsonii* strain 30446 lysate up-regulates IL-1α mRNA expression while IL-1β mRNA is not affected after 48hrs in Caco-2 monolayers.

Fold change in IL-1α and IL-1β mRNA expression compared to control as measured by RT-qPCR after exposure to a *Brachyspira hampsonii* strain 30446 whole cell lysate at five concentrations (0.005-50μg/ml) for a period of 48 hours. IL-1α = interleukin-1 alpha, IL-1β = interleukin-1 beta. Data presented as mean ± SEM, analyzed using one-way ANOVA. * = $P < 0.05$. (n=6).

3.4 Discussion

In humans and swine, diarrhea accompanied by excessive mucus production is a pathology of intestinal spirochetosis caused by *Brachyspira* spp (49, 121, 127, 206, 266). *In vitro*, *Brachyspira pilosicoli* and *Brachyspira hyodysenteriae* have been shown to be attracted to mucin concentrations of 6-8% similar to the viscosity of the mucus layer covering the epithelium in the colon (223). Furthermore, a strong chemotactic response by *Brachyspira hyodysenteriae* to porcine mucin components serine and fucose and binding to mucin carbohydrate structures *in vivo* have been described (161, 207, 251). These previous findings suggest that the niche mucus environment in the colon following *Brachyspira* infection is important for bacterial colonization and growth. This study provides a new understanding of the pathophysiologic and cellular changes resulting in decreased electrogenic anionic transport that supports mucus thickening and disorganization in the colon of diarrheic pigs infected with *Brachyspira hyodysenteriae* and *Brachyspira hampsonii*. These findings further our understanding of animal and human intestinal spirochetosis.

Epithelial ion transport of Cl^- and HCO_3^- heavily influences the properties of mucins and the mucus environment in the gastrointestinal tract (98, 115, 151, 253). Previous research has shown that *Brachyspira hyodysenteriae* and *Brachyspira hampsonii* cause elevated expression and synthesis of gel-forming mucins MUC2 and MUC5AC (251, 323). Gel-forming mucins are stored at a low pH in a high Ca^{2+} concentration within goblet cells and require Ca^{2+} binding following secretion (148). Mucin Ca^{2+} binding typically occurs by binding HCO_3^-, allowing repulsive electrostatic forces to unfold and expand mucins more than 1000-fold in volume (148, 253). Without

HCO_3^- present, mucins aggregate and accumulate, and if not removed will entrap debris and bacteria resulting in tissue damage (98, 114, 253).

Additionally, Cl^- and its interaction with Ca^{2+} is essential for maintaining mucin rheological properties relating to viscosity (90). Anion secretion through apical Cl^- channels, specifically CFTR appears to be critical in the proper expansion of mucins following secretion by goblet cells (98). Mice containing the defective ΔF508 CFTR gene expressed in cystic fibrosis were unable to transport HCO_3^- leading to aggregation and accumulation of mucins in the ileum preventing the clearance of pathogens (253). Additionally, mice suffering from *Citrobacter rodentium* infection had significantly reduced changes in I_{sc} in the colon following activation with cAMP and cholinergic agonists, correlating with thickening of the mucus layer overlying the colonic mucosa (115). It is important to mention that in mice suffering from *Citrobacter rodentium* the authors found that the decrease in agonist-induced I_{sc} correlated with the onset of bacterial clearance (115). However, *Brachyspira hyodysenteriae* infections appear to differ greatly from *Citrobacter* infections in mice as mucin organization was not disrupted, and no MUC5AC expression was detected (115, 251). It is important, however, to acknowledge the effects that apical anion secretion has on modifying the mucus environment within the gastrointestinal tract.

Previous research concluded that Cl^- unidirectional flux from the blood to lumen in pigs experimentally infected with *Brachyspira hyodysenteriae* was unaffected, while absorption was abolished (13). This contrasts with the findings of the present study, where both *Brachyspira hyodysenteriae* and *Brachyspira hampsonii* strain 30446 infections resulted in a significant decrease in cAMP and calcium-activated I_{sc} anionic

current. This decrease correlated with a significant increase in MUC5AC expression throughout the colon, as previously reported (251). Additionally, the current study found no significant effect on tissue resistance, a measure of epithelial barrier function. Thus, my findings partially agree with the previous work, which also reported that barrier function in diarrheic animals infected with *Brachyspira hyodysenteriae* was not compromised (13, 277).

The differences in conclusions between studies maybe a result of assumptions made, and techniques used. Previous work used pilot experiments in healthy pigs demonstrating linear radiolabelled ^{22}Na and ^{36}Cl flux. This led the authors to use a simplified version of the Berger and Steele equation (13, 28, 277), along with the total volume and concentration of cold non-isotope Na^+ and Cl^-, to indirectly calculate the blood to lumen unidirectional flux of Cl^- (13, 277). If the author's assumptions were incorrect, a blood to lumen change in Cl^- flux would be missed, and a decrease in secretion could have been overlooked in a larger decrease in absorption.

Secondly, bicarbonate unidirectional flux was not assessed. Agonist-induced net bicarbonate secretion using 40mM theophylline, which inhibits the degradation of cAMP, was abolished in diarrheic animals (277). Anionic I_{sc} is carried by both Cl^- and HCO_3^-, as HCO_3^- is preferentially transported through CFTR, BEST2, and BEST4 (249, 299, 332). Thus, if the previous authors' assumptions regarding unidirectional fluxes hold true, the decrease in anionic current I_{sc} reported herein could predominately result from a change in HCO_3^- transport. However, a decrease in the transport of HCO_3^- through the characterized transporters I report should also lead to decreased Cl^- transport from the

blood to the lumen, which would be in conflict with conclusion of the previous study (13, 277).

Additionally, previous studies did not take into account regional differences in anion transport which have been described in both rat and human colon (228, 237). Thus, if only one segment of the colon was sampled the results of the current study may have differed due to the anatomical location that colonic samples were taken from. However, analyses of I_{sc} measurements in Ussing chambers revealed that anionic I_{sc} was decreased similarly in all colonic segments of diarrheic pigs infected with *Brachyspira hyodysenteriae* and *Brachyspira hampsonii* strain 30446.

None-the-less, these findings combined with previous conclusions indicate that diarrhea caused by *Brachyspira hyodysenteriae* infections is unlike the diarrhea caused by enteropathogenic *E.coli*'s heat labile and heat stable enterotoxins, and *Vibrio cholerae*'s cholera toxin and NAG-stable toxin that cause excessive Cl^- and HCO_3^- loss (56, 108, 316). The presented study adds to this assertion by confirming a lack of cAMP driven Cl^- and HCO_3^- loss through apical chloride channels. However, the decreased electrogenic anionic secretory response favours mucus thickening and reduced clearance, promoting *spirochete* colonization and growth.

3.4.1 *Decreased channel expression correlates with a decrease in I_{sc}*

Diseases such as inflammatory bowel disease, cystic fibrosis, and models of intestinal inflammation have been associated with decreased anionic secretion, however, not all are due to a decrease in mRNA channel expression (11, 16, 92, 111, 138, 197, 232, 271). In the present study, the decrease in agonist-induced I_{sc} correlated

with a decrease in anion channel expression. Apical Cl^- channels (CFTR, TMEM16A) were found to have decreased gene transcripts or protein expression in the colon explaining the decrease in I_{sc}. The exception to this is BEST2 throughout the colon of diarrheic pigs infected with *Brachyspira hyodysenteriae* and *Brachyspira hampsonii* strain 30446. This overall decrease in anionic secretory function in the colon would be beneficial to the pathogen as a decrease in anionic secretion causes mucus stagnation allowing for greater colonization of *Brachyspira* species and prolonged inflammation (114).

3.4.2 *Increase or no change in channel expression results in a decrease in I_{sc}*

Elevated expression of BEST2 would also favour the altered colonic mucin environment in diarrheic animals. BEST2 is activated by calcium, and expressed on the basolateral membrane of goblet cells with a high permeability to HCO_3^- (332). Given that previous work demonstrated that diarrheic pigs infected with *Brachyspira hyodysenteriae* had an abundance of goblet cells in their colonic epithelium compared to controls, an increase in BEST2 expression is not unexpected (251). This is likely driven by the host's inflammatory response, as cytokines have been shown to differentiate epithelial cells to goblet cells (242, 301). This increased goblet cell population would increase the number of BEST2 channels on the basolateral membrane of the mounted epithelial tissue in the Ussing chamber. This, in turn, would increase the calcium-activated cholinergic induced basolateral entry of bicarbonate into mucin-secreting goblet cells. However, human and mouse goblet cells do not express CFTR suggesting that BEST2 works in concert with the electroneutral Cl^--HCO_3^-

exchanger SLC26A3 (332). Thus, an increase in BEST2 expression would not affect the observed I_{sc}.

TMEM16A, an epithelial, apically located calcium-activated anion channel, had no significant change in mRNA expression when compared to control in all three colonic segments of diarrheic pigs. Paradoxically, the cholinergic calcium-activated I_{sc} was significantly inhibited in all segments of diseased colon samples. Given the apical location of TMEM16A, one would expect no change in I_{sc} in the proximal, apex and distal segments of the colon. One explanation could be the down-regulation of CLCA1 and CLCA4 in all colon segments infected with *Brachyspira* species. CLCA1 has been reported to stabilize TMEM16A on the cell surface, thus increasing surface expression which results in activation of calcium-activated I_{sc} (269). TMEM16A protein expression was significantly reduced in all colonic segments of diarrheic pigs infected with *Brachyspira*. These findings suggest that the decreased expression of CLCA1 could be responsible for the decrease in calcium-activated I_{sc} generated by TMEM16A by protein destabilization. This demonstrates the importance of CLCA1 for proper function of TMEM16A in colonic tissue. Alternatively, a possible mechanism is that these *Brachyspira* species can inhibit the translation of channel mRNA to functional protein by a yet to be determined mechanism.

Although it is clear that changes in expression of anion channels and transporters are responsible in part for the decrease in anionic I_{sc}, it is not clear how *Brachyspira* induces these changes. *Brachyspira* infections appear to inhibit both transcriptional and translational processes. Part of the mechanism by which *Brachyspira* species accomplish this could be by altering of the host's cytokine responses, as

previous work has demonstrated strong cytokine regulation of ion channels (67, 132, 137, 258, 293).

3.4.3 *Cytokines known to regulate anionic secretion do not account for the decrease in I_{sc}*

TNF-α and IFN-γ can cause decreased functionality of CFTR, calcium-activated Cl^- channels, and NKCC1 in human intestinal epithelial cells after 48-hour exposure *in vitro* (67, 132, 258). TNF-α and IFN-γ down-regulate mRNA expression of CFTR, however, this is at a post-transcriptional level since these cytokines do not affect transcription rate (31, 221). Collectively, this post-transcriptional effect occurs by destabilizing CFTR mRNA (31, 221). However, the present study demonstrated decreased or no change in TNF-α and IFN-γ mRNA expression compared to control.

IL-1β has dose-dependent effects on CFTR mRNA and protein expression in human colonic T84 cells *in vitro* (44). Exposure of IL-1β to T84 cells at concentrations between 0.25-0.5ng/ml for 4 hours resulted in increased CFTR mRNA and protein expression (44). In contrast, cells exposed to IL-1β at concentrations of $\geq$1ng/ml significantly down-regulated CFTR mRNA and protein expression (44). In the present study, IL-1β mRNA expression was significantly up-regulated only in the distal segment of diarrheic pigs which does not account for the decrease in cAMP-induced I_{sc} in the proximal and apex segments of pig with diarrhea.

Alternatively, some of the effect may be mediated through lower initial tissue levels of cAMP prior to agonist addition, as previously observed (277). Pro-inflammatory cytokines are responsible for an increase in the expression of the PTGS2 mRNA and

the functional enzyme required for the synthesis of prostanoids (65). Prolonged *in vitro* exposure of Calu-3 cells to IL-1β displayed a significant decrease in cAMP accumulation and secretion of Cl^- in response to PGE_2 (64). This effect was accompanied by PTGS2 induction and was abolished when the cells were treated with specific PTGS2 inhibitors (64). The mechanism by which this occurred was mediated by down-regulation of EP_4 prostanoid receptors and adenylyl cyclase (64). This mechanism may partly explain the lower levels of cAMP found in the colonic epithelium of diarrheic pigs infected with *Brachyspira hyodysenteriae* (277). Collectively, it appears that long-term exposure to IL-1β impairs cAMP and Cl^- responses via an autocrine loop involving PTGS2 induction. Thus, elevated expression of IL-1α and IL-1β would increase expression of PTGS2 and explain the decrease in cAMP-activated I_{sc} observed in diseased colon samples. However, in the present study, tissues were stimulated with isoproterenol, a β_2 adrenergic agonist. Unlike the EP_4 receptor, the β_2 adrenergic receptor is up-regulated by IL-1β (64). Thus, any tissue deficiencies in cAMP would likely be negated by increased receptor activation and cAMP production. Thus, it would seem that a decrease in initial tissue cAMP concentration does not account for the decreased cAMP channel activation.

TGF-β1 is a strong negative regulator of both CFTR and TMEM16A by reducing channel mRNA and protein expression in colonic and airway epithelial cell lines (137, 293). Down-regulation of CFTR was attributed to TGF-β1 activation of p38 MAPK, while activation of pSmad-2/3 contributed to the down-regulation of TMEM16A (293). In my study, however, mRNA expression of TGF-β1, TGF-β2, and TGF-β3 was down-regulated or unchanged in diarrheic pigs compared to controls. Therefore, the

expression of TGF-β does not account for the decreased anion channel mRNA and protein expression in diarrheic pigs infected with either *Brachyspira* species investigated.

3.4.4 *IL-1α is not responsible for the decrease in CFTR mRNA expression*

In the colon of diarrheic pigs infected with *Brachyspira hyodysenteriae* and *Brachyspira hampsonii,* only IL-1α was significantly upregulated in each of the three colonic segments sampled. IL-1α has previously been shown to cause an increase in I_{sc} in rabbit ileum within 30-minutes of exposure to 5ng/ml (50, 58). Furthermore, myofibroblast cells preincubated with IL-1α significantly elevated I_{sc} in acutely juxtaposed T84 monolayers (131). However, the increase in I_{sc} in all cases was attributed to elevated expression of PTGS1 and PTGS2 resulting in elevated production of PGE_2. To determine if IL-1α has concentration-dependent effects on modulating CFTR mRNA expression like IL-1β I exposed polarized Caco-2 monolayers to high levels of human recombinant IL-1α for 24hrs (44). However, my findings do not support the hypothesis that high concentrations of IL-1α have an effect on modulating CFTR mRNA expression in Caco-2 cells. However, IL-1α exposure did elevate PTGS2 mRNA expression in Caco-2 cells confirming that IL-1α had a biological effect. These findings suggest that the decrease in electrogenic I_{sc} and decrease in anion channel mRNA in *Brachyspira* diseased pigs is not attributed to the host's cytokine response. Given these findings, it is more likely that *Brachyspira* spp. are able to inhibit transcriptional and translational processes directly or by the aid of a toxin (49).

3.4.5 *Brachyspira hampsonii lysate down-regulates CFTR mRNA in Caco-2 monolayers*

To determine if a bacterial component of *Brachyspira* was capable of directly modulating CFTR mRNA expression in Caco-2 cells, polarized Caco-2 monolayers were exposed to different concentrations (0.005-50µg/ml) of *Brachyspira hampsonii* lysate for 48hrs. My findings revealed that the bacterial lysate caused a significant decrease in CFTR mRNA expression following lysate exposure at concentrations of 5 and 50µg/ml. Furthermore, a significant increase in IL-1α expression was observed at a lysate concentration of 50µg/ml while IL-1β remained unchanged compared to control. As IL-1α was the only cytokine significantly upregulated in the colon of diarrheic pigs and is not responsible for the down-regulation of CFTR mRNA expression, my research points to a direct effect of the bacteria. This is not the first report of a direct effect caused by *Brachyspira*, as live *Brachyspira hyodysenteriae* exposed to neutrophil elastase resulting in degradation of membrane proteins caused elevated mucin production and mucin transport rates in HT29 MTX-E12 cells (252). This finding along with my current research demonstrates that the destruction of *Brachyspira* releases a bacterial component that results in a direct modification of cellular processes, specifically those that aid in modifying the colonic mucus environment.

3.5 Conclusion

Brachyspira hyodysenteriae and *Brachyspira hampsonii* strain 30446 evoke a decreased electrogenic anionic secretory response in experimentally infected, diarrheic animals, primarily accomplished by decreasing the expression of anionic channels and transporters. This decrease in the anionic secretory response supports the altered

mucin environment observed in diarrheic pigs. These *Brachyspira* spp. induce a strong IL-1α inflammatory response throughout the colon, however, IL-1α was not responsible for the decrease in CFTR mRNA expression. However, exposure of Caco-2 monolayers to a *Brachyspira hampsonii* lysate resulted in down-regulation of CFTR and upregulation of IL-1α gene transcripts. Additionally, loss of ion channel protein TMEM16A throughout the colon without any change in gene expression suggests that these two bacteria can directly impair transcription and translation of ion channels. I present strong evidence for a decrease in blood to lumen movement of anions in diarrheic animals which supports mucus thickening and stagnation favouring spirochete colonization. These findings add new insight into the pathophysiological mechanisms in the development of an altered mucin environment during spirochetosis.

Chapter 4 - Impairment of Electroneutral Na^+ Transport and Associated Down-Regulation of NHE3 Contributes to the Development of Diarrhea Following *in vivo* Challenge with *Brachyspira* spp.

Cole B. Enns[1], John C.S. Harding[2], Matthew E. Loewen[1b]

1. Department of Veterinary Biomedical Sciences, 2. Department of Large Animal Clinical Sciences, Western College of Veterinary Medicine, University of Saskatchewan. 52 Campus Drive. Saskatoon, Saskatchewan, Canada S7N 5B4

Author Contributions

C.E., J.H., and M.L. conceived and designed research; C.E., J.H., and M.L. performed experiments; C.E. analyzed data; C.E. and M.L. interpreted results of experiments; C.E. prepared figures; C.E. and M.L. drafted manuscript; C.E., J.H., and M.L. edited and revised manuscript; C.E., J.H., and M.L. approved final version of manuscript.

*This manuscript has not yet been submitted for publication.

*See Appendix for Descriptive Materials & Methods.

The effects of *Brachyspira hyodysenteriae* and *Brachyspira hampsonii* spirochetosis on Na^+ transport was assessed in the colon to determine its contribution to diarrheal disease, in pigs following experimental infection. Electrogenic and electroneutral Na^+ absorption was assessed in Ussing chambers by radiolabelled ^{22}Na flux and pharmacological inhibitory studies. Basal radiolabelled ^{22}Na flux experiments revealed that J_{ms} was significantly impaired in *B. hyodysenteriae* and *B. hampsonii* diseased pigs. Inhibition of J_{ms} by amiloride was significantly reduced in diseased pigs. This impairment of J_{ms} was not due to changes in electrogenic Na^+ absorption via ENaC. Inhibition of electrogenic short-circuit current (I_{sc}) through ENaC via amiloride in the proximal, apex, and distal colonic segments of diseased pigs were not different from control, suggesting that electroneutral Na^+ absorption is responsible for diarrheal development. These findings were further supported by significant down-regulation of Na^+/H^+ exchanger (NHE1, NHE2, and NHE3) mRNA expression in the proximal, apex and distal colonic segments paired with decreased protein expression of the critical NHE3 isoform. The decrease in NHE3 mRNA expression was not attributed to the host's cytokine response as human IL-1α did not modify NHE3 mRNA expression in Caco-2 cells. However, a whole cell *Brachyspira hampsonii* lysate significantly down-regulated NHE3 mRNA expression in Caco-2 cells. Together these findings provide mechanism for the spirochete induced malabsorptive diarrhea, supported by a decrease in electroneutral Na^+ absorption in the porcine colon due to *Brachyspira's* ability to inhibit NHE3 transcription, driving diarrheal disease.

4.1 Introduction

Electroneutral Na^+/ H^+ exchange is responsible for developing the osmotic drive for fluid absorption along the gastrointestinal tract of mammals. Inhibition of this exchange process has been shown to contribute to diarrheal disease caused by multiple enteric pathogens. However, the effect of the colonic spirochete *Brachyspira* on the electroneutral exchange has not been determined. In humans, colonic spirochetosis is caused by *B. pilosicoli* and *B.* aalborgi (206, 307). In swine, *B. hyodysenteriae* and emergent *Brachyspira hampsonii* cause severe spirochetosis, causing production limiting diarrhea accompanied by varying amounts of fecal blood and mucous (49, 121, 266).

Studies assessing the effect of *Brachyspira* spp. on solute transport have been limited to the swine isolate *B. hyodysenteriae*. *B. hyodysenteriae* has been described as causing malabsorptive diarrhea (13, 277). Ligated colonic loop experiments were utilized to determine the effects on Na^+ and Cl^- transport (13, 277). The authors concluded that *B. hyodysenteriae* abolished the absorptive capacity of the porcine colon while having no effect on secretion (13, 277). However, these studies were performed using a version of the Berger and Steele equation, and nonlinear changes in net electrolyte movement would lead to misinterpretation of the results (13, 28, 277). Additionally, the transporters that would need to be altered to produce this response were not assessed.

The absorptive capacity of the epithelium affected by *Brachyspira* spp. is greatest in the porcine spiral colon which can be divided into the proximal, apex and distal segments. Absorption of Na^+ and Cl^- by the colonic epithelium is primarily

transported by electroneutral Na^+/H^+ (NHE) exchangers found in all three segments (181). The remaining Na^+ absorption is electrogenic and is due to absorption through luminal ENaC which is predominantly expressed in the distal colon (246).

Na^+/H^+ exchangers (NHE) are electroneutral cation exchangers in which a single extracellular Na^+ is exchanged for a cytosolic H^+. NHE isoforms 1-3 are predominantly expressed in intestinal epithelia with NHE2 and NHE3 predominantly expressed on the apical surface of epithelial cells in the ileum and colon (4, 35, 135). NHE1 is localized to the basolateral membrane of epithelial cells and plays an important role in the regulation of cellular pH (35). NHE3 is essential for Na^+, and water absorption in the gastrointestinal tract as NHE3 knockout mice suffered from chronic diarrhea (280). The NHE2 knockout mouse model, however, did not result in diarrhea, suggesting that NHE3 is responsible for the majority of Na^+ absorption and water homeostasis in the gastrointestinal tract (279). Furthermore, electroneutral Na^+ absorption is inhibited by bacterial pathogens such as *S. typhimurium*, *V.* cholerae, and *Campylobacter jejuni* that cause an increase in intracellular Ca^{2+}, cAMP and/or cGMP, inhibiting NHE2 and NHE3 (113, 153, 165, 292). Whereas enteropathogenic *E. coli* (EPEC) infections significantly downregulate NHE3 activity while NHE1 and NHE2 are stimulated in response to the infection *in vitro* however, diarrhea ensues (126).

ENaC is a luminal Na^+ channel responsible for the electrogenic absorption of Na^+ in the distal colon (99, 274). The channel is made up of three homologous subunits α, β, and γ (42). Its function is regulated by mineralocorticoids and glucocorticoids such as aldosterone which have been shown to upregulate mRNA of ENaC's β and γ-subunits.

Here I characterized the pathophysiological effects of *Brachyspira hyodysenteriae* and *Brachyspira* hamposonii on Na^+ absorption in the porcine colon. Electrogenic and electroneutral Na^+ absorption via ENaC and NHE isoforms was assessed in the porcine colon in Ussing chambers. A decrease in electrogenic Na^+ absorption was not observed. However, electroneutral radiolabelled ^{22}Na flux revealed that J_{ms} Na^+ transport was significantly reduced. These findings along with a decrease in NHE isoforms 1-3 mRNA and reduced NHE3 protein expression support a reduction in the ability of the porcine colon to absorb Na^+ during *Brachyspira* diarrhea. Loss of NHE3 gene transcripts was not attributed to the host's cytokine response as IL-1α (Chapter 3)(322) did not reduce NHE3 mRNA expression in Caco-2 cells. However, a whole cell *Brachyspira* lysate significantly reduced NHE3 mRNA expression in Caco-2 cells after 48hrs of exposure. These findings suggest that *Brachyspira* either directly or by aid of a secreted toxin are able to inhibit ion channel transcriptional processes resulting in diarrheal disease.

4.2 Materials & Methods

4.2.1 *Animals*

Thirty 6-8 week-old purebred Yorkshire barrows were housed in pairs with 10 pigs per room and provided an antibiotic-free diet with water *ad libitum*. Treatment groups were each housed in separate BSL2 animal care rooms. Pigs acclimated to their new environment for 7 days before they were inoculated with either *Brachyspira hyodysenteriae* strain G44 (kindly provided by Boehringer-Ingelheim Vet Medica, St. Joseph, MO; n=10), *Brachyspira hampsonii* strain 30446 (n=10) or a mock inoculum of sterile culture media (n=10). Feeders were removed from the pens 12 hours prior to inoculation, but water was not. Inoculation was conducted by passing a stomach tube

and flushing 30ml of 10^8-10^9 cells/ml inoculum into the stomach of a pig, followed by sterile PBS as previously described (266). Pigs were assessed daily for clinical signs of diarrhea, and fecal consistency-scores were taken twice a day to accurately determine the onset of diarrhea. *Brachyspira* challenged pigs developed diarrhea within 3-7 days post inoculation and were euthanized 24 hours after the onset of diarrhea. Control pigs remained healthy (non-diarrheic) and were euthanized on an age-matched basis with *Brachyspira* challenged pigs euthanized the same day. This research was designed and conducted in accordance with the Canadian Council for Animal Care and approved by the University of Saskatchewan Committee on Animal Care and Supply (Protocol #20130034).

4.2.2 *Electrogenic Ussing chamber studies*

Following euthanasia, 17-18 cm segments of proximal (2.5 cm distal of the cecum), apex of the spiral colon (midpoint between cecum and sigmoid colon) and distal (sigmoid colon) were collected and washed with Krebs buffer (pH 7.4) containing (in mM) 113 NaCl, 5 KCl, 1.6 Na_2HPO_4, 0.3 $NaH_2PO_4 \bullet H_2O$, 25 $NaHCO_3$, 1.1 $MgCl_2 \bullet 6H_2O$, 2.2 $CaCl_2 \bullet 2H_2O$ and 10 glucose, and chilled to 4ºC as previously described (61). Samples were immediately transported back to the lab in Krebs buffer gassed with 95% O_2 - 5% CO_2.The colonic segments were then stripped with forceps by removing the serosa (visceral peritoneum) and the longitudinal/circular muscle layers of the intestinal wall, leaving only the submucosal elements, and the epithelium as previously described (61). The stripped tissues (4 tissue replicates of each segment per pig) were then places on 1cm^2 tissue Ussing chamber inserts and inserted into the Ussing chamber (Physiologic Instruments, San Diego, CA). Each reservoir was

independently gassed with 95% O_2-5%CO_2. A heated circulating water bath warmed and maintained the buffer temperature within the Ussing chamber to 37ºC. Transepithelial potential differences were short-circuited to 0 mV with a voltage clamp on the apical and basolateral chambers using Ag-AgCl electrodes and 3M KCl agar bridges as previously described (61).

Tissues were allowed to equilibrate for twenty minutes before the addition of amiloride. Tissues were pulsed every 30 seconds with a 1 mV pulse, and the resulting current was used to determine tissue resistance. After the equilibration period, a 0.1mM (final conc.) amiloride (A7410; Sigma Aldrich) was added to the apical side of the Ussing chamber, selectively inhibiting ENaC.

4.2.3 *Characterization of electroneutral absorptive response in healthy and infected porcine colon ^{2} ^{2}Na flux study*

The apex of the spiral colon was collected following euthanasia and samples were prepared according to the protocol described above in the *Electrogenic Ussing Chamber Studies* section. Once the colon tissues were inserted into the Ussing chambers, short-circuit current was recorded, and two tissues were paired with one another. The tissues were recorded for twenty minutes before the addition of ^{22}Na to reach a steady state current. 1 µCi of ^{22}Na (PerkinElmer, Waltham, MA) was added to the apical side of chamber #1, and 1 µCi was added to the basolateral side of chamber #2. The side of the chamber that ^{22}Na is added too is referred to as the “hot side” and the opposing side is referred to as the “cold side”. After the addition of ^{22}Na, 100µl samples were removed from the hot side of both chambers immediately and placed in glass vials. The 100µl removed from the Ussing chamber was immediately replaced

with 100µl of fresh Krebs buffer. Samples (500µl) were removed from the cold side of both chambers and placed in glass vials and once again replaced with 500µl of fresh Krebs buffer. Samples (500µl) were removed from the cold side for the first 80 minutes for steady-state flux to be achieved.

At 80 minutes 0.1mM (final conc.) amiloride (A7410; Sigma Aldrich) was added to the apical side each tissue in the Ussing chamber. Amiloride, a potent inhibitor of luminal ENaC (276) and NHE isoforms 1 and 2 (100, 200, 239) was selectively used to assess the impact that *Brachyspira hyodysenteriae* and *Brachyspira hampsonii* strain 30446 have on Na^+ transport *in vivo*. Cold samples were removed in five-minute intervals for a total time of 20 minutes following the addition of amiloride. All samples collected were counted on a Titertek Plus Series gamma counter.

Cold samples were used to calculate unidirectional mucosal-to-serosal (J_{ms}), serosal-to-mucosal (J_{sm}) and net flux ($J_{net} = J_{ms} – J_{sm}$) for ^{22}Na as previously described (281). Positive net flux values indicate net absorption while negative values indicate net secretion of the isotope.

4.2.4 *RT-qPCR analysis of ion channel and transporter mRNA expression*

Mucosal samples taken at the time of necropsy were stored in RNAlater® (AM7021; Ambion®) and homogenized in 1ml of TRIzol reagent (15596018; Life Technologies) and RNA extracted according to the manufacturer's protocol. A standard of <500ng/µl was used as exclusion criteria for RNA samples.

cDNA was created from mRNA using the Go Script Reverse Transcription system (A5001; Promega) according to manufactures protocol. cDNA was diluted in

RNase-free water and frozen at -80˚C. Gene expression was assessed by RT-qPCR using GoTaq qPCR Master Mix (A6002; Promega) and Stratagene Mx5000P real-time qPCR machines according to manufactures protocol. The average C_T (cycle threshold) value was used to calculate the fold difference of each gene using the ΔΔCt calculation method. Porcine primers were designed for GAPDH, NHE1, NHE2, NHE3, ENaC-α, ENaC-β and ATP1A1 (Table 4.1). Porcine GAPDH was used as the reference gene for the analysis. Human primers were designed for GAPDH, NHE2, NHE3, and PTGS2 (Table 4.2). Human GAPDH was used as the reference gene for the analysis.

4.2.5 *Western blot analysis of NHE3*

Protein was extracted from control and diarrheic pigs from the apex segment of the colon using the ProteoExtract transmembrane protein kit (71772-3; Novagen®) according to manufactures protocol. Samples were boiled in 2x denaturing buffer (20% glycerol, 4% SDS, 125 mM Tris pH 6.8, 0.3 mM bromophenol blue) containing 10% β-mercaptoethanol (BME; M6250; Sigma-Aldrich) for five minutes and analyzed by 10% SDS-PAGE (286).

For western blot analysis, proteins were transfered onto PVDF membranes (RPN303LFP; GE Healthcare Life Sciences) at 0.2mA for 4 hours at 4ºC with transfer buffer (25mM Tris, 192mM glycine, 20% methanol) (286). Membranes were blocked for 1 hour at room temperature with a 10% RapidBlock™ (M325-AMRESCO®) blocking solution and subsequently probed overnight at 4ºC with primary antibodies anti-NHE3 (ARP43870_P050; AVIVA Biosciences) anti-β-Actin (C-4; sc-47778; Santa Cruz Biotechnology) in a 10% RapidBlock™ solution. The membranes then incubated for 1

Table 4.1. Porcine primer sequences for RT-qPCR

Gene Name	Forward (5'-3')	Reverse (5'-3')
GAPDH	ACATCAAGAAGGTGGTGAAGCAGG	TGAGCTTGACGAAGTGGTCGTTGA
NHE1	CAGAGGACTGCTTCCACAAA	CAAAGTGAGACCTGGGACATAG
NHE2	GGCAGAGACTGGGATGATAAG	TCGCTGACGGATTTGATAGAG
NHE3	GGTGCTCTTCATCATCGTCTTC	CCAGCGTCACGAAAGATTCA
ENaC-α	TGCACTGGGCAAATTCATCTTCGC	ACATCCAGAGGTTGGAGCTGTTCT
ENaC-β	TCTTCCACCCGGATTATGGCAACT	ATGTCCAGGATCAACTTCAGGCC
ATP1A1	TGTGAAGAACTTGGAGGCTGTGGA	TGGCCGAAGTCTTGTCGAATGAGA

Table 4.2. Human primer sequences for RT-qPCR

Gene Name	Forward (5'-3')	Reverse (5'-3')
GAPDH	CAAGGTCATCCATGACAACTTTG	GGGCCATCCACAGTCTTCTG
NHE2	CCGATTTGGGAGTGAGAAG	CGCCCTCCAGAAGTATTTAG
NHE3	GAGACAAGGTCAAGGAGAAG	GAGAGGATGTGGTCGAAAG
PTGS2	GAAGCCTTCTCTAACCTCTC	GGATCAGGGATGAACTTTCT

hour at room temperature with secondary antibodies Alexa Fluor 488 Goat anti-Rabbit IgG antibody (A-11008; Thermo Fisher Scientific) and ECL Plex Goat anti-Mouse IgG-Cy5 antibody (PA45009; Amersham Biosciences) in 10% RapidBlock™ solution. Proteins were subsiquently detected and analyzed using Typhoon Trio and ImageQuant TL System (63005583; GE Healthcare Life Sciences).

4.2.6 *Cell culture*

The Caco-2 cell line derived from human colorectal adenocarcinoma (HTB-37; ATCC, Manassas, VA) were cultured in Dulbecco's modified Eagle medium (DMEM) (10-0130CM, Corning, Manassas, VA) containing 10% heat-inactivated fetal bovine serum (Gibco, Burlington, ONT, Canada) Grand, 1% penicillin-streptomycin (15140-122; Life Technologies), and 1% MEM non-essential amino acids (Gibco, Grand Island, NY) at 37˚C in a humidified atmosphere with 5% CO_2. Cells were plated on polyester Transwell® permeable supports (0.4µm pores, 24 mm in diameter, Corning) and cultured under standard conditions until confluency. Cells were maintained for 10 days after confluency was achieved before being used in downstream experiments.

4.2.7 *Exposure of Caco-2 monolayers to recombinant human IL-1α*

To determine if the single pro-inflammatory cytokine that was significantly up-regulated throughout the colon of pigs infected with *Brachyspira hyodysenteriae* and *Brachyspira hampsonii* strain 30446 (Chapter 3) was responsible for the decrease in NHE3 mRNA expression *in vivo*, polarized Caco-2 monolayers were exposed to human recombinant IL-1α (I2778; Sigma Aldrich) and subsequently probed for changes in NHE2 and NHE3 mRNA expression by RT-qPCR. Both apical and basolateral surfaces

were exposed to IL-1α at concentrations of 10, 100 and 500 ng/ml for 24hrs. The Caco-2 cell line was chosen as no porcine colon-derived cell lines are commercially available. To ensure that IL-1α had a biological effect on Caco-2 monolayers, qPCR primers were developed for prostaglandin-endoperoxide synthase 2 (PTGS2) which has been previously shown to become up-regulated in multiple cell types after IL-1α exposure (58, 131, 259).

4.2.8 *Caco-2 monolayer exposure to Brachyspira hampsonii lysate*

To determine if *Brachyspira* has a direct effect on modulating ion channel expression I wanted to determine if a whole cell *Brachyspira* lysate was capable of down-regulating CFTR mRNA expression in Caco-2 cells. The *Brachyspira hampsonii* strain 30446 lysate was prepared by centrifuging 50ml of culture broth containing actively motile spirochete bacteria (10^8/ml) at 10,000 X *g* for 40 min, after which the supernatant was poured off (224). Bacterial pellets were resuspended in phosphate buffered saline (Gibco; 10010-023, Life Technologies) and vortexed until the pellet completely dissolved. This material was subsequently disrupted by sonication (Sonics & Materials Inc., Danbury, CT, USA) at 50% duty for 120 s at 4˚C (224). Lysate total protein concentrations were determined using BCA protein assay (ThermoFisher; Rockford, IL) using bovine serum albumin (BSA) as a standard according to the manufacture's protocol. Polarized Caco-2 monolayers were exposed apically to the whole cell *Brachyspira hampsonii* lysate (0.005-50µg/ml) in PBS or a PBS control for 48hrs. 50µg/ml of total bacterial protein was determined to be ~10^8 CFU/ml and considered a physiological concentration.

4.2.9 *Statistical analysis*

Data for electrogenic Ussing chamber studies, ^{22}Na Flux studies data was not normally distributed (Shapiro-Wilk test; $P < 0.05$) and is expressed as median ± interquartile range (IQR). Data obtained by RT-qPCR is expressed as mean ± standard error of the mean (SEM) (Shapiro-Wilk test; $P > 0.05$). Western blot data is normally distributed (Shapiro-Wilk test; $P > 0.05$) and expressed as mean ± SEM. Change in I_{sc} between diseased and control colon segments was analyzed by Kruskal-Wallis one-way analysis of variance. Changes in the rate of ^{22}Na transport was analyzed by Kruskal-Wallis one-way analysis of variance and Dunn's test. Fold changes in mRNA expression of diseased colonic segments compared to control obtained by RT-qPCR was log transformed (log10) and analyzed by one-way ANOVA and Tukey post-hoc. Western blot analysis of NHE3 protein was analyzed by Student's t-test (control vs. *Brachyspira* species in two separate analyses). Fold changes obtained by RT-qPCR for *in vitro* data was analyzed by Student's *t*-test. Significance was set *a priori* at $P < 0.05$.

4.3 Results

4.3.1 *Brachyspira hyodysenteriae and Brachyspira hampsonii reduce Na^+ absorption in the apex of the porcine spiral colon during ^{22}Na equilibration*

During the 80-minute ^{22}Na equilibration, diseased colon tissues had a significantly decreased unidirectional J_{ms} flux at all time points when compared to control ($P < 0.05$) (Figure 4.1A). Interestingly, at no point was there a significant difference in J_{ms} between bacterial strains. Additionally, at no point was J_{sm} ^{22}Na flux (Figure 4.1B) significantly different in *Brachyspira hyodysenteriae* infected tissues when compared to

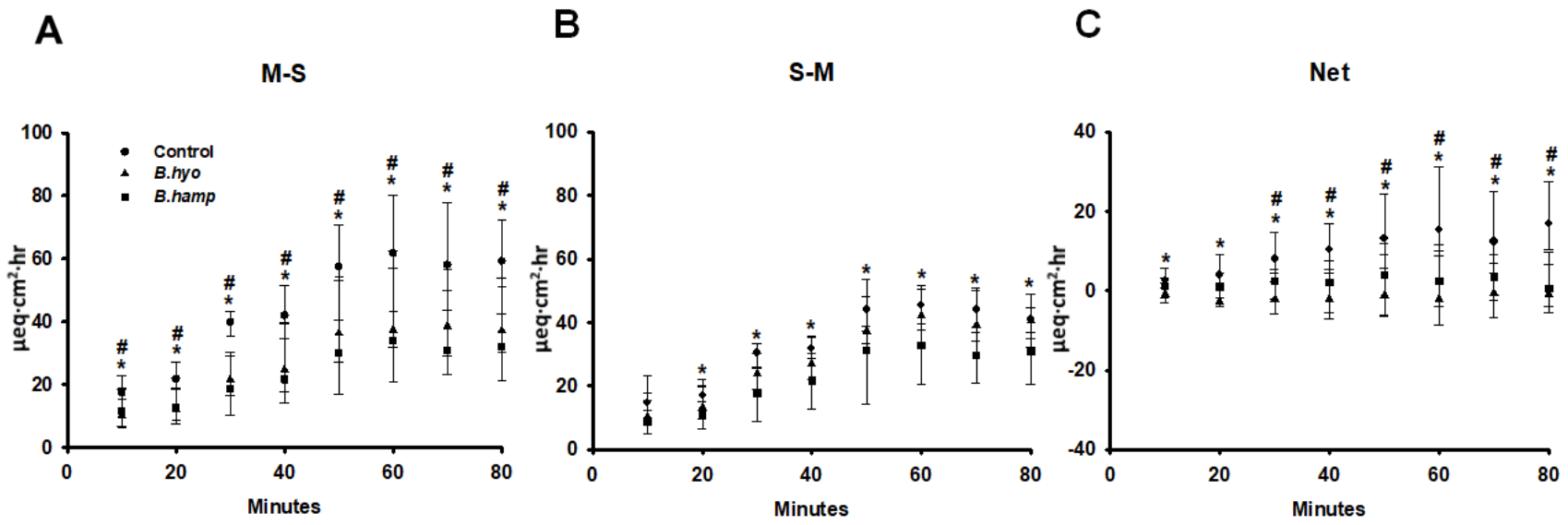

Figure 4.1. *Brachyspira hyodysenteriae* and *Brachyspira hampsonii* strain 30446 decrease basal J_{ms} and net Na^+ absorption during ^{22}Na equilibration in the apex of the porcine spiral colon.

Basal J_{ms} (A), J_{sm} (B), and net (C) flux rates during ^{22}Na equilibration across apex colonic segments from control, *B. hyodysenteriae*, and *B. hampsonii* diseased pigs. M-S, unidirectional mucosal-to-serosal ^{22}Na flux; S-M, unidirectional serosal-to-mucosal ^{22}Na flux; Net, net ^{22}Na flux. Data presented as median ± IQR, analyzed using Kruskal-Wallis one-way analysis of variance and Dunn's Post Hoc. Significant differences between control and *B. hyodysenteriae* are represented by * = $P < 0.05$; Significant differences between control and *B. hampsonii* are represented by # = $P < 0.05$. (n=12 ctrl, n=12 *B. hyodysenteriae*, n=12 *B. hampsonii* strain 30446).

control. However, a significant reduction in J_{sm} flux was observed in *Brachyspira hampsonii* strain 30446 infected tissues when compared to control ($P < 0.05$) after 20-minutes of fluxing. After 50-minutes of fluxing a significant difference in J_{sm} between *Brachyspira hampsonii* strain 30446 and *Brachyspira hyodysenteriae* ($P < 0.05$) developed. J_{net} revealed that control colonic tissues exhibited net Na^+ absorption during the equilibration period (Figure 4.1C). *Brachyspira hyodysenteriae* diseased tissues had a net secretory response at all time points during the equilibration and a significant difference ($P < 0.05$) compared to control was noted at only 10-minutes after the beginning of the equilibration period. *Brachyspira hampsonii* strain 30446 exhibited a different trend with a small rate of net Na^+ absorption. However, this rate was significantly less ($P < 0.05$) than the net absorption observed in control tissues and was not significantly different than the net secretion noted in tissues infected with *Brachyspira hyodysenteriae* (Figure 4.1C).

Overall the unidirectional J_{ms} flux suggests that diseased tissues have a reduced absorptive capacity when compared to control tissues. J_{sm} flux did not account for the decrease in net Na^+ absorption in diseased samples. Na^+ absorption in the colon is primarily due to the electroneutral movement of Na^+ and H^+ through NHEs and electrogenic absorption via ENaC. The unidirectional J_{ms} suggests that either one or both of these routes of absorption have been negatively altered contributing to malabsorptive diarrhea in experimentally challenged pigs.

4.3.2 *Brachyspira hyodysenteriae and Brachyspira hampsonii infections reduce electroneutral but not electrogenic Na^+ absorption in the porcine spiral colon*

Addition of amiloride to the mucosa of colonic tissues in Ussing chambers during ^{22}Na flux was used to inhibit Na^+ absorption. The maximal inhibitory effect on unidirectional J_{ms} flux in both control and diseased colon samples was observed 10-minutes after amiloride addition. However, the addition of amiloride resulted in a significantly greater decrease in flux rate in control tissues (-9.06 $\pm$ 6.77 $\mu eq \cdot cm^{-2} \cdot h^{-1}$) when compared to *B. hyodysenteriae* (-6.49 $\pm$ 6.64 $\mu eq \cdot cm^{-2} \cdot h^{-1}$) ($P < 0.05$) and *B. hampsonii* (-2.88 $\pm$ 5.92 $\mu eq \cdot cm^{-2} \cdot h^{-1}$) ($P < 0.05$) (Table 4.3). The unidirectional J_{sm} flux was similarly decreased in all tissues. Control tissues had a decreased J_{sm} flux rate (-7.45 $\pm$ 5.19 $\mu eq \cdot cm^{-2} \cdot h^{-1}$) compared to *B. hyodysenteriae* (-6.2 $\pm$ 11.78 $\mu eq \cdot cm^{-2} \cdot h^{-1}$) and *B. hampsonii* (-5.55 $\pm$ 5.53 $\mu eq \cdot cm^{-2} \cdot h^{-1}$) (Table 4.3). Indicating little change in paracellular movement of Na^+ and tight junction disruption between control and diarrheic pigs.

The electrogenic Na^+ absorptive capacity of the porcine spiral colon was measured in diseased and healthy colon segments in Ussing chambers, to determine its contribution to the reduction in ^{22}Na J_{ms} flux. The addition of amiloride to the mucosa of proximal, apex and distal colon segments revealed a decreased trend in inhibitable I_{sc} throughout all segments of diarrheic pigs however, no significant difference was noted when compared to control (Figure 4.2). It was noted, however, that electrogenic inhibitable I_{sc} via amiloride was greater in the distal colonic segment compared to the proximal. These data suggest that electrogenic Na^+ absorption throughout the colon is

Table 4.3. Effect of 0.1mM amiloride on unidirectional Na^+ fluxes across control, *B. hyodysenteriae*, and *B. hampsonii* infected colon.*

	J^{Na+} ($\mu eq \cdot cm^2 \cdot h$)					
	M-S			S-M		
	Basal	*Amiloride*	*Δ*	*Basal*	*Amiloride*	*Δ*
Control	59.32 ± 18.10	51.15 ± 21.19	-9.06[a] ± 6.77	40.94 ± 7.70	31.54 ± 10.64	-7.45[a] ± 5.19
B. hyo	37.15 ± 22.53	34.37 ± 20.53	**-6.49[b] ± 6.64**	40.62 ± 15.11	34.41 ± 21.45	-6.20[a] ± 11.78
B. hamp	31.95 ± 19.53	26.22 ± 13.02	**-2.88[b] ± 5.92**	30.86 ± 16.43	23.75 ± 11.89	-5.55[a] ± 5.53

*Values represent medians ± IQR, analyzed using Kruskal-Wallis one-way analysis of variance and Dunn's Post Hoc. Change in ^{22}Na flux rate (*Δ*) 10-minutes after the addition of amiloride. *Δ* values for *B. hyodysenteriae* and *B. hampsonii* diseased tissues were compared to control and significant differences ($P < 0.05$) are marked with a different superscript. Significantly different values are marked in bold. M-S, mucosal-to-serosal; S-M, serosal-to-mucosal. (n=12 ctrl, n=12 *B. hyodysenteriae*, n=12 *B. hampsonii* strain 30446).

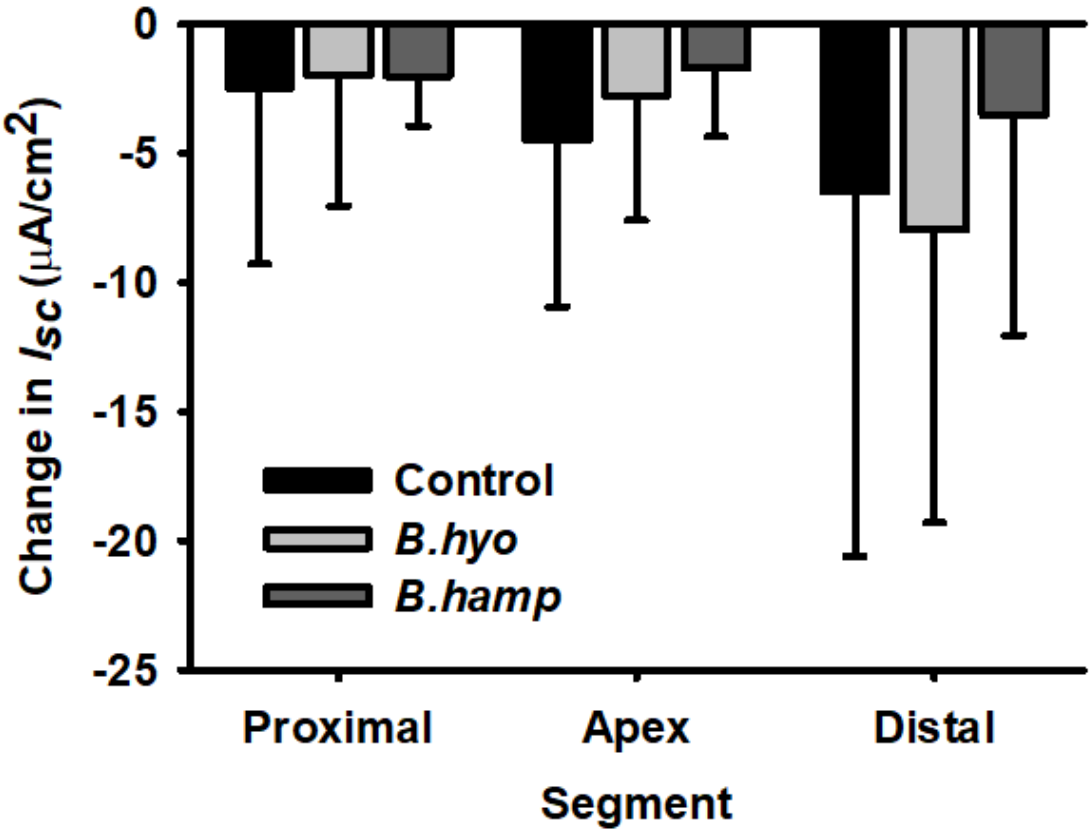

Figure 4.2. *Brachyspira hyodysenteriae* and *Brachyspira hampsonii* strain 30446 do no affect electrogenic Na^+ absorption through ENaC.

Change in I_{sc} in response to the addition of ENaC channel inhibitor amiloride in the proximal, apex, and distal colonic segments of control and diseased pigs. ENaC = epithelial sodium channel; I_{sc} = short-circuit current. Data presented as median ± IQR, analyzed using Kruskal-Wallis one-way analysis of variance. (n=18 ctrl, n=17 *B. hyodysenteriae*, n=16 *B. hampsonii* strain 30446)

not affected significantly in diseased animals, leading to the conclusion that the significant decrease in J_{ms} is due to loss of electroneutral Na^+ transport in the spiral colon of diarrheic pigs.

4.3.3 *RT-qPCR analyses of Na^+ channels and transporters*

Results from the ^{22}Na flux experiments indicated that unidirectional J_{ms} was significantly impaired in the apex of diarrheic pigs. To determine if these differences were attributed to altered Na^+ channel and transporter mRNA expression, colonic mucosal samples were analyzed by RT-qPCR. In diseased pigs down-regulation of NHE isoforms, 1-3 in the proximal, apex and distal colonic segments of diarrheic pigs experimentally challenged with *B. hyodysenteriae* and *B. hampsonii* further supports the decreased J_{ms}. NHE2 and NHE3 had significant reductions ($P < 0.05$) in mRNA transcripts when compared to controls in all three segments of the colon (Table 4.4). These two transporters have been shown to drive electroneutral Na^+ absorption and be involved in diarrheal disease (279).

In contrast, NHE1 is primarily localized to the basolateral membrane of epithelial cells and plays a key role in the regulation of cellular pH (35). NHE1 was down-regulated ($P < 0.05$) in the proximal, apex and distal segments of the colon in diarrheic pigs infected with *B. hyodysenteriae* and the apex and distal segments infected with *B. hampsonii* (Table 4.4). Loss of NHE1 mRNA and protein has been observed in colonic biopsies from patients with inflammatory bowel disease which has been suggested to be a contributing factor of the pathogenesis of the disease (164). Electrogenic Na^+ transporter ENaC had significant down-regulated mRNA expression of the channels α sub-unit ($P < 0.05$) in the apex of diarrheic pig infected with *B.*

Table 4.4. Fold changes in Na^+ channel and transporter mRNA expression in the porcine colon.*

	Segment of Porcine Colon								
	Proximal			Apex			Distal		
Ion Channel	Ctrl	*B. hyo*	*B. hamp*	Ctrl	*B. hyo*	*B. hamp*	Ctrl	*B. hyo*	*B. hamp*
NHE1	$2.15^a \pm 1.42$	**$0.27^b \pm 0.10$**	**$0.33^b \pm 0.08$**	$1.02^a \pm 0.11$	**$0.44^b \pm 0.11$**	**$0.47^b \pm 0.10$**	$1.76^a \pm 0.49$	**$0.51^b \pm 0.24$**	**$0.38^b \pm 0.08$**
NHE2	$1.30^a \pm 0.47$	**$0.38^b \pm 0.12$**	**$0.31^b \pm 0.06$**	$1.04^a \pm 0.13$	**$0.08^b \pm 0.01$**	**$0.18^b \pm 0.09$**	$1.42^a \pm 0.38$	**$0.26^b \pm 0.03$**	**$0.32^b \pm 0.11$**
NHE3	$1.16^a \pm 0.30$	**$0.11^b \pm 0.02$**	**$0.24^b \pm 0.04$**	$1.17^a \pm 0.36$	**$0.36^b \pm 0.11$**	**$0.28^b \pm 0.11$**	$1.33^a \pm 0.44$	**$0.29^b \pm 0.10$**	**$0.14^b \pm 0.04$**
ENaC-α	$1.49^a \pm 0.61$	$0.76^a \pm 0.29$	$0.38^a \pm 0.13$	$1.05^a \pm 0.17$	**$0.09^b \pm 0.04$**	**$0.03^b \pm 0.01$**	$1.59^a \pm 0.67$	$0.44^a \pm 0.10$	**$0.17^b \pm 0.05$**
ENaC-β	$1.45^a \pm 0.76$	$0.26^a \pm 0.06$	$2.32^a \pm 0.98$	$1.21^a \pm 0.31$	$0.47^a \pm 0.13$	$1.42^a \pm 0.28$	$1.61^a \pm 0.65$	$1.44^a \pm 0.18$	$2.66^a \pm 0.88$
ATP1A1	$1.36^a \pm 0.48$	**$0.21^b \pm 0.03$**	**$0.31^b \pm 0.06$**	$1.27^a \pm 0.45$	$0.57^a \pm 0.16$	$0.47^a \pm 0.09$	$1.48^a \pm 0.44$	$0.85^a \pm 0.12$	$0.60^a \pm 0.10$

*Fold changes in Na^+ channel and transporter mRNA expression in three segments (proximal, apex, distal) of the colon in control, *B. hyodysenteriae*, and *B. hampsonii* diseased pigs. Data presented as mean ± SEM of fold difference in gene expression measured by RT-qPCR. For each gene marked with a different superscript differ by at least $P < 0.05$ compared to control in each segment. NHE1 = Na^+/H^+ exchanger 1; NHE2 = Na^+/H^+ exchanger 2; NHE3 = Na^+/H^+ exchanger 3; ENaC-α = epithelial sodium channel subunit α; ENaC-β = epithelial sodium channel subunit β; ATP1A1 = ATPase Na+/K+ transporting subunit alpha 1. Significantly different values are marked in bold. (n=6 ctrl, n=6 *B. hyodysenteriae,* n=6 *B. hampsonii* strain 30446).

hyodysenteraie and the apex and distal segments of pigs infected with *B. hampsonii* (Table 4.4). ENaC's β sub-unit was unchanged from control in all three segments of colon when compared to control (Table 4.4). Previous findings have suggested that ENaC is capable of forming a functional channel capable of transporting Na^+ without all three subunits (123). Thus, down-regulation of ENaC's α sub-unit in diseased colonic samples may not translate to a decrease in amiloride inhibitable I_{sc}. Na^+/K^+- ATPase α1 subunit is responsible for the transport of three Na^+ out of the cell and two K^+ in, maintaining the cells osmotic balance (188). Its reduction could impact the ^{22}Na flux. However, Na^+/K^+- ATPase α1 expression was unaffected in all segments, except the proximal colon in diarrheic pigs infected with *B. hyodysenteriae* and *B. hampsonii* which was significantly down-regulated ($P < 0.05$) (Table 4.4). This finding indicates that the impaired ^{22}Na flux in the apex of diseased pigs is not due to changes in this transporter. Furthermore, the decrease in Na^+/K^+- ATPase α1 did not significantly affect electrogenic Na^+ transport via ENaC, indicating that the decrease in expression had a minimal effect on contributing to diarrheal development.

4.3.4 *Western blot analysis of NHE3*

Although all three NHE isoforms were down-regulated, previous studies have indicated that the NHE3 isoform is critical for Na^+ absorption in the gastrointestinal tract (280). Thus, western blot for NHE3 was performed to support inhibitor and RT-qPCR results for this vital transporter. NHE3 channel protein was significantly decreased in the apex of diarrheic pigs infected with *B. hyodysenteriae* ($P < 0.001$) and *B. hampsonii* ($P < 0.001$) when compared to control (Figure 4.3). The decrease in channel protein correlates with the decrease in mRNA expression of NHE3 and impairment of Na^+

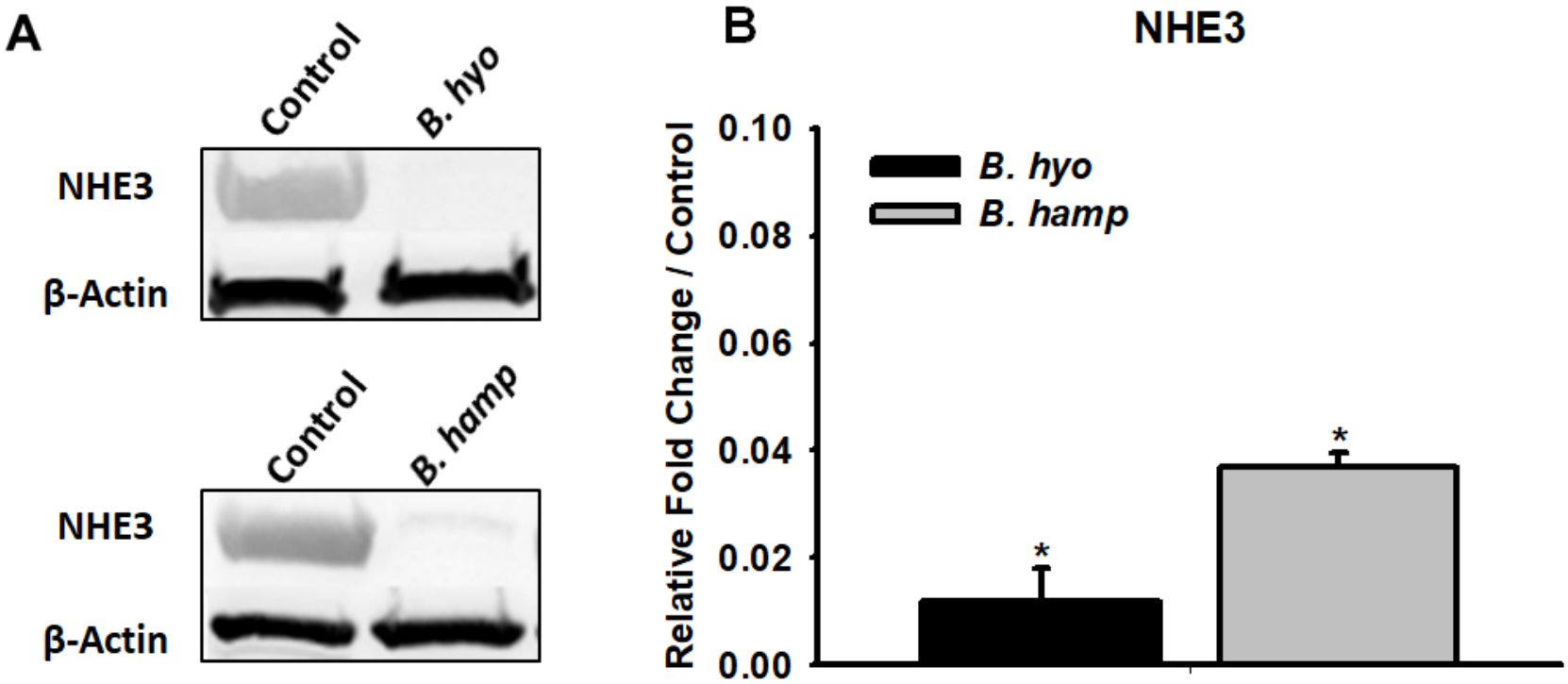

Figure 4.3. *Brachyspira hyodysenteriae* and *Brachyspira hampsonii* strain 30446 significantly reduce NHE3 protein expression in the apex of the porcine colon.

Western blot (A) and densitometry (B) of NHE3 (~93 kDa) compared to β-actin (~43 kDa) reference for *B. hyodysenteriae* and *B. hampsonii* strain 30446 infected apex porcine colon relative to control. NHE3 = Na^+/H^+ exchanger 3; β-actin = beta actin. Data presented as mean ± SEM, analysed using Student's *t*-test. * = $P < 0.05$ (n=3 ctrl, n=3 *B. hyodysenteriae,* n=3 *B. hampsonii* strain 30446)

absorption in the colon of *Brachyspira* infected pigs.

4.3.5 *IL-1α does not decrease NHE3 mRNA expression in polarized Caco-2 monolayers*

To investigate whether the up-regulation of IL-1α mRNA expression throughout the colon of diarrheic pigs which I have previously reported (Chapter 3) was responsible for the decreased expression of NHE3 mRNA, polarized Caco-2 monolayers were exposed to varying concentrations (10, 100 and 500ng/ml) of human recombinant IL-1α for 24hrs. RT-qPCR revealed that IL-1α had no effect on modulating NHE3 gene expression at any concentration when compared to control (Table 4.5). To ensure that IL-1α was biologically active in my model, PTGS2 mRNA expression assessed. IL-1α exposure has been shown to result in elevated PTGS2 mRNA expression in several cell types (58, 131, 259). I found that all monolayers independent of IL-1α concentration had a significant 2-fold increase in PTGS2 mRNA expression ($P < 0.05$) (Table 4.5).

4.3.6 *Brachyspira hampsonii lysate decreases NHE3 mRNA expression in polarized Caco-2 monolayers*

As IL-1α had no effect on NHE3 mRNA expression, I elected to test if a *Brachyspira* lysate was capable of directly altering NHE3 mRNA expression. Polarized Caco-2 monolayers were exposed to varying concentrations of lysate (0.005-50µg/ml) for 48hrs. My results revealed that a lysate concentration of 50µg/ml was capable of significantly down-regulating NHE3 expression ($P = 0.009$) compared to control (Figure 4.4A). My previous findings revealed that this *Brachyspira* lysate significantly upregulated IL-1α in exposed monolayers, recapitulating other cellular events observed

in vivo (Chapter 3). Together these findings provide evidence that loss of NHE3 mRNA transcripts is due to either a direct effect of the bacteria or by a toxin.

Table 4.5. Fold changes in NHE3 and PTGS2 mRNA expression in polarized Caco-2 cell monolayers after 24hr exposure to IL-1α.*

	Concentration of recombinant human IL-1α			
Gene Name	**Control**	**10ng/ml**	**100ng/ml**	**500ng/ml**
NHE3	$1.07^{a} \pm 0.18$	$1.48^{a} \pm 0.32$	$1.60^{a} \pm 0.49$	$1.28^{a} \pm 0.29$
PTGS2	$1.00^{a} \pm 0.07$	**$2.22^{b} \pm 0.23$**	**$2.41^{b} \pm 0.29$**	**$2.21^{b} \pm 0.21$**

*Fold changes in NHE3 and PTGS2 mRNA expression in polarized Caco-2 monolayers exposed to human recombinant IL-1α for 24hrs. Data presented as mean ± SEM of fold differences in gene expression measured by RT-qPCR. For each gene marked with a different superscript differ by at least $P < 0.05$ compared to control. PTGS2 data is duplicated from Table 3.7. NHE3 = Na^{+}/H^{+} exchanger 3; PTGS2 = prostaglandin-endoperoxide synthase 2. Significantly different values are marked in bold. (n=6).

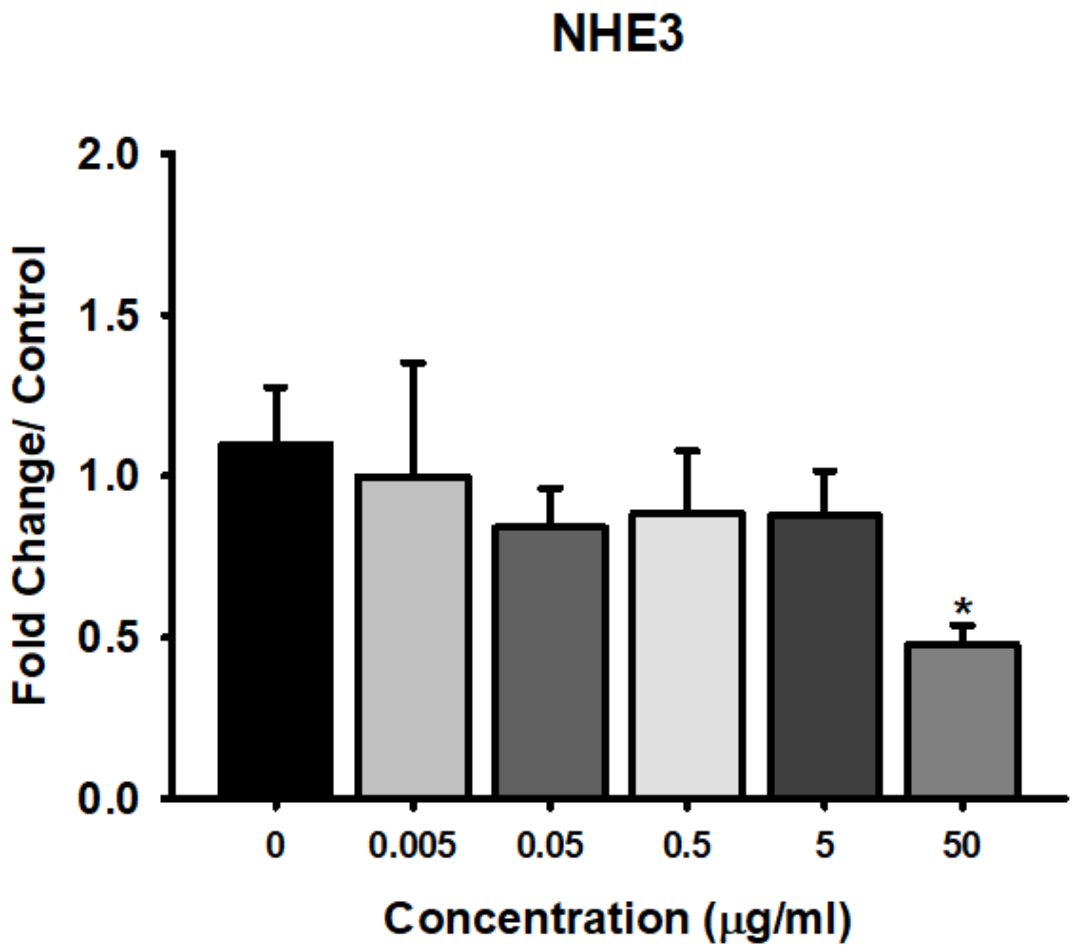

Figure 4.4. *Brachyspira hampsonii* strain 30446 lysate down-regulates NHE3 mRNA expression in Caco-2 monolayers.

Fold change in NHE3 mRNA expression compared to control as measured by RT-qPCR after exposure to a *Brachyspira hampsonii* strain 30446 whole cell lysate at five concentrations (0.005-50μg/ml) for a period of 48hrs. NHE3 = Na^+/H^+ exchanger 3. Data presented as mean ± SEM, analyzed using one-way ANOVA. * = $P < 0.05$. (n=6).

4.4 Discussion

Here I identify colonic electroneutral Na^+ absorption and associated genes as the cause of spirochete induced diarrheal disease caused by *B. hyodysenteriae* and *B. hamposonii*. Diarrhea in pigs caused by *B. hyodysenteriae* has been previously described as malabsorptive in which Na^+ and Cl^- absorption is abolished in diarrheic animals (13, 277). An increase in luminal anion secretion does not contribute to the development of diarrheal disease (13, 277)(Chapter 3). However, a decrease in agonist-induced anion secretion in diarrheic pigs experimentally challenged with *B. hyodysenteriae* and *B. hampsonii* throughout the colon, due to down-regulation of anion channel mRNA and protein, is thought to modify mucin properties and aid in the colonization and development of spirochetosis (Chapter 3). Furthermore, colonic permeability to mannitol and PEG-400 in the porcine colon remained unchanged, and transepithelial electrical resistances were not different from control, suggesting that tight junction integrity is not compromised (13) (Chapter 3). The pathophysiological mechanism of transporter and transporter regulation during spirochetosis causing malabsorptive diarrhea has not been characterized in any *Brachyspira* spp.

4.4.1 *Impairment of electroneutral Na^+ absorption contributes to diarrheal development*

The current study provides strong evidence supporting the loss of the Na^+ absorptive capacity of the colon in diarrheic pigs infected with *B. hyodysenteriae* and *B. hampsonii*. The ^{22}Na flux equilibration period further supports previous findings, by which J_{ms} is severely impaired in the colon of diseased pigs (13, 277). Furthermore, the significant decrease in amiloride inhibitable J_{ms} flux in pigs infected with *B.*

hyodysenteriae or *B. hampsonii* suggests a decrease in Na^+ channels and transporters on the mucosal surface. J_{sm} flux appears to be reduced in diarrheal animals but not significantly, leading to the conclusion that the loss of net Na^+ absorption in diarrheic pigs is attributed to a decrease in J_{ms} alone. Inhibition of electrogenic Na^+ transport via ENaC in Ussing chambers revealed that there was no significant difference in inhibitable current between control and diseased tissues. Therefore, these findings point to impairment of electroneutral Na^+ transport as the driving force responsible for the production of diarrhea in *Brachyspira* diseased pigs.

Gene transcripts of colonic samples taken from diarrheic pigs revealed that electroneutral Na^+ transporters NHE isoforms 1-3 were significantly down-regulated when compared to control throughout the three segments of the colon. Loss of NHE3 in a complete *Slc9a3*$^{-/-}$ mouse model resulted in mild diarrhea, enlargement of the gastrointestinal tract, increase in GI-contents, and a decrease in pH in the colon relative to the cecum (279). Interestingly, NHE2 knockout (*Slc9a2*$^{-/-}$) mice showed no changes in acid-base homeostasis or disruptions in electrolyte absorption suggesting that the NHE3 isoform is of greater importance in the gastrointestinal tract (279). Significant down-regulation of NHE3 protein expression in the apex of diarrheic pigs further supports the conclusion that impairment of electroneutral Na^+ absorption is responsible for the development of diarrhea.

During diarrheal episodes, chronic stimulation by mineralocorticoids elicits the expression of ENaC throughout the colon and into the ileum to help mitigate fluid and electrolyte loss (279, 324). This compensatory mechanism appears not to be present in diarrheic pigs suffering from *Brachyspira* colitis. Interestingly, ENaC's α-subunit mRNA

was significantly down-regulated in some segments of the colon in diseased pigs while the β-subunit was unchanged from control. However, previous studies have suggested that not all sub-units are required to form a functional channel supporting the transport of Na^+ (123). The current electrogenic Ussing chamber studies lead to the conclusion that electrogenic Na^+ absorption is not significantly affected in the colon of diarrheic pigs. It is possible, however, that Na^+ absorption through ENaC accounts for the majority of Na^+ absorption in diseased pigs when electroneutral Na^+ absorption is impaired.

Na^+/K^+ ATPase's α-subunit was down-regulated in the proximal segment of the colon in *B. hyodysenteriae* and *B. hampsonii* diseased pigs. Na^+/K^+ ATPase is essential for maintaining the electrolyte gradient across the cellular membrane, regulating osmotic balance and cell volume (33, 155). The α-subunit of the Na^+/K^+ ATPase pump is responsible for the transport of three Na^+ out of the cell and two K^+ in, which maintains low Na^+ concentrations in the cell driving ion transport (188). Malabsorption of bile acids in the colon associated with chronic diarrhea in human patients has been shown to cause down-regulation of Na^+/K^+ ATPase's subunits (36). This was further supported with T84 cells exposed to 150 μM deoxycholic acid for 48 hours which down-regulated both ATP1A1 and ATP1B1 at both the mRNA and protein level *in vitro* (36). Since Na^+/K^+ ATPase is essential for driving ion transport within enterocytes, loss of its function would be a main contributor to the production of diarrhea observed in animals infected with *Brachyspira* species. However, it was not down-regulated in the apex of the colon, thus it is unlikely to have been responsible for the decrease in Na^+ absorption observed. Additionally, the decrease in mRNA expression in the proximal colon did not

have a significant effect on electrogenic Na^+ absorption in this segment. Together these findings suggest that down-regulation of ATP1A1 in the proximal segment is of minimal importance during spirochetosis.

4.4.2 *IL-1α does not decrease NHE3 mRNA expression in polarized Caco-2 monolayers*

Cytokines have been previously shown to have strong negative regulation of Na^+ channel and transporters (9, 260, 337). Kruse et al. reported that pigs experimentally challenged with *B. hyodysenteraie* had elevated levels of IL-1β and TNF-α in their blood during peak dysentery while IFN-γ was not detected (176). Furthermore, colonic explants exposed to live *B. hyodysenteriae* had elevated IL-1α expression after 8hrs of exposure (322). My previous findings have shown that diarrheic pigs challenged with *B. hyodysenteiae* or *B. hampsonii* strain 30446 had significantly elevated mRNA expression of Th1 cytokine IL-1α throughout their colons while TNF-α and IFN-γ were down-regulated or unchanged compared to control (Chapter 3).

The majority of previous research on cytokine modification of electroneutral Na^+ transporters has focused on pro-inflammatory cytokines IFN-γ, TNF-α, and IL-1β. This is likely due to the elevated expression of these pro-inflammatory cytokines in patients suffering from inflammatory bowel disease (17, 94, 204, 215). IFN-γ has been shown to decrease NHE2 and NHE3 mRNA and protein expression in Caco-2 BBE cells, rat ileum and colon in a dose and time-dependent manner (9, 260). Additionally, TNF-α also decreased NHE3 gene expression in C2BBe1 cells (9). Both IFN-γ and TNF-α repress the NHE3 gene by phosphorylation of Sp1 and Sp3 transcription factors by a cAMP-dependent protein kinase (9).

A recent study has shown that IL-1β strongly reduces mRNA and protein expression of $PDZK_1$ (NHERF3) in Caco-2BBE cells (194). Reduced expression of $PDZK_1$ has been identified in the inflamed intestine of both ulcerative colitis patients and murine colitis models (186, 330). Absence of $PDZK_1$ leads to dysfunction of NHE3, however, it is not a result of decreased mRNA or protein expression but rather an increase in protein turnover due to reduced membrane retention time (59, 130). Other studies have shown that NHERF1 and NHERF2 deficient mice have reduced NHE3 activity and transporter abundance on the brush border membrane of jejunum and colon while mRNA levels remain unchanged (40, 54).

These three cytokines do not account for the decrease in NHE2 and NHE3 mRNA and protein expression in the colon of *Brachyspira* diseased pigs. As IL-1α was the only cytokine upregulated throughout the colon of diarrheic pigs I tested whether IL-1α was capable of down-regulating NHE3 mRNA expression in polarized Caco-2 monolayers. I found that recombinant IL-1α did not down-regulate NHE3 in Caco-2 cells at any concentration (10, 100, and 500 ng/ml) after 24hrs of exposure. However, the elevated mRNA expression of PTGS2 confirmed that IL-1α had a biological effect (58, 131, 259).

Previous studies have found that basolateral stimulation of rabbit ileum with human IL-1α decreases both Na^+ and Cl^- absorption while stimulating Cl^- secretion (58). These effects were mirrored closely when ileal samples were stimulated with PGE_1, however, when ileal samples were first treated with IL-1α and subsequently exposed to PGE_1 the magnitude of change in net flux and electrical properties was reduced (58). These findings suggested that the effects of IL-1α and PGE_1 are not additive in nature

(58). Additionally, in another study assessing enterocyte-subepithelial myofibroblast interaction exposure of 18Co or P2JF cells preincubated with IL-1α grown acutely juxtaposed to T84 cells significantly elevated basal I_{sc} (131). This effect was attributed to upregulation of PTGS1 and PTGS2 expression in 18Co and P2JF cell lines and production of PGE_2 (131). Additional studies have identified that prostanoids stimulate Cl^- secretion and inhibit electroneutral Na^+ absorption by elevating cAMP (12, 238, 340). However, in the colon of diarrheic pigs infected with *Brachyspira*, anion secretion is impaired, and there is a reduction in NHE3 mRNA and protein expression. Prostanoids do not generally decrease mRNA or protein, suggesting that prostanoid induction by IL-1α is not responsible for the observed decrease in Na^+ absorption. Thus, the reduction in Na^+ channel mRNA and protein *in vivo*, the inability of IL-1α to down-regulate NHE3 in Caco-2 cells, and previous literature suggest that *Brachyspira* or a secreted toxin are capable of modulating Na^+ transporter transcriptional processes.

4.4.3 *Brachyspira hampsonii lysate down-regulates NHE3 mRNA expression in Caco-2 cells*

As IL-1α was not capable of down-regulating NHE3 mRNA in Caco-2 cells, a whole cell *Brachyspira hampsonii* lysate was used to determine its effect on NHE3 gene expression. Exposure of polarized Caco-2 monolayers to a lysate concentration of 50µg/ml caused a significant decrease in NHE3 mRNA. This suggests that a component of the bacterial is responsible for the decrease in transporter mRNA expression. This is not the first time that disruption of *Brachyspira* results in modification of cellular processes (252)(Chapter 3). Live *B. hyodysenteraie* accompanied with neutrophil elastase causing degradation of outer membrane proteins caused elevated mucin

production and transport rates in HT29 MTX-E12 cells (252). Furthermore, I have previously shown that a *Brachyspira hampsonii* strain 30446 lysate decreased CFTR mRNA expression in polarized Caco-2 monolayers (Chapter 3). Thus, I provide strong evidence supporting the direct effects of *Brachyspira* spp. that contribute to diarrheal development in the colon of infected pigs.

4.5 Conclusion

The current study provides new insight into the pathophysiological mechanisms involved during *B. hyodysenteraie* and *B. hampsonii* strain 30446 infections contributing to the development of diarrheal disease. Impairment of the electroneutral Na^+ absorptive capacity of the porcine colon is a major contributor to the development of diarrhea. This decrease in Na^+ absorption is supported by the down-regulation of NHE isoforms 1-3 mRNA and reduced protein expression of the critical NHE3 isoform in the colon of diseased pigs. The examined host cytokine response appears not to be responsible for the decrease in NHE3 mRNA expression as human recombinant IL-1α had no effect on modulating NHE3 expression in Caco-2 monolayers. A *Brachyspira hampsonii* lysate, however, decreased NHE3 mRNA expression in Caco-2 monolayers providing further evidence that *Brachyspira* are able to impair ion channel and transporter transcriptional processes. Together these findings provide new evidence supporting a decrease in electroneutral Na^+ absorption contributing to diarrheal development during episodes of spirochetosis.

Chapter 5 - Decreased Expression of DRA (SLC26A3) by IL-1α Contributes to Development of Diarrheal Disease Following *in vivo* Challenge with *Brachyspira* spp.

Cole B. Enns[1], John C.S. Harding[2], Matthew E. Loewen[1b]

1. Department of Veterinary Biomedical Sciences, 2. Department of Large Animal Clinical Sciences, Western College of Veterinary Medicine, University of Saskatchewan. 52 Campus Drive. Saskatoon, Saskatchewan, Canada S7N 5B4

Author Contributions

C.E., J.H., and M.L. conceived and designed research; C.E., J.H., and M.L. performed experiments; C.E. analyzed data; C.E. and M.L. interpreted results of experiments; C.E. prepared figures; C.E. and M.L. drafted manuscript; C.E., J.H., and M.L. edited and revised manuscript; C.E., J.H., and M.L. approved final version of manuscript.

*This publication has not yet been submitted for publication.

*See Appendix for Descriptive Materials & Methods.

The effects of spirochetosis by *Brachyspira hyodysenteriae* and *Brachyspira hampsonii* on electroneutral Cl^- transport in the porcine colon was assessed to determine its contribution to the development of diarrheal disease. Barrier function was evaluated, as a significant portion of Cl^- absorption occurs paracellularly. Ussing chamber radiolabeled ^{36}Cl, and ^{3}H-mannitol fluxes were used to determine changes in transport and barrier function. The basal J_{ms} radiolabeled ^{36}Cl flux was significantly impaired in the colon of diarrheic pigs infected with *B. hyodysenteriae* and *B. hampsonii*. This decrease was not a result of increased paracellular movement of solutes in the colon as unidirectional, and net ^{3}H-mannitol fluxes in diarrheic pigs were not different from control. This suggested that the decrease in ^{36}Cl J_{ms} flux was attributed to electroneutral Cl^- absorption via chloride/bicarbonate exchanger, SLC26A3 also known as DRA (down-regulated in adenoma). Flux experiments were supported by a significant decrease in both SLC26A3 mRNA and protein expression in the colon of diarrheic pigs. The decrease in DRA mRNA expression is potentially attributed to the host's cytokine response as human IL-1α decreased DRA mRNA in Caco-2 cells. Together these findings provide mechanism for the spirochete-induced malabsorptive diarrhea, supported by a decrease in electroneutral Cl^- absorption while demonstrating novel downregulation of DRA by IL-1α.

5.1 Introduction

Colonic spirochetosis occurs in many species including humans and swine resulting in diarrheal disease. Colonization of the human colon by *Brachyspira aalborgi* and *Brachyspira pilosicoli* leads to moderate inflammation and diarrhea (307). In swine, *Brachyspira hyodysenteriae* and *Brachyspira hampsonii* cause severe colonic inflammation accompanied by severe bloody mucoid diarrhea (49, 121, 266). The pathophysiological mechanism by which *Brachyspira pilosicoli* and *Brachyspira aalborgi* cause diarrhea in the human colon is unknown. Our group has recently made advances in characterizing the pathophysiological mechanisms of *Brachyspira hyodysenteriae* and *Brachyspira hampsonii* in a porcine model *in vivo*.

Brachyspira hyodysenteriae was originally described as malabsorptive diarrhea by which Na^+ and Cl^- lumen-to-blood fluxes were impaired in isolated colonic loops in diarrheal pigs (13). These findings were further supported by my findings revealing that electroneutral Na^+ absorption was abolished in diarrheal animals correlating with significantly decreased Na^+-H^+ exchanger 3 (NHE3) mRNA and protein expression (Chapter 4). Furthermore, *Brachyspira* associated diarrhea is not driven by an increase in anion secretion, rather decreased agonist-induced electrogenic anionic secretory response was observed (Chapter 3). This decrease contributes to increased mucus thickening and disorganization within the porcine colon allowing for greater bacterial colonization (Chapter 3)(251). This altered ion transport in the colon of diarrheic pigs appeared to be caused by a direct effect of *Brachyspira* spp. (Chapter 3), and not attributed to the elevated expression of pro-inflammatory cytokine IL-1α, the only significantly upregulated cytokine noted throughout the colon at peak clinical signs.

Although great advances have been made in determining the cellular mechanisms responsible for this malabsorptive diarrhea (Chapters 3 & 4), the role of Cl^- absorption has not been characterized.

The predominant route of chloride absorption in the colon is electroneutral (Cl^--HCO_3^-) in nature and coupled with electroneutral Na^+ - H^+ exchange (270). *In vivo* perfusion studies in the human colon suggests that 25% of Cl^- absorbed is due to Cl^--HCO_3^- exchange while the remainder is due to paracellular transport due to luminal negative potential difference generated by electrogenic Na^+ absorption (71). This electroneutral Cl^- absorption is primarily achieved by the Cl^--HCO_3^- exchangers SLC26A3 downregulated in adenoma (DRA) and SLC26A6 (PAT-1) located on the apical membrane of enterocytes in the gastrointestinal tract (43, 320). PAT-1 is primarily expressed in the small intestine while DRA is predominantly expressed in the colon (81, 157, 318, 320). DRA appears to be the critical transporter as alterations in DRA function and expression have been implicated in diarrheal disorders such as congenital chloride diarrhea (CLD) and inflammatory bowel disease (IBD) (162, 321, 327). Furthermore, knockdown of DRA in mice results in a diarrheal phenotype, while knockdown of PAT-1 does not (157).

The proinflammatory cytokines IL-1β and IFN-γ have been shown to have a significant effect reducing DRA gene and protein expression in Caco-2 cells (268, 328). Additionally, *Clostridium difficile* toxins A and B and enteropathogenic *E. coli* were found to have a direct effect on DRA, by reducing protein expression (66, 107). The role of DRA in the development of *Brachyspira* induced diarrhea has not yet been explored.

The purpose of this study was to determine the pathophysiologic and molecular effect on Cl^- absorption in the colon of control and experimentally infected pigs with two *Brachyspira* spp. resulting in spirochetosis. Cl^- absorption was assessed in the apex of the porcine spiral colon in Ussing chambers using radiolabelled ^{36}Cl flux. J_{ms} flux in diarrheic pigs infected with *B. hyodysenteriae* and *B. hampsonii* was severely reduced. This decrease in J_{ms} was not attributed to an increase in transcellular or paracellular Cl^- movement as indicated by J_{sm} unidirectional fluxes with ^{36}Cl or ^{3}H-mannitol. This decrease in Cl^- absorption correlated with a significant decrease in DRA gene and protein expression in the apex of the colon in diarrheic pigs. To assess whether the host cytokine response was responsible for the decrease in DRA expression, Caco-2 monolayers were exposed to human recombinant IL-1α for 24hrs. IL-1α decreased DRA mRNA expression in Caco-2 cells leading us to the conclusion that IL-1α is responsible for modulating DRA expression, contributing to diarrheal disease.

5.2 Materials & Methods

5.2.1 *Animals*

Thirty 6-8 week-old purebred Yorkshire barrows were housed in pairs with 10 pigs per treatment group housed in separate BSL2 animal care rooms. Pigs were acclimated to their new environment for 7 days and provided an antibiotic-free diet with water *ad libitum*. After 7 days pigs were orally challenged with either *Brachyspira hyodysenteriae* strain G44 (kindly provided by Boehringer-Ingelheim Vet Medica, St. Joseph, MO; n=10), *Brachyspira hampsonii* strain 30446 (n=10) or a mock inoculum of sterile culture media (n=10). Feed was removed 12 hours prior to inoculation, but water was not. Inoculation was conducted by passing a stomach tube and flushing 30ml of

10^8-10^9 cells/ml inoculum into the stomach of a pig, followed by sterile PBS as previously described (266). Pigs were assessed daily for clinical signs of diarrhea, and fecal consistency-scores were taken two times daily to accurately determine the onset of diarrhea. *Brachyspira* challenged pigs developed diarrhea within 3-7 days post inoculation and were euthanized 24 hours after the onset of diarrhea. Control pigs remained healthy (non-diarrheic) and were euthanized on an age-matched basis with *Brachyspira* challenged pigs euthanized the same day. This research was designed and conducted in accordance with the Canadian Council for Animal Care and approved by the University of Saskatchewan Committee on Animal Care and Supply (Protocol #20130034).

5.2.2 *Characterization of the electroneutral absorptive response in healthy and diseased porcine colon - ^{36}Cl flux study*

Following euthanasia by intracranial captive bolt and exsanguination, 17-18 cm of the apex segment of the spiral colon (midpoint between cecum and sigmoid colon) was collected and washed with Krebs buffer (pH 7.4) containing (in mM) 113 NaCl, 5 KCl, 1.6 Na_2HPO_4, 0.3 $NaH_2PO_4 \bullet H_2O$, 25 $NaHCO_3$, 1.1 $MgCl_2 \bullet 6H_2O$, 2.2 $CaCl_2 \bullet 2H_2O$ and 10 glucose, and chilled to 4ºC as previously reported (61). Samples were immediately transported back to the lab in Krebs buffer gassed with 95% O_2 - 5% CO_2.The colonic segment was then stripped with forceps by removing the serosa (visceral peritoneum) and the longitudinal/circular muscle layers, leaving only the underlying submucosal elements, remnants of muscle, and the epithelium as previously described (61). The stripped tissues (12 tissue replicates per pig) were then placed on 1cm^2 tissue Ussing chamber inserts and inserted into the Ussing chamber (Physiologic

Instruments, San Diego, CA). Each reservoir was independently gassed with 95% O_2-5%CO_2. A heated circulating water bath warmed and maintained the buffer temperature within the Ussing chamber to 37ºC. Transepithelial potential differences were short-circuited to 0 mV with a voltage clamp on the apical and basolateral chambers using Ag-AgCl electrodes and 3M KCL agar bridges as previously described (61).

Tissue were allowed to equilibrate for twenty minutes before the addition of ^{36}Cl. Tissues were pulsed every 30 seconds with a 1 mV pulse, and the resulting current was used to determine tissue resistance. Tissues were paired with one another, and subsequently, 0.25 µCi of ^{36}Cl and 1 µCi of ^{3}H-mannitol (PerkinElmer, Waltham, MA) was added to the apical side of chamber #1 and the same to the basolateral side of chamber #2. After the addition of isotope, 100µl samples were immediately removed from the apical side of chamber #1, and basolateral side of chamber #2 referred to as "hot samples" and placed in 5ml of Ultima Gold™ scintillation cocktail (PerkinElmer, Waltham, MA). The 100µl samples were then immediately replaced with 100µl of fresh Krebs buffer. Samples (500µl) were removed from the basolateral side of chamber #1, and apical side of chamber #2 referred to as "cold samples" every ten minutes for 60 minutes and subsequently replaced with fresh Krebs buffer. Cold samples were used to calculate unidirectional mucosal-to-serosal (J_{ms}), serosal-to-mucosal (J_{sm}) and net flux ($J_{net} = J_{ms} – J_{sm}$) for ^{36}Cl and ^{3}H-mannitol as previously described (281). Positive net flux values indicate net absorption while negative values indicate net secretion of the isotope.

5.2.3 *RT-qPCR analysis of DRA mRNA expression*

Mucosal samples taken at the time of necropsy were stored in RNAlater® (AM7021; Ambion®) and homogenized in 1ml of TRIzol reagent (15596018; Life Technologies) and RNA extracted according to the manufacturer's protocol. A standard of <500ng/µl was used as exclusion criteria for RNA samples.

cDNA was created from mRNA using the Go Script Reverse Transcription system (A5001; Promega) according to the manufacture's protocol. cDNA was diluted in RNase-free water and frozen at -80˚C. Gene expression was assessed by RT-qPCR using GoTaq qPCR Master Mix (A6002; Promega) and Stratagene Mx5000P real-time qPCR machines according to the manufacture's protocol. The average C_T (cycle threshold) value was used to calculate the fold difference of each gene using the ΔΔCt calculation method. Porcine primers were designed for GAPDH and SLC26A3 (Table 5.1). Porcine GAPDH was used as the reference gene for the analysis. Human primers were designed for GAPDH, SLC26A3, and PTGS2 (Table 5.1). Human GAPDH was used as the reference gene for the analysis.

5.2.4 *Western blot analysis of DRA*

Protein was extracted from control and diarrheic pigs from the apex segment of the colon using the ProteoExtract transmembrane protein kit (71772-3; Novagen®) according to the manufacture's protocol. Samples were boiled in 2x denaturing buffer (20% glycerol, 4% SDS, 125 mM Tris pH 6.8, 0.3 mM bromophenol blue) containing 10% β-mercaptoethanol (BME; M6250; Sigma-Aldrich) for five minutes and analyzed by 10% SDS-PAGE (286).

Table 5.1. Porcine and human primer sequences for RT-qPCR

Gene Name	Forward (5'-3')	Reverse (5'-3')
Porcine GAPDH	ACATCAAGAAGGTGGTGAAGCAGG	TGAGCTTGACGAAGTGGTCGTTGA
Porcine SLC26A3	CCTGACGCACAGACTTTA	CACTCCCAAGGCTATTAACT
Human GAPDH	CAAGGTCATCCATGACAACTTTG	GGGCCATCCACAGTCTTCTG
Human SLC26A3	GGCCGTACTACAAGGTTTA	GCTAGTCCCACCATCATAC
Human PTGS2	GAAGCCTTCTCTAACCTCTC	GGATCAGGGATGAACTTTCT

For western blot analysis, proteins were transferred onto PVDF membranes (RPN303LFP; GE Healthcare Life Sciences) at 0.2mA for 4 hours at 4ºC transfer buffer (25mM Tris, 192mM glycine, 20% methanol) as previously described (286). Membranes were blocked for 1 hour at room temperature with a 10% RapidBlock™ (M325-AMRESCO®) blocking solution and subsequently probed overnight at 4ºC with primary antibodies anti-SLC26A3 (PA5-68530; Invitrogen) anti-β-Actin (C-4; sc-47778; Santa Cruz Biotechnology) in a 10% RapidBlock™ solution. The membranes were then incubated for 1 hour at room temperature with secondary antibodies Alexa Fluor 488 Goat anti-Rabbit IgG antibody (A-11008; Thermo Fisher Scientific) and ECL Plex Goat anti-Mouse IgG-Cy5 antibody (PA45009; Amersham Biosciences) in 10% RapidBlock™ solution. Proteins were subsiquently detected and analyzed using Typhoon Trio and ImageQuant TL System (63005583; GE Healthcare Life Sciences).

5.2.5 *Cell culture*

The Caco-2 cell line derived from human colorectal adenocarcinoma (HTB-37; ATCC, Manassas, VA) were cultured in Dulbecco's modified Eagle medium (DMEM) (10-0130CM, Corning, Manassas, VA) containing 10% heat-inactivated fetal bovine serum (Gibco, Burlington, ONT, Canada), 1% penicillin-streptomycin (15140-122; Life Technologies), and 1% MEM non-essential amino acids (Gibco, Grand Island, NY) at 37˚C in a humidified atmosphere with 5% CO_2. Cells were plated on polyester Transwell® permeable supports (0.4µm pores, 24 mm in diameter, Corning) and cultured under standard conditions until confluency. Cells were maintained for 10 days after confluency was achieved before being used in downstream experiments.

5.2.6 *Caco-2 monolayer exposure to recombinant human IL-1α*

My previous research has identified IL-1α as the only cytokine that is up-regulated throughout the colon of diarrheic pigs experimentally challenged with *B. hyodysenteriae* and *B. hampsonii* (Chapter 3). To identify if IL-1α was responsible for the decreased expression of DRA, polarized Caco-2 monolayers were exposed to human recombinant IL-1α (I2778; Sigma Aldrich) on both apical and basolateral surfaces at varying concentrations (10, 100, and 500 ng/ml) for 24hrs. The human-derived colon adenocarcinoma Caco-2 cell line was chosen as no commercial porcine colonic cell lines are currently available. To ensure that IL-1α had a biological effect on Caco-2 monolayers, RT-qPCR was performed for prostaglandin-endoperoxide synthase 2 (PTGS2) which becomes up-regulated in many cell types after IL-1α exposure (58, 131, 259).

5.2.7 *Statistical analysis*

^{36}Cl flux data was not normally distributed (Shapiro-Wilk test; $P < 0.05$) and is expressed as median $\pm$ interquartile range (IQR). RT-qPCR and western blot data is normally distributed (Shapiro-Wilk test; $P > 0.05$) and expressed as mean $\pm$ standard error of the mean (SEM). Changes in the rate of ^{36}Cl transport was analyzed by Kruskal-Wallis one-way analysis of variance and Dunn's test. Fold changes in mRNA expression of diseased colonic segments compared to control obtained by RT-qPCR was long transformed (log10) and analyzed by one-way ANOVA and Tukey post-hoc. Western blot analysis of DRA protein was analyzed with Student's t-test (control vs. *Brachyspira* species in two separate analyses). Significance was set *a priori* at $P < 0.05$.

5.3 Results

5.3.1 *Brachyspira hyodysenteriae and Brachyspira hampsonii reduce Cl^- absorption in the apex of the porcine spiral colon during ^{36}Cl equilibration*

During the 60-minute ^{36}Cl equilibration period, a significant decrease in unidirectional J_{ms} flux was observed in *B. hyodysenteriae* diseased colon ($P < 0.05$) after only 20 minutes of flux, the rate of flux remained significantly decreased for the remainder of the equilibration period compared to healthy colon samples (Figure 5.1A). Furthermore, a significant decrease in J_{ms} flux in *B. hamp* infected colon samples ($P < 0.05$) was observed after 30 minutes and remained significantly decreased for the remainder of the equilibration period. Interestingly, after 30 minutes of flux, the J_{sm} flux was significantly reduced in *B. hyodysenteriae* and *B. hampsonii* diseased pigs compared to control ($P < 0.05$) (Figure 5.1B). This Indicated that *Brachyspira* induced diarrhea is not secretory in nature, which is in agreement with my previous findings (Chapter 3)(277).

J_{net} revealed that healthy unchallenged pigs had net Cl^- absorption in the apex of their spiral colon (Figure 5.1C). *B. hyodysenteriae* diseased pigs had a net secretory response during the equilibration period (Figure 5.1C). However, this response was attributed to a decrease in Cl^- secretion and an even greater decrease in Cl^- absorption rather than an increase in Cl^- secretion. Interestingly, *B.hamp* infected colon samples had net absorption of Cl^- which was reduced compared to controls, but not significantly. It appeared that net Cl^- absorption was unaffected, however, unidirectional fluxes revealed that a reduction in J_{ms} paired with a greater reduction in J_{sm} was the reason for the altered absorptive response suggesting that Cl^- absorption is also impaired in the

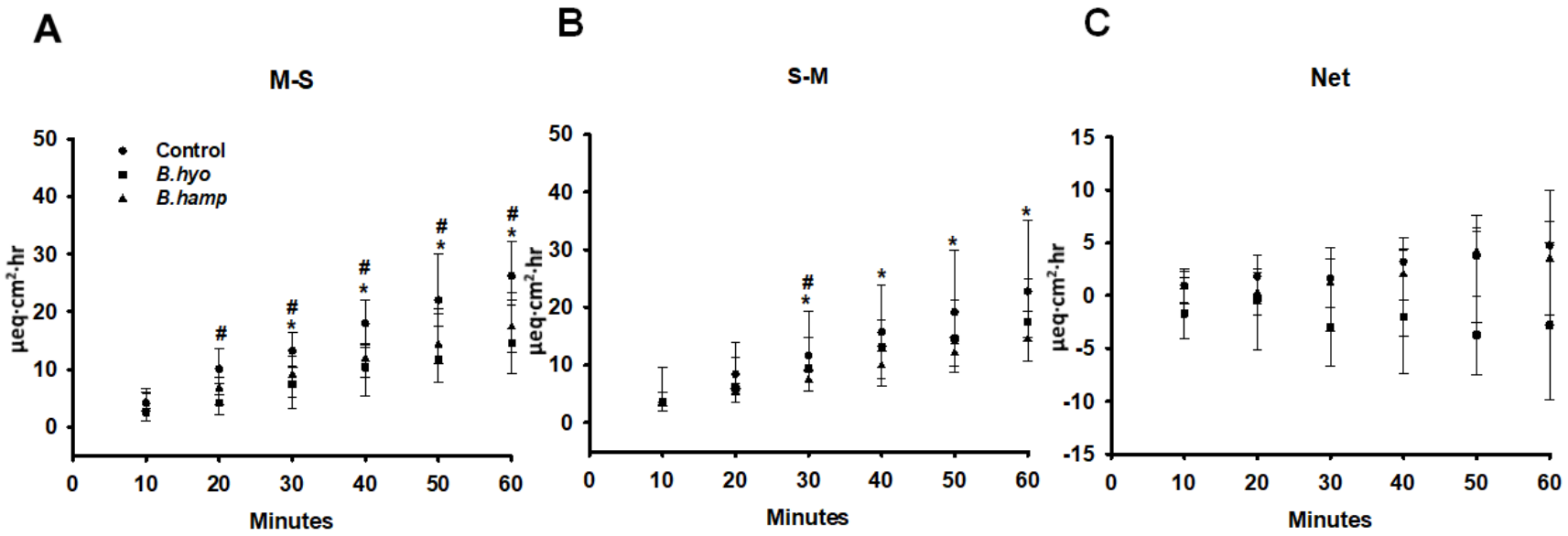

Figure 5.1. *Brachyspira hyodysenteriae* and *Brachyspira hampsonii* strain 30446 decrease basal J_{ms} Cl^- absorption during ^{36}Cl equilibration in the apex of the porcine spiral colon.

Basal J_{ms} (A), J_{sm} (B), and net (C) flux rates during ^{36}Cl equilibration across apex colonic segments from control, *B. hyodysenteriae*, and *B. hampsonii* diseased pigs. M-S, unidirectional mucosal-to-serosal ^{36}Cl flux; S-M, unidirectional serosal-to-mucosal ^{36}Cl flux; Net, net ^{36}Cl flux. Data presented as median $\pm$ IQR, analyzed using Kruskal-Wallis one-way analysis of variance and Dunn's Post Hoc. Significant differences between control and *B. hyodysenteriae* are represented by ***** = $P < 0.05$; Significant differences between control and *B. hampsonii* are represented by # = $P < 0.05$. (n=12 ctrl, n=12 *B. hyodysenteriae*, n=12 *B. hampsonii* strain 30446).

apex of *B.hamp* diseased pigs. Overall, close analysis of unidirectional flux clearly demonstrates a decrease in the absorption of Cl^- in diarrheic pigs.

5.3.2 *DRA inhibition by carbachol reveals reduced Cl^- transport in the apex of diarrheic pigs*

Following the equilibration period, DRA was inhibited through the addition of carbachol causing an increase in intracellular Ca^{2+} (183). In control tissues, carbachol resulted in a decrease in J_{ms} (-2.23 $\pm$ 3.84 µmol·cm^{-2}·h^{-1}) while increasing J_{sm} (3.30 $\pm$ 4.31 µmol·cm^{-2}·h^{-1}) flux, resulting in net Cl^- secretion (Table 5.2). Interestingly, carbachol had little effect inhibiting DRA in diarrheic pigs as J_{ms} flux was not inhibited in *B.hyodysenteriae* (0.20 $\pm$ 3.61 µmol·cm^{-2}·h^{-1}) and *B. hampsonii* (1.73 $\pm$ 6.92 µmol·cm^{-2}·h^{-1}) infected animals. When compared to control, *B. hyodysenteriae* and *B. hampsonii* infected tissues had significantly less inhibition ($P < 0.05$) ($P < 0.05$) of Cl^- J_{ms} following carbachol addition (Table 5.2). J_{sm} in *B. hyodysenteriae* infected tissues did not increase following carbachol addition (-0.08 $\pm$ 3.97 µmol·cm^{-2}·h^{-1}) while tissues from *B. hamp* diseased pigs had an increase in luminal Cl^- secretion (3.25 $\pm$ 3.14 µmol·cm^{-2}·h^{-1}) comparable to control. These findings suggest that diarrheic pigs have reduced levels of functional DRA protein on the mucosal surface of their colons resulting in decreased transporter-mediated Cl^- absorption.

Table 5.2. Effect of 0.1mM carbachol on Cl^- fluxes across control, *B. hyo*, and *B. hamp* infected colon.*

	J^{Cl-} ($\mu eq \cdot cm^2 \cdot h$)							
	M-S			S-M			Net	
	Basal	*Carbachol*	*Δ*	*Basal*	*Carbachol*	*Δ*	*Basal*	*Carbachol*
Control	34.30 ± 10.8	32.95 ± 11.16	-2.23[a] ± 3.84	33.62 ± 16.27	32.74 ± 20.11	3.30[a] ± 4.31	6.73 ± 13.96	-0.49 ± 13.89
B. hyo	23.08 ± 18.23	21.04 ± 15.62	**0.20[b] ± 3.61**	24.33 ± 13.45	24.69 ± 10.46	-0.08[a] ± 3.97	-3.76 ± 21.60	-0.07 ± 17.58
B. hamp	24.30 ± 11.80	28.43 ± 11.95	**1.73[b] ± 6.92**	21.13 ± 8.71	24.28 ± 8.44	3.25[a] ± 3.14	5.31 ± 11.10	3.69 ± 8.79

*Values represent medians ± IQR, analyzed using Kruskal-Wallis one-way analysis of variance and Dunn's Post Hoc. Change in ^{36}Cl flux rate (*Δ*) 10-minutes after the addition of carbachol. *Δ* values for *B. hyodysenteriae* and *B. hampsonii* diseased tissues were compared to control and significant differences ($P < 0.05$) are marked with a different superscript. Significantly different values are marked in bold. M-S, mucosal-to-serosal; S-M, serosal-to-mucosal. (n=12 ctrl, n=12 *B. hyodysenteriae*, n=12 *B. hampsonii* strain 30446).

5.3.3 *Brachyspira hyodysenteriae and Brachyspira hampsonii do not cause an increase in paracellular movement of ^{3}H-mannitol in the apex of the porcine spiral colon*

As previously described chloride absorption in the colon is closely tied to electroneutral sodium absorption (270). Chloride absorption is primarily achieved by paracellular movement following electroneutral sodium transport. To assess if barrier function was compromised in *B. hyodysenteriae* and *B. hampsonii* diseased animals, ^{3}H-mannitol flux was examined in Ussing chambers. No significant difference in J_{ms}, J_{sm} or J_{net} was observed during the 60-minute equilibration period between control or diarrheic pigs (Figure (5.2A-C). This finding was not surprising as my previous work has shown that tissue resistance, an indicator of barrier function is not affected by *Brachyspira* infection (Chapter 3). Furthermore, this finding points to the importance of DRA in facilitating Cl^- absorption in the colon.

5.3.4 *The decrease in DRA mRNA & protein expression correlates with decreased Cl^- absorption in the colon of diarrheic pigs*

To determine if the decrease in Cl^- absorption was attributed to down-regulation of DRA, mRNA and protein expression was measured by RT-qPCR and western blot. DRA was determined to be significantly down-regulated in the apex of the colon in diarrheic animals infected with *Brachyspira hyodysenteriae* ($P < 0.05$) and *Brachyspira hampsonii* ($P < 0.05$) when compared to control (Figure 5.3)

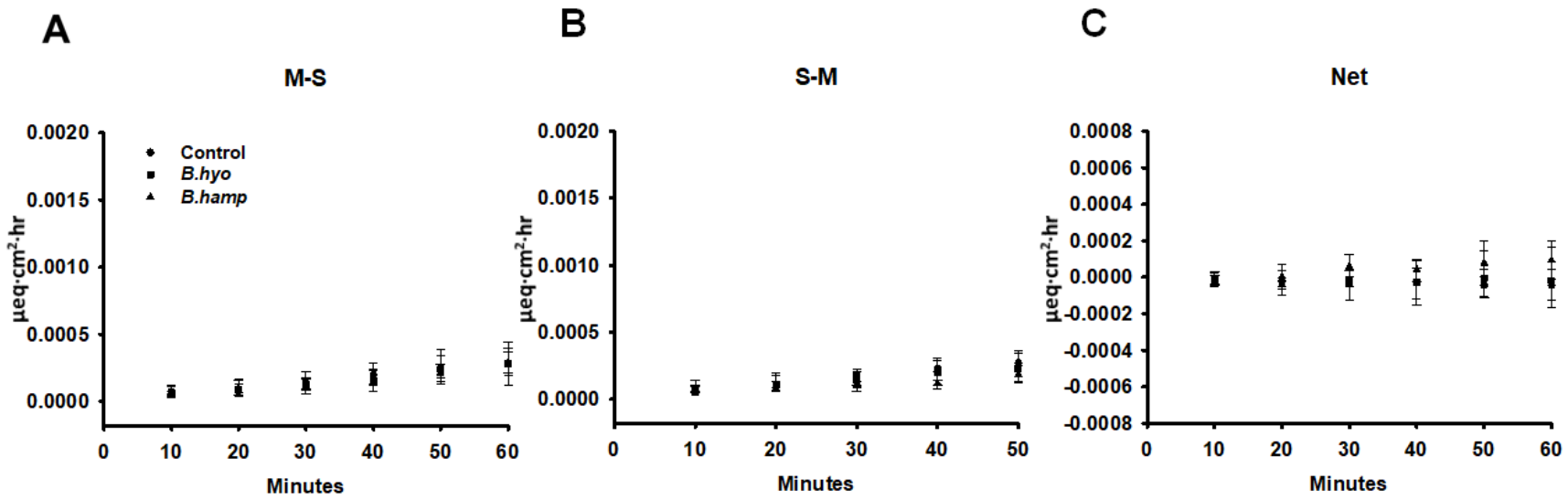

Figure 5.2. *Brachyspira hyodysenteriae* and *Brachyspira hampsonii* strain 30446 do not affect paracellular solute movement.

Basal J_{ms} (A), J_{sm} (B), and net (C) flux rates during ^{3}H-mannitol equilibration across apex colonic segments from control, *B. hyodysenteriae*, and *B. hampsonii* diseased pigs. M-S, unidirectional mucosal-to-serosal ^{3}H-mannitol flux; S-M, unidirectional serosal-to-mucosal ^{3}H-mannitol flux; Net, net ^{3}H-mannitol flux. Data presented as median $\pm$ IQR, analyzed using Kruskal-Wallis one-way analysis of variance and Dunn's Post Hoc. Significant differences between control and *B. hyodysenteriae* are represented by ***** = $P < 0.05$; Significant differences between control and *B. hampsonii* are represented by # = $P < 0.05$. (n=12 ctrl, n=12 *B. hyodysenteriae*, n=12 *B. hampsonii* strain 30446).

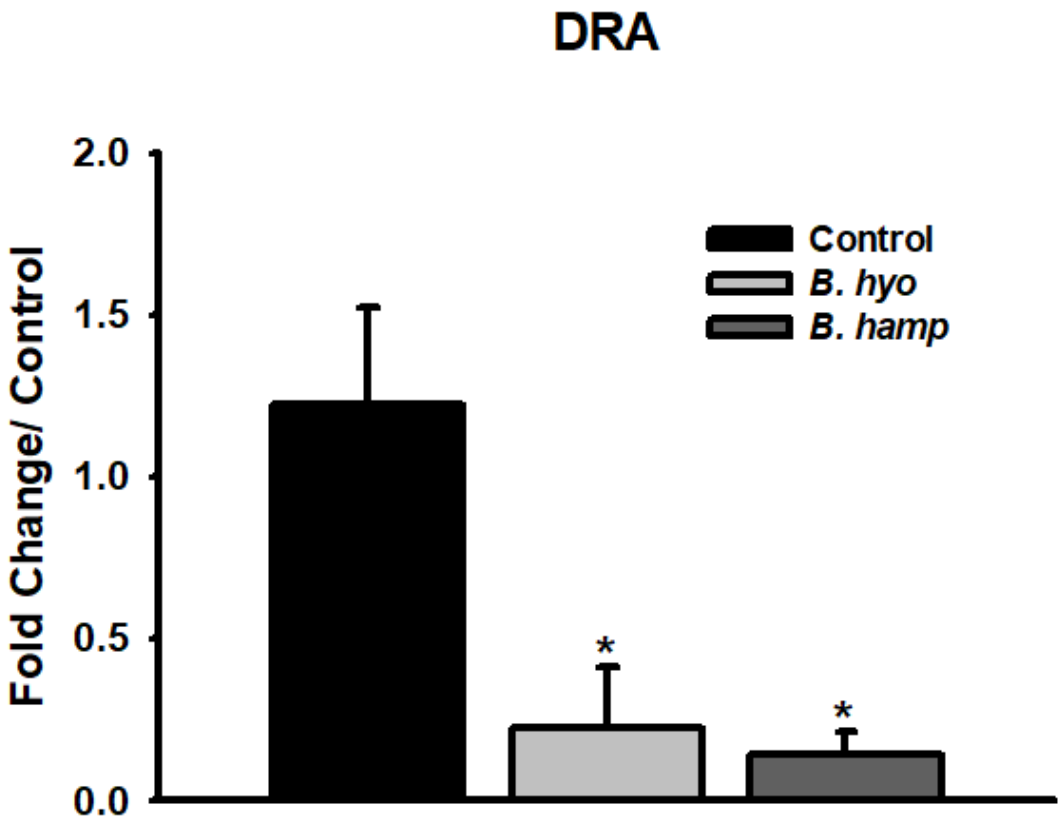

Figure 5.3. *Brachyspira hyodysenteriae* and *Brachyspira hampsonii* strain 30446 decrease DRA mRNA expression in the apex of the porcine colon.

Change in DRA mRNA compared to control as measured by RT-qPCR. DRA, down-regulated in adenoma. DRA = downregulated-in0adenoma. Data presented as mean ± SEM, analyzed using one-way ANOVA. * = $P < 0.05$ (n=6 ctrl, n=6 *B. hyodysenteriae,* n=6 *B. hampsonii* strain 30446).

Upon western blot analysis, it was determined that DRA protein expression was significantly reduced in the apex of disease pigs ($P < 0.05$) ($P < 0.05$) (Figure 5.4). The decrease in DRA mRNA and protein expression supports the observed decrease in Cl^- absorption in the colon of diarrheic pigs.

5.3.5 *Human IL-1α decreases DRA mRNA expression in polarized Caco-2 monolayers*

To determine if IL-1α, the only cytokine up-regulated throughout the colon of diarrheic pigs was responsible for the decrease in DRA mRNA expression observed *in vivo*, polarized Caco-2 monolayers were exposed to human recombinant IL-1α for 24hrs (Chapter 3). I found that IL-1α significantly decreased DRA mRNA expression at a dose of 500ng/ml when compared to control ($P < 0.05$) (Table 5.3). Furthermore, I observed a significant increase ($P < 0.05$) in PTGS2 expression in all Caco-2 monolayers treated with IL-1α, confirming that the cytokine had a biological effect (Table 5.3). These results suggest that IL-1α is responsible for the down-regulation of DRA contributing to the formation of diarrhea in *B. hyodysenteriae* and *B. hampsonii* diseased pigs.

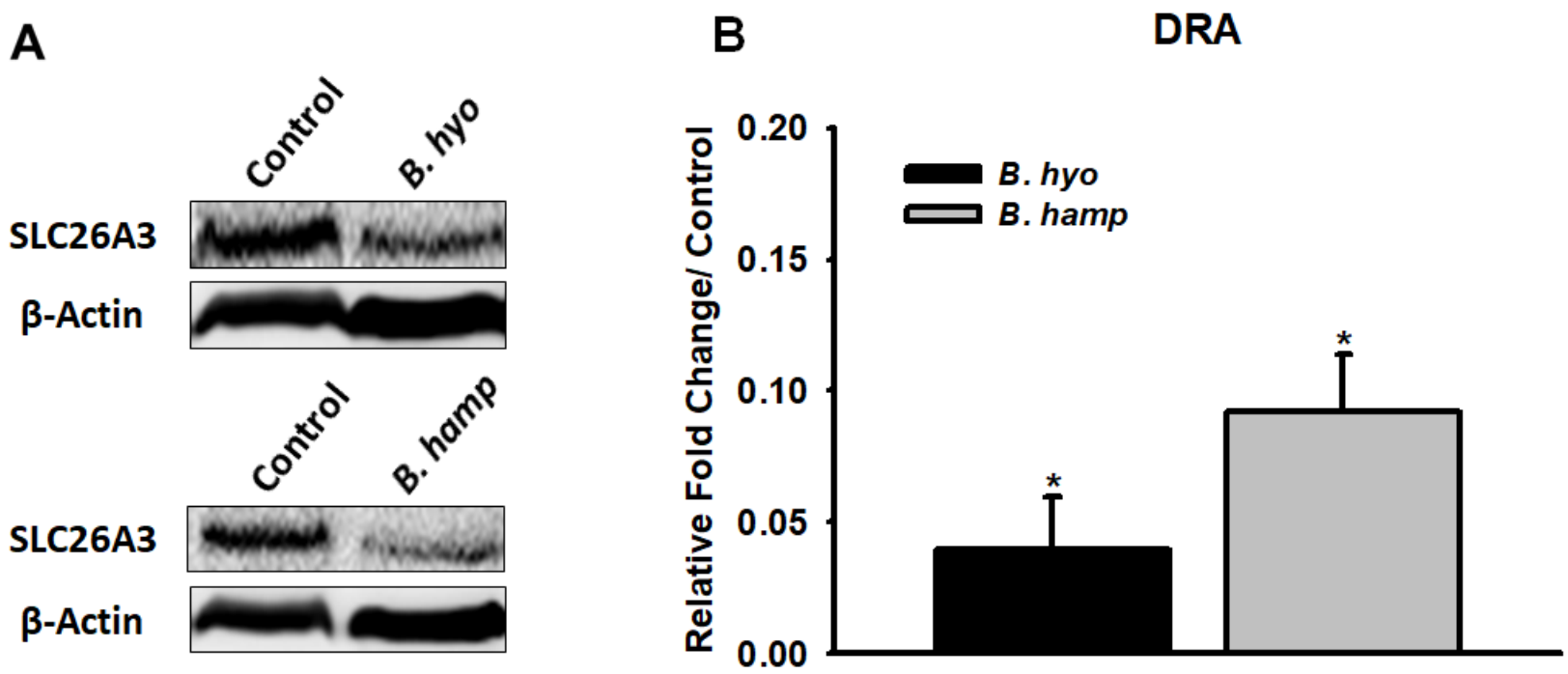

Figure 5.4. *Brachyspira hyodysenteriae* and *Brachyspira hampsonii* strain 30446 significantly reduce DRA protein expression in the apex of the porcine colon.

Western blot (A) and densitometry (B) of DRA (~85 kDa) compared to β-actin (~43 kDa) reference for *B. hyodysenteriae* and *B. hampsonii* strain 30446 infected apex porcine colon compared to control. DRA = down-regulated in adenoma; β-actin = beta-actin. Data presented as mean ± SEM, analyzed using Student's *t*-test. * = $P < 0.05$ (n=3 ctrl, n=3 *B. hyodysenteriae,* n=3 *B. hampsonii* strain 30446).

Table 5.3. Fold changes in SLC26A3 and PTGS2 mRNA expression in polarized Caco-2 cell monolayers after 24hr exposure to IL-1α.*

	Concentration of recombinant human IL-1α			
Gene Name	**Control**	**10ng/ml**	**100ng/ml**	**500ng/ml**
SLC26A3	$1.12^{a} \pm 0.23$	$0.63^{a} \pm 0.09$	$0.67^{a} \pm 0.14$	**$0.47^{b} \pm 0.09$**
PTGS2	$1.00^{a} \pm 0.07$	**$2.22^{b} \pm 0.23$**	**$2.41^{b} \pm 0.29$**	**$2.21^{b} \pm 0.21$**

*Fold changes in SLC26A3 and PTGS2 mRNA expression in polarized Caco-2 monolayers exposed to human recombinant IL-1α for 24hrs. Data presented as mean ± SEM of fold difference in gene expression measured by RT-qPCR. For each gene marked with a different superscript differ by at least $P < 0.05$ compared to control. PTGS2 data is duplicated from Tables 3.7 and 4.5. SLC26A3 = solute carrier family 26 member 3; PTGS2 = prostaglandin-endoperoxide synthase 2 Significantly different values are marked in bold. (n=6).

Discussion

Despite the high prevalence of diarrheal disease caused by *Brachyspira* spp. in both humans and swine, little is known regarding the pathophysiology of diarrheal disease caused by *Brachyspira* spp. In the current study, I examined the role of the Cl^- - HCO_3^- exchanger DRA (SLC26A3) and found that DRA protein expression and function was significantly reduced in the apex of the colon of pigs suffering from *B. hyodysenteriae* and *B. hamp* infection. Furthermore, my study revealed that IL-1α was responsible for the down-regulation of DRA mRNA expression in Caco-2 monolayers, unlike the direct effect of *Brachyspira* on ion channel and transporter transcriptional processes, which were unaffected by IL-1α.

Previous studies assessing the disruption in electrolyte movement following *Brachyspira* infection had been limited to *B.* hyodysenteriae in swine (13, 277). Diarrhea caused by *B. hyodysenteriae* has been historically characterized as a malabsorptive diarrhea in which Na^+ and Cl^- absorption is abolished in the colon of diseased animals (13, 277). However, these studies were performed using a modified version of the Berger and Steele equation in which nonlinear changes in electrolyte movement could lead to erroneous results (277). Additionally, mRNA and protein expression of transporters were not assessed to support the author's findings. Furthermore, the impact of the inflammatory response was not assessed to give mechanism to the observations made.

5.4.1 *Reduced DRA mRNA and protein expression support impaired Cl^- absorption in the apex of the porcine colon following Brachyspira hyodysenteriae and Brachyspira hampsonii infection*

Electroneutral NaCl absorption in the colon primarily occurs through the coupled function of Na^+/H^+ exchanger 3 (NHE3) and Cl^-/HCO_3^- exchanger (DRA) (248). These electroneutral exchangers appear to be critical in maintaining homeostasis as knockout of NHE3 or DRA in mouse models resulted in the development of diarrhea (100, 282). The importance of DRA is further confirmed in patients suffering from inheritable congenital chloride diarrhea who have mutations in the SLC26A3 gene which results in reduced Cl^-/ HCO_3^- exchange and persistent diarrhea (162, 163, 199). These findings provide strong evidence to support the conclusion that loss of DRA function alone is capable of causing diarrheal disease. However, my previous findings have shown that NHE2 and NHE3 isoforms were down-regulated in diarrheic pigs infected with *B. hyodysenteriae* or *B. hampsonii* at both transcriptional and translational levels (Chapter 4). The current study revealed that Cl^- absorption was impaired in diarrheal animals which correlated with reduced DRA mRNA and protein expression. It is important to note that the decrease in Cl^- absorption was not attributed to paracellular loss of Na^+ as barrier function was not compromised in diseased pigs as indicated by the ^{3}H-mannitol flux and previous findings (13)(Chapter 3). Thus, these findings point to the importance of DRA in maintaining electroneutral Cl^- absorption within the colon, and loss of function contributes to diarrhea in *Brachyspira* infected pigs.

5.4.2 *DRA mechanistic loss during Brachyspira infection is unlike that of other enteric pathogens*

Loss of DRA exchange processes have been noted in diarrheal disease caused by other enteric pathogens such as *C. difficile* and enteropathogenic *E. coli* (66, 107). Interestingly, these two pathogens result in decreased DRA function, achieved through the secretion of toxins or effector proteins (66, 107). Purified *C. difficile* toxins TcdA and TcdB decreased DRA proteins expression at low doses at 6 and 24hrs in a dose-dependent manner *in vitro* and *in vivo* (66). This effect appeared to occur via a posttranscriptional mechanism as *C. difficile* toxins did not affect DRA mRNA expression in Caco-2 cells or in the colon of mice (66). These findings were further confirmed by a significant reduction in DRA protein expression in colonic biopsies from patients suffering from *C. difficile* infection (66). Similarly, enteropathogenic *E. coli* infection of Caco-2 and T84 cells reduced DRA function, however, this was not due to a decrease in total protein expression (107). Rather, a decrease in apical DRA expression was due to redistribution to intracellular compartments achieved by secreted effector proteins EspG and EspG2 (107). The redistribution of DRA was attributed to disruption of the microtubular network as EspG and EspG2 have been shown to play an important role in the disruption of microtubules (107, 202, 303). Unlike these two pathogens the *Brachyspira* spp. assessed in the current study caused a significant decrease in DRA mRNA expression in the colon of infected pigs. These findings suggest that the mechanism responsible for the decrease in DRA function and protein expression is unlike that of *C. difficile* and enteropathogenic *E. coli*.

5.4.3 *Paracellular movement of solute is not altered in the porcine colon during Brachyspira infection*

Many bacterial pathogens cause disruption of tight junction proteins leading to increased paracellular movement of solutes and water, contributing to diarrheal development. Bacterial pathogens such as *C. difficile* and enteropathogenic *E. coli* disrupt tight junctions by causing alterations in the cell's cytoskeleton (29, 231, 283). Moreover, other enteric pathogens such as *Bacteroides fragilis* and *Vibrio cholerae* disrupt tight junctions by producing bacterial proteases (29, 216, 217, 325, 326). Infections caused by *B. hyodysenteraie* and *B. hampsonii* appear to be different from many of other enteric pathogens as no significant difference in ^{3}H-mannitol fluxes were observed in colonic samples obtained from diseased and control pigs. My findings are in agreement with previous studies that observed no change in paracellular movement of solutes in diarrheic pigs infected with *B. hyodysenteriae* (13). These findings provide strong evidence supporting the theory that diarrhea caused by *Brachyspira* is strictly malabsorptive in nature.

5.4.4 *IL-1α is responsible for the decrease in DRA mRNA expression*

Reduced gene expression of DRA has been noted in patients suffering from inflammatory bowel disease (IBD) and linked to the direct effects of pro-inflammatory cytokines IL-1β, TNF-α, and IFN-γ (178, 268, 328). My previous findings determined that TNF-α and IFN-γ were either down-regulated or unchanged throughout the colon of *Brachyspira* infected pigs (Chapter 3). Furthermore, IL-1β was upregulated but, only in the distal segment of the colon suggesting that these cytokines are not responsible for the down-regulation of DRA mRNA expression in the apex of diseased pigs (Chapter 3).

IL-1α was the only pro-inflammatory cytokine that was determined to be upregulated throughout the colon of diarrheic pigs and in colonic explants exposed to live *B. hyodysenteriae* (322)(Chapter 3). Previous studies have shown that direct administration of human recombinant IL-1α in Ussing chambers was capable of decreasing both Na^+ and Cl^- absorption in rabbit ileum while eliciting Cl^- secretion (58). However, studies assessing Cl^- secretion in T84 cells grown acutely juxtaposing 18Co cells exposed to IL-1α revealed an increase in PTGS1 and PTGS2 expression resulting in PGE_2 production and Cl^- secretion (131). Based on these findings it appears that IL-1α causes an increase in PGE_2 synthesis which acts on EP_2 and EP_4 receptors on intestinal epithelial cells resulting in elevated cAMP production (72, 297). Thus, electroneutral Na^+ and Cl^- absorption is inhibited by second messenger-mediated inhibition of NHE3 and DRA, rather than altering transporter transcription (74, 82).

I have previously shown that diarrheic pigs suffering from *B. hyodysenteriae* or *B. hampsonii* have significantly reduced anionic secretion throughout the colon which does not agree with what is currently known regarding IL-1α (58). However, previous studies only looked at the effects of IL-1α at concentrations < 5μg/ml. Some cytokines such as IL-1β has been shown to have dose-dependent effects on ion channel transcription in which low doses result in increased expression of CFTR while high doses have an inhibitory effect (44). I have provided strong evidence that polarized Caco-2 monolayers exposed to high concentrations (500μg/ml) of human recombinant IL-1α significantly reduce DRA mRNA expression after 24hrs. This is the first report of IL-1α's ability to modulate DRA mRNA expression *in vitro*. It is possible that IL-1α is responsible for the decrease in DRA gene expression in the colon of diarrheic pigs infected with

Brachsypira, translating into a reduction in DRA protein expression. This study provides strong evidence supporting the conclusion that the loss of Cl^- absorption in the colon of diarrhea pigs through DRA is achieved by the host's cytokine response, ultimately contributing to the development of diarrhea.

5.5 Conclusion

Brachyspira hyodysenteriae and *Brachyspira hampsonii* cause diarrheal disease in swine by evoking a strong pro-inflammatory response leading to a significant decrease in Cl^- absorption. This decrease in Cl^- absorption was attributed to a decrease in DRA mRNA and protein expression in the colon of diseased pigs. To determine if the previously described pro-inflammatory cytokine response was responsible for modulation of DRA expression, Caco-2 cells were exposed to human recombinant IL-1α. DRA was down-regulated in Caco-2 cells after being exposed to IL-1α for 24hrs, thus describing new regulation of DRA by IL-1α. None the less, I provide strong evidence supporting a decreased Cl^- absorptive response in the colon of *Brachyspira* diseased pigs contributing to the development of diarrhea and providing new insight into the pathophysiological mechanisms of spirochetosis.

Chapter 6 - General Discussion

6.1 Implications

Diarrheal disease caused by *Brachyspira* spp. results in production limiting diarrhea in swine worldwide. Pigs suffering from *Brachyspira* colitis experience massive diarrhea accompanied by blood and large amounts of mucus (290). Colonization of the colon results in severe inflammation and activation of the innate immune system. Although this response is important for elimination and clearance of *Brachyspira* spp. I have shown in three studies that destruction of *Brachyspira* and pro-inflammatory cytokine IL-1α alter ion channel and transporter transcription. These alterations in ion transport likely contribute to the development of an altered colonic mucin environment potentially favouring *Brachyspira* colonization resulting in diarrheal disease.

Elevated luminal anion secretion has been associated with many enteric pathogens and is responsible for driving the development of diarrhea. Additionally, anion secretion is also important in maintaining mucin rheological properties, specifically in secreted gel-forming mucins. In chapter 3, I assessed the agonist-induced electrogenic anionic secretory response throughout the spiral colon of pigs experimentally challenged with *B. hyodysenteriae* and *B. hampsonii*. Rather than an elevated anionic secretory response, I found that diarrheic pigs had a significantly reduced agonist-induced anionic secretory response. I also assessed whether a decrease in K^+ flux might be responsible for the decrease in anion secretion observed through the use of ^{86}Rb flux studies in Ussing chambers. ^{86}Rb is effectively transported through K^+ channels and is used as a radiolabelled marker to replace radiolabelled K^+ (201). However, during the equilibration period, there was no significant difference in

J_{ms}, J_{sm}, or J_{net} fluxes (Figure A). Gene expression of the major anionic transporters in the colon revealed reduced levels of CFTR throughout the colon of diseased pigs. TMEM16A was not reduced at the mRNA level however, western blot analysis revealed that TMEM16A protein expression was significantly reduced in all three segments of diarrheic pigs compared to controls. I was unable to measure CFTR protein expression as no CFTR antibodies tested reacted with pig colonic tissue. However, a recent study has shown that knockout of TMEM16A eliminated cAMP and Ca^{2+} activated anionic currents in the adult murine colon, providing evidence that TMEM16A is required for CFTR expression and function (26). These findings suggest that the decrease in anionic secretion is not due to reduced K^+ conductance but rather a decrease in mRNA and protein expression of apically expressed anion channels.

Using a Caco-2 cell culture model I analysed the effects of IL-1α and a *B. hampsonii* lysate on modifying CFTR mRNA expression to determine which treatment may account for the decrease observed *in vivo*. I found that IL-1α was unable to decrease CFTR mRNA expression but, the *B. hampsonii* lysate did at my pathophysiologic concentration. Thus, it appears that the decrease in anion secretion is attributed to a direct effect of the *Brachyspira* lysate. However, this decrease in anion secretion does not drive the development of diarrhea, rather it likely influences mucin rheological properties, possibly creating a favourable environment for *Brachyspira* colonization.

Many enteric pathogens utilize or modify the mucin environment within the host's gastrointestinal tract as part of their pathogenesis. Pathogens such as *V. cholerae* cause depletion of mucus in the small intestine likely allowing for greater access to the epithelium for binding of GM1 ganglioside receptors (134, 185, 227). In contrast,

ETEC's heat labile enterotoxin induces MUC2 secretion in the host's small intestine. This change in the mucin environment is favoured by ETEC as it secretes EtpA, an adhesin that allows binding to both secreted and transmembrane mucins (179). Previous studies have shown that *B. hyodysenteriae* and *B. hampsonii* alter the colonic mucin environment by elevating production of MUC2 and MUC5AC and subsequently binding to these mucin carbohydrate structures, suggesting that mucins are important for *Brachyspira's* pathogenesis (251, 323). As mucin rheological properties are heavily influenced by anion secretion, I believe that *Brachyspira* spp. likely produce a toxin or molecule which is responsible for the decrease in anion secretion. This pathophysiological mechanism has been observed in cystic fibrosis airways, as the lack of anion secretion through CFTR causes mucus thickening leading to the formation of mucus plaques, contributing to *Pseudomonas aeruginosa* colonization (139, 144, 250, 305). Thus, I believe that this decrease in anion secretion results in an altered colonic mucin environment which likely promotes *Brachyspira* colonization. However, the question still remains whether the thickening and aggregation of the mucins allow motile *Brachyspira* to outcompete other bacteria present in the colon or it may be possible that the reduction in mucus clearance due to altered rheological properties potenitally drives colonization.

In chapter 4, I assessed Na^+ absorption in diarrheic pigs as a potential contributor to the development of diarrhea. I found that electroneutral (NHE) but, not electrogenic (ENaC) Na^+ absorption was impaired in diarrheic pigs. Loss of NHE isoforms 2 and 3 have been observed in diarrheal disease caused by other enteric pathogens (113, 125, 292). I found that downregulation of NHE3 was not attributed to

the host's inflammatory response as IL-1α was not capable of decreasing NHE3 mRNA in Caco-2 cells. Rather NHE3 mRNA was decreased after exposure to a pathophysiologic concentration of *B. hampsonii* lysate *in vitro*. My findings suggest that loss of electroneutral Na^+ absorption in the colon of diseased pigs through NHE isoforms 2 and 3 is a major contributor to diarrhea caused by these two *Brachyspira* spp.

Interestingly, electrogenic Na^+ via ENaC was not significantly different between control and diseased pigs in any segment of the porcine colon sampled. Furthermore, gene expression of ENaC subunits supported this observation. Although speculative, the ability of diarrheic pigs to continue to absorb Na^+ via ENaC during diarrheal episodes may prevent severe ionic imbalances and fluid loss, which would result in death. Previous research has shown that mineralocorticoids such as aldosterone elevate ENaC expression throughout the colon (279, 324). My electrophysiological and gene expression data, however, does not show elevated expression of ENaC throughout the colon thus leading me to believe that mineralocorticoids are not involved in diarrheal disease caused by *B. hyodysenteriae* and *B. hampsonii*.

In chapter 5, I assessed Cl^- absorption and barrier function in diarrheic pigs. A portion of Cl^- absorption occurs paracellularly as Cl^- follows Na^+, the second route in the colon is via electroneutral Cl^-/HCO_3^- exchange through DRA (SLC26A3) (270). I determined that paracellular transport of solute was unaffected in diarrheic pigs, however, electroneutral Cl^- absorption was significantly impaired. Loss of anion exchange through DRA has been associated with diarrheal disease (66, 162, 321, 327). In the case of DRA, the significant increase in pro-inflammatory cytokine IL-1α observed

throughout the colon of diseased pigs was responsible for the downregulation of DRA. This is the first time that regulation of DRA transcription by IL-1α has been described. In addition to new cytokine regulation of DRA, I have shown that impairment of DRA in diseased pigs contributes to diarrheal development in addition to the decrease in electroneutral Na^+ absorption.

Together these three studies provide new insight into the pathophysiological mechanisms of *B. hyodysenteriae* and *B. hampsonii*. Previous studies assessing ion transport in isolated colonic loops in *B. hyodysenteriae* diseased pigs observed that Na^+ and Cl^- absorption was inhibited while anion secretion and paracellular transport was not different from control (13, 277). My studies largely agreed with these original observations with the exception of the unchanged anion secretion. This is likely due to the authors using a simplified version of the Berger and Steele equation to indirectly calculate the blood to lumen change in anionic flux (277). Thus, a decrease in anion secretion would have been overlooked as a larger decrease in absorption was present (277).

This decrease in anion secretion and the resulting modification of the colonic mucin environment potentially initiates the pathogenesis of *B. hyodysenteriae* and *B. hampsonii* by promoting a favourable colonic mucin environment for colonization. Thus, a decrease in anion secretion lends new insight into the pathogenesis of these two *Brachyspira spp..* Furthermore, my studies have identified NHE2, NHE3, and DRA as the transporters responsible for the development of diarrheal disease following *Brachyspira* infection, which has not been described previously. I have also provided novel mechanisms for the observed changes in ion transport observed *in vivo*. The

decrease in anion secretion and loss of NHE isoform mRNA and protein was attributed to direct effects of *Brachyspira*, potentially a secreted toxin. The decrease in DRA mRNA and protein, however, was attributed to the host's profound IL-1α response noted throughout the colon.

Understanding the pathophysiological mechanisms associated with the pathogenesis of *Brachyspira* spp. in swine could provide new vaccine targets to help mitigate this disease. I know that a *B. hampsonii* lysate is capable of modifying ion channel gene expression, however, at the current time it is unknown whether a specific protein or toxin is responsible for this effect. Purification of toxins produced by *Brachyspira* spp. resulting in similar pathophysiological effects *in vitro* and/or *in vivo* can be used as tools in developing a subunit vaccine. Furthermore, these studies may provide new insight into the potential mechanisms associated with human intestinal spirochetosis caused by *B. pilosicoli* and *B. aalborgi*.

6.2 Limitations of this Research

As with all research utilizing different scientific models creates limitations to what can be studied and how and how those studies can be conducted. Using a porcine model comes with a variety of limitations and challenges that make researching specific aspects very difficult to impossible. Thus, this section will discuss the major limitations that I encountered during the duration of my program.

I assessed changes in ion transport in the porcine colon after the onset of peak clinical signs (bloody-mucoid diarrhea). However, due to the nature of my study, I was not able to assess the changes in ion transport during the development of diarrhea.

Variability in the time it took pigs to progress from a fecal score of 0 to 4 was high, making it impossible to know when to euthanize pigs to assess other time points other than peak clinical signs. Furthermore, assessing ion transport at other time points was beyond the scope of my research, however, it would provide valuable information on gene and protein expression in the mucosa during the early stages of the disease. Thus, these experiments should be conducted in the future to fully characterize the pathophysiological mechanism of diarrhea caused by *B.hyodysenteriae* and *B. hampsonii.*

In chapter 3 I concluded that changes in anion secretion specifically secretion of HCO_3^- was responsible for altering mucin rheological properties in the porcine colon which likely favoured *Brachyspira* colonization and growth. However, in this study, I was unable to directly measure HCO_3^- transport through the colonic tissues. Radiolabelled HCO_3^- fluxes were not ran for safety reasons as HCO_3^- and H^+ is turned into CO_2 and H_2O via the carbonic anhydrase reaction. Our Ussing chamber setup is not secured in a fume hood so these experiments could not be run. I could have utilized gut loop studies which were previously used (13, 277), however, these studies do not account for the serosal to mucosal movement of ions, which was the main focus of this study.

Utilizing a porcine model created a major challenge as many commercial, scientific products, specifically antibodies for ion channels, are not created to react with pig tissue. Thus, a major limitation of my first study in chapter 3 was the inability to directly measure CFTR protein expression in the porcine colon by western blot or any other antibody reliant scientific technique as none of the antibodies tested reacted with porcine colon (Table A).

A major limitation of all three studies in this thesis was that no commercially available immortalized porcine colonic epithelial cell lines currently exist. I experimented with polarized primary colonic epithelial cultures, however, once these primary cells reached confluency they would die before they could be subject to the *Brachyspira* lysate. This led me to immortalize my own porcine colonic epithelial cell line using a retrovirus, however, this cell line was not ready to be used for experimentation during my research program. As a result, I utilized Caco-2 cells, which are derived from human colon to test my *B. hampsonii* lysate on. Thus, although I observed results that favoured my observations *in vivo,* it is difficult if not impossible to conclude that the *Brachyspira* lysate would cause the same pathophysiologic effects in porcine colonic epithelial cells.

Another limitation of utilizing cell culture models is that they need to be grown in an oxygen rich environment. *Brachyspira* spp. are anaerobic making it impossible to co-culture live bacteria on polarized monolayers. I attempted this multiple times and was unable to culture the *Brachyspira* on blood-agar plates after co-culture of the bacteria and cells in the CO_2 incubator. However, through use of 3D printing, it could be possible to develop an apparatus that allowed for co-culturing polarized monolayers with anaerobic bacteria so that the cells could be grown in 100% CO_2 while being fed nutrients and oxygen through the basolateral membrane. Although nothing like this currently exists it could be the focus of future research.

This inability to co-culture *Brachyspira* with Caco-2 cells caused me to use a whole cell *B. hampsonii* lysate. This lysate, however, contains all cellular components of the bacteria including LPS which may be responsible for the pathophysiological changes observed. The next step in this experiment would be to fraction out proteins in

the lysate based on size to determine which proteins are responsible for the observations made in my studies.

Many of these limitations created new questions which need to be addressed by future research. In section 6.3 the next steps to fully characterize the pathophysiological mechanism of diarrhea caused by *B. hyodysenteriae* and *B. hampsonii* will be discussed.

6.3 Future Research

In my three studies, I have characterized the pathophysiologic and molecular mechanisms involved in the pathogenesis and development of *Brachyspira* induce diarrhea in swine. I along with others have identified that destruction of *Brachyspira* causes changes in ion transport and mucus secretion. However, at the current time, it is unknown what toxin or protein associated with *Brachyspira* is responsible for this cellular response. I have concluded that both the host's cytokine response and direct effects off the bacteria are responsible for changes in ion transport in the porcine colon resulting in diarrheal disease.

Future studies need to identify what proteins or molecules associated with *Brachyspira* are capable of modifying ion transport and invoking the inflammatory response. I utilized a whole cell *B. hampsonii* lysate; the next step would be to isolate proteins based on their molecular size to determine what size of protein(s) can mirror my results. Currently, in our lab purification of hemolysins produced by *Brachyspira* spp. by HPLC is being conducted. It is possible that these bacterial associated proteins may aid in the pathogenesis of the disease by modifying the host's cytokine response or by

directly modifying transcription and/or translation of ion channels in the porcine colon. It is important to note, however, that I did not assess all known cytokines. Thus, an untested cytokine may be responsible for the decreased ion channel mRNA and protein expression observed *in vivo*.

I used a human colonic cell line model to assess molecular changes in ion channel mRNA expression after exposure to a *B. hampsonii* lysate. Limitations of this approach have been discussed in section 6.2. Thus, use of immortalized colonic cell lines created by myself and others in our lab can be used to assay the lysate and other proteins of interest to determine which target(s) are responsible for the alterations in ion transport.

The limitations of assessing colonic ion transport in pigs at several time points during the development of diarrheal disease have been discussed in section 6.2. However, this study would provide a lot of information regarding the entire pathophysiological mechanism of *Brachyspira* induced diarrhea. Although speculative it is possible that diarrhea caused by *Brachyspira* spp. is initiated by an increase in anion secretion. Furthermore, the host's cytokine response may be significantly different during the onset of the disease compared to peak clinical signs. This study, however, is logistically challenging as there is high variability in the development of diarrhea between pigs and additional lab equipment and skilled persons would be required. Thus, development of an *in vitro* co-culture method with *Brachyspira* spp. and porcine colonic epithelial cells would be very useful to determine the pathophysiological changes occurring at multiple time points. The use of organoids may be a potential way to assess these changes *in vitro* as opposed to traditional cell monolayer models.

Diarrhea caused by *B. hyodysenteriae* and *B. hampsonii* is accompanied by what is thought to blood. This observation, however, has never been confirmed that whole red blood cells are present is the feces of diseased pigs. I have shown that both TEER and paracellular movement of mannitol is unchanged in the colon of diarrheic pigs compared to control. These findings suggest that disruption of tight junctions does not contribute to the development of diarrhea or allow for the movement of red blood cells into the lumen of the colon in diseased pigs. Thus, future work needs to determine if blood is actually present in the feces of diseased pigs, and if so, how this pathophysiological mechanism occurs.

Appendix

Descriptive Materials & Methods

As this thesis was written in a manuscript style format, more descriptive materials and methods have been added to this thesis.

Animals

Fifty-four 6-8 week-old purebred Yorkshire barrows were housed in pairs with 12 pigs per room and provided antibiotic-free diet high in soybean meal and water *ad libitum*. Treatment groups were each housed in separate BSL2 animal care rooms at 18˚C. Pigs were acclimated to their new environment for 7 days before inoculation with either *Brachyspira hyodysenteriae* strain G44 (kindly provided by Boehringer-Ingelheim Vet Medica, St. Joseph, MO; n=17), *Brachyspira hampsonii* strain 30446 (n=16), or a mock inoculum of sterile liquid culture media (n=18). The number of pigs in each group differed slightly because inoculated pigs that did not develop bloody-mucoid diarrhea were not used. Feeders were removed from pens 12 hours prior to inoculation to simulate a feed outage, but water was not. Inoculation was conducted by passing a stomach tube and flushing 30ml of 10^8-10^9 cells/ml inoculum into the stomach of a pig, followed by sterile PBS as previously described (266). Pigs were then assessed daily for clinical signs of disease, and fecal consistency-scores were graded twice daily using a 0-4-point scale (0=formed, normal; 1=soft, wet cement consistency; 2=runny or watery; 3=mucoid diarrhea; or 4=bloody-mucoid diarrhea) to accurately determine the onset and severity of diarrhea as previously described (266). *Brachyspira hyodysenteriae* and *Brachyspira hampsonii* strain 30446 pigs developed bloody-mucoid

diarrhea within 3-7 days after inoculation and were euthanized 24 hours after onset of dysentery. Control pigs remained healthy (non-diarrheic) and were euthanized on an age-matched basis with inoculated pigs euthanized the same day. Pigs were euthanized by intracranial captive bolt and exsanguination. This research was designed and conducted in accordance with the Canadian Council for Animal Care and approved by the University of Saskatchewan Committee on Animal Care and Supply (Protocol #20130034).

Electrogenic Ussing chamber studies

After euthanasia, 17-18 cm segments of proximal (2.5 cm distal from the cecum), apex of the spiral colon (midpoint between the cecum and sigmoid colon) and distal (sigmoid colon) colon were collected and washed with Krebs buffer (pH 7.4) containing (in mM) 113 NaCl, 5 KCl, 1.6 Na_2HPO_4, 0.3 $NaH_2PO_4 \bullet H_2O$, 25 $NaHCO_3$, 1.1 $MgCl_2 \bullet 6H_2O$, 2.2 $CaCl_2 \bullet 2H_2O$ and 10 glucose, and chilled to 4ºC. Samples were immediately transported to the lab in Krebs buffer gassed with 95% O_2 -5% CO_2 where the serosa (visceral peritoneum) and longitudinal and circular muscle layers of the colonic wall were removed with forceps (stripped) from all segments leaving only the mucosa and submucosal rudiments as previously described (61). Pieces of stripped mucosa (2-4 tissue replicates of each segment per pig) were then placed on $1cm^2$ tissue Ussing chamber inserts and inserted into the Ussing chamber (Physiologic Instruments, San Diego, CA). Each reservoir was independently gassed with 95% O_2-5%CO_2. A heated circulating water bath maintained the buffer in the Ussing chamber at 37ºC. Transepithelial potential differences were short-circuited to 0 mV with a voltage

clamp using Ag-AgCl electrodes and 3M KCL agar bridges (Physiologic Instruments, San Diego, CA) on apical and basolateral sides as previously described (61).

Tissues were allowed to equilibrate for twenty minutes before the addition of any drugs. A 1mV pulse every 30 seconds was used to determine the resistance and tissue viability from the resulting current. After the equilibration period, 0.1mM amiloride (A7410; Sigma Aldrich) was added to the apical side of the Ussing chamber to selectively inhibit ENaC. Once steady state was reached, 10µM of the adrenergic agonist isoproterenol (I6504; Sigma Aldrich) was added to the basolateral side of the chamber to increase cAMP physiologically and stimulate cAMP-activated channels, such as CFTR. After steady state was reached, 0.1mM of carbachol (C4382; Sigma Aldrich) was added to the basolateral side of the chamber. This cholinergic agonist increases intracellular Ca^{2+} activating calcium-activated channels. After steady state was reached, 10µM forskolin (F6886; Sigma Aldrich) and 1mM of 1M 3-isobutyl-1-methylxanthine (IBMX) (I5879; Sigma Aldrich) were added to the apical and basolateral sides of the Ussing chamber causing a massive irreversible and sustained elevation in cAMP to fully activate cAMP-activated secretion. Finally, after steady state was reached 0.1mM bumetanide (B3023; Sigma Aldrich) was added to the basolateral side of the Ussing chamber to inhibit the basolateral Na^+-K^+-$2Cl^-$ co-transporter 1 (NKCC1). Changes in short-circuit current were recorded and analyzed using LabChart 7 software (ADInstruments, Colorado Springs, CO).

Characterization of electroneutral absorptive response in healthy and diseased porcine colon - radiolabelled isotope flux studies

The apex of the spiral colon was collected following euthanasia and samples were prepared according to the protocol described above in the *Electrogenic Ussing Chamber Studies* section. Once the colonic tissues (12 tissue replicates per pig) were inserted into the Ussing chambers, short-circuit current was recorded, and tissues were paired with the tissue next to it. Tissues were recorded for twenty minutes before the addition of a radiolabelled isotope to reach a steady state current. One µCi of isotope (^{22}Na, ^{36}Cl, ^{3}H-mannitol, ^{86}Rb) was added to the apical side of chamber #1, and one µCi was added to the basolateral side of chamber #2. The side of the chamber that isotope is added too is referred to as the "hot side," and the opposing side is referred to as the "cold side." After the addition of isotope, 100µl samples were removed from the hot sides of both chambers #1 and #2 immediately and placed in glass (^{22}Na) or scintillation (^{36}Cl, ^{3}H-mannitol, ^{86}Rb) vials containing 5ml of Ultima Gold™ scintillation cocktail (PerkinElmer, Waltham, MA). The 100µl removed from the Ussing chamber was immediately replaced with 100µl of fresh Krebs buffer. 500µl samples were removed from the cold side of chambers #1 and #2 and placed in the appropriate vials and immediately replaced with 500µl of fresh Krebs buffer. 500µl samples were removed from the cold side for the first 60 (^{36}Cl, ^{3}H-mannitol) to 80 (^{22}Na, ^{86}Rb) minutes for steady-state flux to be achieved. Different activators or inhibitors of electroneutral ion transport were then added to determine their effect on electroneutral transport. These specific drugs are described in the materials and methods within each data chapter. ^{22}Na samples were counted on a Titertek Plus gamma counter while ^{36}Cl, ^{3}H-mannitol,

and ^{86}Rb were counted on a beta counter to determine cpm values.

Tissues were then paired based on upon each tissue's resistance. Tissues which had resistances that differed <15% of each other were paired. cpm values were used to calculate unidirectional mucosal-to-serosal (J_{ms}) and serosal-to-mucosal (J_{sm}) fluxes based on the following equation (281):

$\Phi_{ms/sm} = v_s(p_{s2} – cp_{s1})/(\Delta t \cdot p^* \cdot A)$

Where: $\Phi_{ms/sm}$ = the unidirectional isotopic flux J_{ms} or J_{sm} ($\mu mol/cm^2 \cdot hr$) or ($\mu eq./cm^2 \cdot hr$)

v_s = volume (cm^3) of buffer on the serosal surface (cold side)

p_s = cpm/cm^3 on the cold side reservoir

c = dilution correction factor

Δt = the time between sample collection (hr)

p^* = the specific activity of the isotope on the hot side (cpm/µmol of total ion of interest in 1ml of buffer)

A = area of the tissue in Ussing chamber insert = 1.0 cm^2

Net flux was then calculated from the resulting values ($J_{net} = J_{ms} – J_{sm}$) for each isotope as previously described (281). Positive net flux values indicate net absorption while negative values indicate net secretion of the isotope.

RNA isolation from porcine colon and polarized Caco-2 monolayers

Mucosal samples collected at the time of euthanasia and subsequently stored in RNAlater® (AM7021; Ambion®) at -80˚C were homogenized in 1ml of TRIzol reagent (15596018; Life Technologies). Likewise, polarized Caco-2 monolayers were harvested by the addition of 1ml of TRIzol to each 24mm Transwell® permeable support and

subsequently pipetting up and down allowing for the removal of all cells. TRIzol works by maintaining RNA integrity during tissue homogenization, while at the same time breaking down cells and cell components. Following the homogenization, the samples were centrifuged for 10 minutes at 12,000 x g at 4ºC, and the supernatant containing the RNA was transferred to a new tube. The samples were then incubated at room temperature for 5 minutes to permit complete dissociation of the nucleoprotein complex. 0.2 ml of chloroform was then added to each sample and tubes were shaken by hand for 15 seconds. The chloroform is used for purifying the nucleic acids and eliminating proteins by causing them to be separated into the organic phase while the RNA remains in the aqueous phase. Samples were incubated at room temperature for 3 minutes and then centrifuged for 15 minutes at 12,000 x g at 4ºC. The aqueous phase was then transferred into a new tube to begin the RNA isolation procedure.

100µl of RNase-free glycogen was then added to each sample. Glycogen acts as a carrier to the aqueous phase, but does not inhibit first-strand synthesis, and does not inhibit PCR. 0.5ml of 100% isopropanol was added to the aqueous phase which rids the aqueous phase of alcohol soluble salts. RNA is insoluble in isopropanol thus, during centrifugation RNA will aggregate forming a pellet. Samples were incubated at room temperature for 10 minutes and subsequently centrifuged for an additional 10 minutes at 12,000 x g at 4ºC. After centrifuging the samples, an RNA pellet became visible on the bottom of each tube. However, if an RNA pellet was not formed an additional 100µl of RNase-free glycogen was added, and the sample was centrifuged for an additional 10 minutes.

Washing of the RNA pellet was conducted by removing the supernatant from each sample by vacuum suction and replaced with 1ml of 75% ethanol. 75% ethanol is used to wash the RNA pellet because at this concentration of ethanol proteins and salts remain in solution while RNA remains insoluble which allows for purification of the RNA pellet. After the addition of 75% ethanol, the samples were centrifuged for 5 minutes at 7500 x g at 4ºC and following this step the aqueous phase was removed by vacuum suction and discarded. The RNA wash with 75% ethanol was subsiquently conducted a second time. Following the second ethanol wash, the RNA pellets were air dried for 10 minutes to allow any remaining ethanol in the tube to evaporate.

RNA pellets were resuspended in 100µl of RNase-free water and subsequently passed up and down several times through a pipette tip. The resuspended pellets were then placed in a heat block for 12 minutes at 56ºC. RNA samples were then tested on one of two nanodrop machines to determine the concentrations of RNA present in each sample. A standard of <500ng/µl was used as exclusion criteria for RNA samples.

Reverse transcription

cDNA was created from mRNA using the GoScript Reverse Transcription system (A5001; Promega). The reverse transcriptase procedure was carried out by mixing 3µl of RNA with 1.75µl of RNase-free water, 0.5 µl D.P, 0.5 µl R.P, 0.5 µl dNTP, 1µl $MgCl_2$, 2µl Buffer, 0.25 µl RNase and 0.5 µl RT per sample to give a total volume of 10 µl. Samples were then transferred into the thermocycler to create cDNA. Samples were subject to 25˚C for 5 minutes, followed by 42˚C for 30 minutes, and finally 85˚C for 5 minutes. cDNA was then diluted with 200µl of RNase-free water and frozen at -80ºC.

Quantivative PCR and fold difference calculation

Quantitative PCR was performed by mixing 12.5µl PCR mix, 6.5µl RNase-free water and 1µl of a combined mixture of gene specific forward and reverse primers. qPCR was performed in duplicate and 2.5µl of cDNA was then added to each well resulting in a total volume of 12.5µl. Samples were run in a Stratagene Mx5000P real-time qPCR machines for 40 cycles. The average C_T (cycle threshold) value was used to calculate the fold difference of each gene between control and diseased colonic samples as well as control and treated cell cultures using the ΔΔCt calculation method:

$$\text{Ratio} = \frac{(\text{Eff}_{\text{target}})^{\Delta\text{CT target (Mean control – Mean sample)}}}{(\text{Eff}_{\text{ref}})^{\Delta\text{CT ref (Mean control – Mean sample)}}}$$

Primer design and efficiency calculation

Porcine primers were designed for GAPDH, CFTR, TMEM16A, ANO6, ANO9, ANO10, BEST2, BEST4, CLCA1, CLCA4, NKCC1, NHE1, NHE2, NHE3, ENaC-α, ENaC-β, ATP1A1, SLC26A3, IL-1α, IL-1β, IL-6, IL-8, IL-10, IL-17A, IL-18, TNF-α, IFN-γ, TGF-β1, TGF-β2, TGF-β3. MUC1, MUC2, MUC4, and MUC5AC (Tables 3.1, 4.1, 5.1). Porcine GAPDH was used as the reference gene for analyses. Human primers were designed for GAPDH, CFTR, NKCC1, NHE2, NHE3, SLC26A3, IL-1α, IL-1β, and PTGS2 (Table 3.2, 4.2, 5.2). Human GAPDH was used as the reference gene for analyses.

Primers were developed in house and designed with PrimerQuest (Integrated DNA Technologies) to span exon-exon junctions and subsequently checked for cross-reaction by using NCBI's Nucleotide-BLAST. Primers were also designed to target all known target gene transcript variants. Standard curves were created by running primer

sets with cDNA serial dilutions ($1 \times 10^{0} – 1 \times 10^{-6}$) to calculate the primer efficiency (Efficiency (%) = $10^{(-1/slope)}$) and to ensure that only a single product was amplified. Only primers amplifying a single product and having a primer efficiency greater than 85% were used. qPCR was performed in duplicate, and a negative control was used to verify the absence of genomic DNA contamination All Ct values used in the analysis for control and diseased pigs were between 15-35.

Western blot and densitometry analysis

Protein was extracted from stripped control and diseased colonic samples from the proximal, apex and distal sections of the porcine colon using the ProteoExtract transmembrane protein kit (71772-3; Novagen®). Colonic samples were sliced in to ~2mm^3 pieces and added to 2ml of ice-cold PBS. Samples were subsequently centrifuged at 100 x g for 2 minutes at 4˚C, and the supernatant was discarded, and this step was repeated. Tissues were then homogenized in the presence of 2ml of ice-cold Extraction Buffer 1 containing 5µl of Protease Inhibitor Cocktail Set III. Samples were incubated on ice for 10 minutes with gentle agitation and then centrifuged at 1000 x g for 5 minutes at 4˚C. The supernatant (cytosolic fraction) was removed and stored at -80˚C, while the tissue pellets were resuspended in 5ml of ice-cold PBS and centrifuged at 1000 x g for 5 minutes at 4˚C and the supernatant, was discarded. The tissue pellets were then resuspended in 200µl of Extraction Buffer 2B in the presence of 5µl Protease Inhibitor Cocktail III and incubated on ice with gentle agitation for 1 hour. Following the incubation period, samples were centrifuged at 16,000 x g for 15 minutes at 4˚C, and

the supernatant containing the integral membrane proteins were transferred to a new tube and stored at -80˚C.

Protein samples were boiled in 2x denaturing buffer (20% glycerol, 4% SDS, 125 mM Tris pH 6.8, 0.3 mM bromophenol blue) containing 10-20% β-mercaptoethanol (BME; M6250; Sigma-Aldrich) for five minutes and analyzed by 10% SDS-PAGE (286).

For western blot analysis, proteins were transferred onto PVDF membrane (RPN303LFP; GE Healthcare Life Sciences) at 0.2mA for 4 hours at 4ºC with transfer buffer (25mM Tris, 192mM glycine, 20% methanol) (286). Membranes were blocked for an hour at room temperature with a 10% RapidBlock™ (M325-AMRESCO®) blocking solution and subsequently probed overnight at 4˚C with primary antibodies anti-TMEM16A (1:1000) (QC13356-42173; AVIVA Biosciences), anti-NHE3 (1:1000) (ARP43870_P050; AVIVA Biosciences), anti-SLC26A3 (1:500) (PA5-68530; Invitrogen), and anti-β-Actin (1:2000) (C-4; sc-47778; Santa Cruz Biotechnology) verified by the supplier to react with pig in PBST or a 10% RapidBlock™ solution. Membranes were washed with PBST a total of three times to remove all primary antibody. Membranes were then incubated for 1 hour at room temperature with secondary antibodies Alexa Fluor 488 Goat anti-Rabbit IgG antibody (1:2000) (A-11008; Thermo Fisher Scientific) and ECL Plex Goat anti-Mouse IgG-Cy5 antibody (1:2000) (PA45009; Amersham Biosciences) in PBST. Membranes were then washed with PBST three times and then four additional times with gentle agitation for 5 minutes each. Membranes were then washed three times with PBS and allowed to dry. Proteins were subsiquently detected and analyzed using Typhoon Trio and ImageQuant TL System (63005583; GE Healthcare Life Sciences).

Densitometry was conducted using ImageQuant software (63005583; GE Healthcare Life Sciences). Background from each blot was subtracted from the densitometry value of each target and house keeping band. The target band was then normalized to the house keeping protein (β-actin), and relative protein expression for diseased tissues were compared to the mean relative protein expression for control tissues. The data was then presented as relative fold change in protein expression compared to control.

Cell culture

The Caco-2 cell line derived from human colorectal adenocarcinoma (HTB-37; ATCC, Manassas, VA) were cultured in Dulbecco's modified Eagle medium (DMEM) (10-0130CM, Corning, Manassas, VA) containing 10% heat-inactivated fetal bovine serum (Gibco, Burlington, ONT, Canada) Grand, 1% penicillin-streptomycin (15140-122; Life Technologies), and 1% MEM non-essential amino acids (Gibco, Grand Island, NY) at 37˚C in a humidified atmosphere with 5% CO_2. Cells were plated on polyester Transwell® permeable supports (0.4µm pores, 24 mm in diameter, Corning) and cultured under standard conditions until confluency (1 x 10^6 cells). Cells were maintained for 10 days after confluency was achieved and media was replaced every two days before being used in downstream experiments.

Exposure of Caco-2 monolayers to recombinant human IL-1α

Polarized human colorectal adenocarcinoma (Caco-2) monolayers were exposed to human recombinant IL-1α (I2778; Sigma Aldrich). Polarized Caco-2 monolayers were subsequently probed for changes in CFTR, NHE2, NHE3, SLC26A3, and PTGS2 mRNA expression by RT-qPCR. Both apical and basolateral surfaces were exposed to

IL-1α at concentrations of 10, 100 and 500 ng/ml for 24hrs in the presence of fetal bovine serum. The Caco-2 cell line was chosen as no porcine colon-derived cell lines are commercially available. To ensure that IL-1α had a biological effect on Caco-2 monolayers, qPCR primers were developed for prostaglandin-endoperoxide synthase 2 (PTGS2) which has been previously shown to become up-regulated in multiple cell types after IL-1α exposure (58, 131, 259).

Caco-2 monolayer exposure to Brachyspira hampsonii lysate

To determine if *Brachyspira* has a direct effect on modulating ion channel expression I wanted to determine if a whole cell *Brachyspira* lysate was capable of down-regulating CFTR, NHE3, and SLC26A3 mRNA expression in Caco-2 cells. The *Brachyspira hampsonii* strain 30446 lysate was prepared by centrifuging 50ml of culture broth containing actively motile spirochete bacteria (10^8/ml) at 10,000 X *g* for 40 min, after which the supernatant was poured off (224). Bacterial pellets were resuspended in phosphate buffered saline (Gibco; 10010-023, Life Technologies) and vortexed until the pellet completely dissolved. This material was subsequently disrupted by sonication (Sonics & Materials Inc., Danbury, CT, USA) at 50% duty for 120 s at 4˚C (224). Lysate total protein concentrations were determined using BCA protein assay (ThermoFisher; Rockford, IL) using bovine serum albumin (BSA) as a standard according to the manufacture's protocol. Polarized Caco-2 monolayers were exposed apically to the whole cell *Brachyspira hampsonii* lysate (0.005-50µg/ml) in PBS or a PBS control for 48hrs. 50µg/ml of total bacterial protein was determined to be ~10^8 CFU/ml and corresponded to 1 x 10^6 cells thus, considered a pathophysiological concentration.

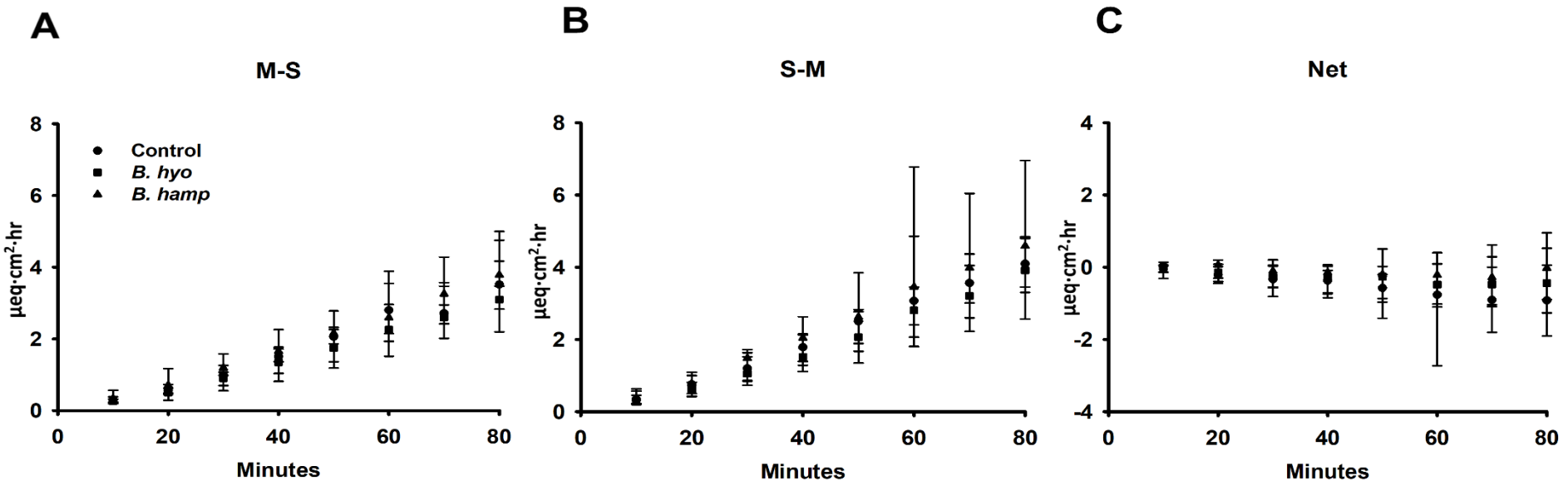

Figure A.1. *Brachyspira hyodysenteriae* and *Brachyspira hampsonii* strain 30446 do not affect K^+ transport during ^{86}Rb equilibration in the apex of the porcine spiral colon.

Basal J_{ms} (A), J_{sm} (B), and net (C) flux rates during ^{86}Rb equilibration across apex colonic segments from control, *B. hyodysenteriae*, and *B. hampsonii* diseased pigs. M-S, unidirectional mucosal-to-serosal ^{86}Rb flux; S-M, unidirectional serosal-to-mucosal ^{86}Rb flux; Net, net ^{86}Rb flux. Data presented as median $\pm$ IQR, analyzed using Kruskal-Wallis one-way analysis of variance. (n=12 ctrl, n=12 *B. hyodysenteriae*, n=12 *B. hampsonii* strain 30446).

Table A.1. CFTR antibodies tested

CFTR Antibody	Manufacturer
CFTR H-182	Santa Cruz Biotechnology
596	Chapel Hill
1I22	Chapel Hill
217	Chapel Hill
450	Chapel Hill
570	Chapel Hill
660	Chapel Hill

References

1. Shigellosis. http://www.cdc.gov/nczved/divisions/dfbmd/diseases/shigellosis/#germ Center for Disease Control and Prevention, 2009.
2. **Abdullah LH, Conway JD, Cohn JA, and Davis CW.** Protein kinase C and Ca2+ activation of mucin secretion in airway goblet cells. *Am J Physiol* 273: L201-210, 1997.
3. **Aimoto S, Takao T, Shimonishi Y, Hara S, Takeda T, Takeda Y, and Miwatani T.** Amino-acid sequence of a heat-stable enterotoxin produced by human enterotoxigenic *Escherichia coli*. *Eur J Biochem* 129: 257-263, 1982.
4. **Akhter S, Cavet ME, Tse C-M, and Donowitz M.** C-terminal domains of Na^+/H^+ exchanger isoform 3 are involved in the basal and serum-stimulated membrane trafficking of the exchanger. *Biochem* 39: 1990-2000, 2000.
5. **Akira S and Hemmi H.** Recognition of pathogen-associated molecular patterns by TLR family. *Immunol Lett* 85: 85-95, 2003.
6. **Akira S, Uematsu S, and Takeuchi O.** Pathogen recognition and innate immunity. *Cell* 124: 783-801, 2006.
7. **Aktories K and Wegner A.** Mechanisms of the cytopathic action of actin-ADP-ribosylating toxins. *Mol Microbiol* 6: 2905-2908, 1992.
8. **Alvarez-Ordóñez A, Martínez-Lobo FJ, Arguello H, Carvajal A, and Rubio P.** Swine dysentery: aetiology, pathogenicity, determinants of transmission and the fight against the disease. *Int J Environ Res Public Health* 10: 1927-1947, 2013.
9. **Amin MR, Malakooti J, Sandoval R, Dudeja PK, and Ramaswamy K.** IFN-gamma and TNF-alpha regulate human NHE3 gene expression by modulating the Sp family transcription factors in human intestinal epithelial cell line C2BBe1. *Am J Physiol Cell Physiol* 291: C887-896, 2006.
10. **Amin MR, Orenuga T, Tyagi S, Dudeja PK, Ramaswamy K, and Malakooti J.** Tumor necrosis factor-alpha represses the expression of NHE2 through NF-kappaB activation in intestinal epithelial cell model, C2BBe1. *Inflamm Bowel Dis* 17: 720-731, 2011.
11. **Archampong EQ, Harris J, and Clark CG.** The absorption and secretion of water and electrolytes across the healthy and the diseased human colonic mucosa measured in vitro. *Gut* 13: 880-886, 1972.
12. **Argenzio RA, Lecce J, and Powell DW.** Prostanoids inhibit intestinal NaCl absorption in experimental porcine cryptosporidiosis. *Gastroenterology* 104: 440-447, 1993.
13. **Argenzio RA, Whipp SC, and Glock RD.** Pathophysiology of swine dysentery: colonic transport and permeability studies. *J Infect Dis* 142: 676-684, 1980.
14. **Arguello H, Alvarez-Ordonez A, Carvajal A, Rubio P, and Prieto M.** Role of slaughtering in *Salmonella* spreading and control in pork production. *J Food Prot* 76: 899-911, 2013.
15. **Arnold JW, Klimpel GR, and Niesel DW.** Tumor Necrosis Factor (TNFα) Regulates Intestinal Mucus Production during Salmonellosis. *Cell Immunol* 151: 336-344, 1993.
16. **Asfaha S, MacNaughton WK, Appleyard CB, Chadee K, and Wallace JL.** Persistent epithelial dysfunction and bacterial translocation after resolution of intestinal inflammation. *Am J Physiol Gastrointest Liver Physiol* 281: G635-644, 2001.
17. **Bamias G, Nyce MR, De La Rue SA, and Cominelli F.** New concepts in the pathophysiology of inflammatory bowel disease. *Ann Intern Med* 143: 895-904, 2005.
18. **Baniak N, Luan X, Grunow A, Machen TE, and Ianowski JP.** The cytokines interleukin-1beta and tumor necrosis factor-alpha stimulate CFTR-mediated fluid secretion by swine airway submucosal glands. *Am J Physiol Lung Cell Mol Physiol* 303: L327-333, 2012.
19. **Barbut F, Decre D, Lalande V, Burghoffer B, Noussair L, Gigandon A, Espinasse F, Raskine L, Robert J, Mangeol A, Branger C, and Petit JC.** Clinical features of *Clostridium difficile*-associated

diarrhoea due to binary toxin (actin-specific ADP-ribosyltransferase)-producing strains. *J Med Microbiol* 54: 181-185, 2005.
20. **Barker N, van Es JH, Kuipers J, Kujala P, van den Born M, Cozijnsen M, Haegebarth A, Korving J, Begthel H, Peters PJ, and Clevers H.** Identification of stem cells in small intestine and colon by marker gene Lgr5. *Nature* 449: 1003-1007, 2007.
21. **Barmeyer C, Rahner C, Yang Y, Sigworth FJ, Binder HJ, and Rajendran VM.** Cloning and identification of tissue-specific expression of KCNN4 splice variants in rat colon. *Am J Physiol Cell Physiol* 299: C251-263, 2010.
22. **Barrow PA, Huggins MB, and Lovell MA.** Host specificity of *Salmonella* infection in chickens and mice is expressed in vivo primarily at the level of the reticuloendothelial system. *Infect Immun* 62: 4602-4610, 1994.
23. **Basalingappa KM, Rajendran VM, and Wonderlin WF.** Characteristics of Kcnn4 channels in the apical membranes of an intestinal epithelial cell line. *Am J Physiol Gastrointest Liver Physiol* 301: G905-911, 2011.
24. **Beg AA, Ruben SM, Scheinman RI, Haskill S, Rosen CA, and Baldwin AS, Jr.** I kappa B interacts with the nuclear localization sequences of the subunits of NF-kappa B: a mechanism for cytoplasmic retention. *Genes Dev* 6: 1899-1913, 1992.
25. **Bellono NW, Bayrer JR, Leitch DB, Castro J, Zhang C, O'Donnell TA, Brierley SM, Ingraham HA, and Julius D.** Enterochromaffin cells are gut chemosensors that couple to sensory neural pathways. *Cell* 170: 185-198.e116, 2017.
26. **Benedetto R, Ousingsawat J, Wanitchakool P, Zhang Y, Holtzman MJ, Amaral M, Rock JR, Schreiber R, and Kunzelmann K.** Epithelial chloride transport by CFTR requires TMEM16A. *Sci Rep* 7: 12397, 2017.
27. **Berger A.** Th1 and Th2 responses: what are they? *BMJ* 321: 424, 2000.
28. **Berger EY and Steele JM.** The calculation of transfer rates in two compartment systems not in dynamic equilibrium. *J Gen Physiol* 41: 1135-1152, 1958.
29. **Berkes J, Viswanathan VK, Savkovic SD, and Hecht G.** Intestinal epithelial responses to enteric pathogens: effects on the tight junction barrier, ion transport, and inflammation. *Gut* 52: 439-451, 2003.
30. **Bertelsen LS, Paesold G, Eckmann L, and Barrett KE.** *Salmonella* infection induces a hypersecretory phenotype in human intestinal xenografts by inducing cyclooxygenase 2. *Infect Immun* 71: 2102, 2003.
31. **Besancon F, Przewlocki G, Baro I, Hongre AS, Escande D, and Edelman A.** Interferon-gamma downregulates CFTR gene expression in epithelial cells. *Am J Physiol* 267: C1398-1404, 1994.
32. **Binder HJ, Foster ES, Budinger ME, and Hayslett JP.** Mechanism of electroneutral sodium chloride absorption in distal colon of the rat. *Gastroenterology* 93: 449-455, 1987.
33. **Blanco G, Sánchez G, and Mercer RW.** Differential regulation of Na, K-ATPase isozymes by protein kinases and arachidonic acid. *Arch Biochem Biophys* 359: 139-150, 1998.
34. **Blocker A, Gounon P, Larquet E, Niebuhr K, Cabiaux V, Parsot C, and Sansonetti P.** The tripartite type III secreton of *Shigella flexneri* inserts IpaB and IpaC into host membranes. *J Cell Biol* 147: 683-693, 1999.
35. **Bookstein C, DePaoli AM, Xie Y, Niu P, Musch MW, Rao MC, and Chang EB.** Na^+/H^+ exchangers, NHE-1 and NHE-3, of rat intestine. Expression and localization. *J Clin Invest* 93: 106-113, 1994.
36. **Borg JF, Yde J, Wu Q, Lajczak N, Keely S, Fenton RA, and Moeller H.** Regulated expression of the Na^+/K^+-ATPase pump in colonic epithelium by bile acids. *FASEB* 31: 856.810-856.810, 2017.
37. **Bowman CC and Bost KL.** Cyclooxygenase-2-mediated prostaglandin E2 production in mesenteric lymph nodes and in cultured macrophages and dendritic cells after infection with *Salmonella*. *J Immunol* 172: 2469-2475, 2004.

38. **Bradbury NA.** Protein kinase-A-mediated secretion of mucin from human colonic epithelial cells. *J Cell Physiol* 185: 408-415, 2000.
39. **Branka JE, Vallette G, Jarry A, Bou-Hanna C, Lemarre P, Van PN, and Laboisse CL.** Early functional effects of *Clostridium difficile* toxin A on human colonocytes. *Gastroenterology* 112: 1887-1894, 1997.
40. **Broere N, Chen M, Cinar A, Singh A, Hillesheim J, Riederer B, Lünnemann M, Rottinghaus I, Krabbenhöft A, and Engelhardt R.** Defective jejunal and colonic salt absorption and altered Na^+/H^+ exchanger 3 (NHE3) activity in NHE regulatory factor 1 (NHERF1) adaptor protein-deficient mice. *Pflugers Arch* 457: 1079, 2009.
41. **Bueno SM, Wozniak A, Leiva ED, Riquelme SA, Carreno LJ, Hardt WD, Riedel CA, and Kalergis AM.** *Salmonella* pathogenicity island 1 differentially modulates bacterial entry to dendritic and non-phagocytic cells. *Immunology* 130: 273-287, 2010.
42. **Butterworth MB.** Regulation of the epithelial sodium channel (ENaC) by membrane trafficking. *Biochim Biophys Acta* 1802: 1166-1177, 2010.
43. **Byeon MK, Westerman MA, Maroulakou IG, Henderson KW, Suster S, Zhang XK, Papas TS, Vesely J, Willingham MC, Green JE, and Schweinfest CW.** The down-regulated in adenoma (DRA) gene encodes an intestine-specific membrane glycoprotein. *Oncogene* 12: 387-396, 1996.
44. **Cafferata EG, Gonzalez-Guerrico AM, Giordano L, Pivetta OH, and Santa-Coloma TA.** Interleukin-1beta regulates CFTR expression in human intestinal T84 cells. *Biochim Biophys Acta* 1500: 241-248, 2000.
45. **Cafferata EG, Guerrico AM, Pivetta OH, and Santa-Coloma TA.** NF-kappaB activation is involved in regulation of cystic fibrosis transmembrane conductance regulator (CFTR) by interleukin-1beta. *J Biol Chem* 276: 15441-15444, 2001.
46. **Cassell JT.** Neil A. Dayton 1893-1977. A personal tribute. *Am J Ment Defic* 82: 227-228, 1977.
47. **Castagliuolo I, Wang CC, Valenick L, Pasha A, Nikulasson S, Carraway RE, and Pothoulakis C.** Neurotensin is a proinflammatory neuropeptide in colonic inflammation. *J Clin Invest* 103: 843-849, 1999.
48. **Chakravortty D and Hensel M.** *Salmonella* selectively stops traffic: response from Chakravortty and Hensel. *Trends Microbiol* 10: 392-393, 2002.
49. **Chander Y, Primus A, Oliveira S, and Gebhart CJ.** Phenotypic and molecular characterization of a novel strongly hemolytic *Brachyspira* species, provisionally designated *"Brachyspira hampsonii"*. *J Vet Diagn Invest* 24: 903-910, 2012.
50. **Chang EB, Musch MW, and Mayer L.** Interleukins 1 and 3 stimulate anion secretion in chicken intestine. *Gastroenterology* 98: 1518-1524, 1990.
51. **Chang WW and Leblond CP.** Renewal of the epithelium in the descending colon of the mouse. II. Renewal of argentaffin cells. *Am J Anat* 131: 101-109, 1971.
52. **Chao AC, de Sauvage FJ, Dong YJ, Wagner JA, Goeddel DV, and Gardner P.** Activation of intestinal CFTR Cl^- channel by heat-stable enterotoxin and guanylin via cAMP-dependent protein kinase. *EMBO J* 13: 1065-1072, 1994.
53. **Charon NW and Goldstein SF.** Genetics of motility and chemotaxis of a fascinating group of bacteria: the spirochetes. *Annu Rev Genet* 36: 47-73, 2002.
54. **Chen M, Sultan A, Cinar A, Yeruva S, Riederer B, Singh AK, Li J, Bonhagen J, Chen G, and Yun C.** Loss of PDZ-adaptor protein NHERF2 affects membrane localization and cGMP-and $[Ca^{2+}]$-but not cAMP-dependent regulation of Na^+/H^+ exchanger 3 in murine intestine. *J Physiol* 588: 5049-5063, 2010.
55. **Cheng H and Leblond CP.** Origin, differentiation and renewal of the four main epithelial cell types in the mouse small intestine. V. Unitarian Theory of the origin of the four epithelial cell types. *Am J Anat* 141: 537-561, 1974.

56. **Cheng SH, Rich DP, Marshall J, Gregory RJ, Welsh MJ, and Smith AE.** Phosphorylation of the R domain by cAMP-dependent protein kinase regulates the CFTR chloride channel. *Cell* 66: 1027-1036, 1991.
57. **Ching JC, Lobanova L, and Loewen ME.** Secreted hCLCA1 is a signaling molecule that activates airway macrophages. *PLoS One* 8: e83130, 2013.
58. **Chiossone DC, Simon PL, and Smith PL.** Interleukin-1: effects on rabbit ileal mucosal ion transport in vitro. *Eur J Pharmacol* 180: 217-228, 1990.
59. **Cinar A, Chen M, Riederer B, Bachmann O, Wiemann M, Manns M, Kocher O, and Seidler U.** NHE3 inhibition by cAMP and Ca^{2+} is abolished in PDZ-domain protein PDZK1-deficient murine enterocytes. *J Physiol* 581: 1235-1246, 2007.
60. **Clark MA, Jepson MA, Simmons NL, and Hirst BH.** Preferential interaction of *Salmonella typhimurium* with mouse Peyer's patch M cells. *Res Microbiol* 145: 543-552, 1994.
61. **Clarke LL.** A guide to Ussing chamber studies of mouse intestine. *Am J Physiol Gastrointest Liver Physiol* 296: G1151-1166, 2009.
62. **Clarke LL and Harline MC.** CFTR is required for cAMP inhibition of intestinal Na^+ absorption in a cystic fibrosis mouse model. *Am J Physiol* 270: G259-267, 1996.
63. **Clauss W, Schafer H, Horch I, and Hornicke H.** Segmental differences in electrical properties and Na-transport of rabbit caecum, proximal and distal colon in vitro. *Pflugers Arch* 403: 278-282, 1985.
64. **Clayton A, Holland E, Pang L, and Knox A.** Interleukin-1beta differentially regulates beta2 adrenoreceptor and prostaglandin E2-mediated cAMP accumulation and chloride efflux from Calu-3 bronchial epithelial cells. Role of receptor changes, adenylyl cyclase, cyclo-oxygenase 2, and protein kinase A. *J Biol Chem* 280: 23451-23463, 2005.
65. **Clayton A and Knox AJ.** COX-2: a link between airway inflammation and disordered chloride secretion in cystic fibrosis? *Thorax* 61: 552-553, 2006.
66. **Coffing H, Priyamvada S, Anbazhagan AN, Salibay C, Engevik M, Versalovic J, Yacyshyn MB, Yacyshyn B, Tyagi S, Saksena S, Gill RK, Alrefai WA, and Dudeja PK.** *Clostridium difficile* toxins A and B decrease intestinal SLC26A3 protein expression. *Am J Physiol Gastrointest Liver Physiol* 315: G43-G52, 2018.
67. **Colgan SP, Resnick MB, Parkos CA, Delp-Archer C, McGuirk D, Bacarra AE, Weller PF, and Madara JL.** IL-4 directly modulates function of a model human intestinal epithelium. *J Immunol* 153: 2122, 1994.
68. **Colwill T.** Unmet market needs. http://www.spirogene.com/market.php, 2010.
69. **Cui J, Yang H, and Lee US.** Molecular mechanisms of BK channel activation. *Cell Mol Life Sci* 66: 852-875, 2009.
70. **Davis CW and Dickey BF.** Regulated airway goblet cell mucin secretion. *Annu Rev Physiol* 70: 487-512, 2008.
71. **Davis GR, Morawski SG, Santa Ana CA, and Fordtran JS.** Evaluation of chloride/bicarbonate. Exchange in the human colon in vivo. *J Clin Invest* 71: 201-207, 1983.
72. **Dey I, Lejeune M, and Chadee K.** Prostaglandin E2 receptor distribution and function in the gastrointestinal tract. *Br J Pharmacol* 149: 611-623, 2006.
73. **Donowitz M, Keusch GT, and Binder HJ.** Effect of *Shigella* enterotoxin on electrolyte transport in rabbit ileum. *Gastroenterology* 69: 1230-1237, 1975.
74. **Donowitz M and Welsh MJ.** Ca^{2+} and cyclic AMP in regulation of intestinal Na, K, and Cl transport. *Annu Rev Physiol* 48: 135-150, 1986.
75. **Doyle LP, Spray RS, and Whiting RA.** *Swine dysentery*: Purdue University Agricultural Experiment Station, 1937.
76. **Doyle SL and O'Neill LA.** Toll-like receptors: from the discovery of NFkappaB to new insights into transcriptional regulations in innate immunity. *Biochem Pharmacol* 72: 1102-1113, 2006.

77. **Ek CE, Nosach R, Fernando C, Huang Y, Perez JBDS, Costa MO, Ekanayake S, Hill JE, and Harding JCS.** An optimized swine dysentery murine model to characterize shedding and clinical disease associated with "*Brachyspira hampsonii*" infection. *BMC Vet Res* 13: 261, 2017.
78. **Eng S-K, Pusparajah P, Ab Mutalib N-S, Ser H-L, Chan K-G, and Lee L-H.** *Salmonella*: A review on pathogenesis, epidemiology and antibiotic resistance. *Frontiers in Life Science* 8: 284-293, 2015.
79. **Engevik MA, Yacyshyn MB, Engevik KA, Wang J, Darien B, Hassett DJ, Yacyshyn BR, and Worrell RT.** Human *Clostridium difficile* infection: altered mucus production and composition. *American Journal of Physiology - Gastrointestinal and Liver Physiology* 308: G510-G524, 2015.
80. **Eveillard M, Fourel V, Barc MC, Kerneis S, Coconnier MH, Karjalainen T, Bourlioux P, and Servin AL.** Identification and characterization of adhesive factors of *Clostridium difficile* involved in adhesion to human colonic enterocyte-like Caco-2 and mucus-secreting HT29 cells in culture. *Mol Microbiol* 7: 371-381, 1993.
81. **Farkas K, Yeruva S, Rakonczay Z, Jr., Ludolph L, Molnar T, Nagy F, Szepes Z, Schnur A, Wittmann T, Hubricht J, Riederer B, Venglovecz V, Lazar G, Kiraly M, Zsembery A, Varga G, Seidler U, and Hegyi P.** New therapeutic targets in ulcerative colitis: the importance of ion transporters in the human colon. *Inflamm Bowel Dis* 17: 884-898, 2011.
82. **Field M.** Ion transport in rabbit ileal mucosa. II. Effects of cyclic 3', 5'-AMP. *Am J Physiol* 221: 992-997, 1971.
83. **Field M, Graf LH, Laird WJ, and Smith PL.** Heat-stable enterotoxin of *Escherichia coli*: in vitro effects on guanylate cyclase activity, cyclic GMP concentration, and ion transport in small intestine. *Proceedings of the National Academy of Sciences* 75: 2800, 1978.
84. **Finlay BB and Falkow S.** Common themes in microbial pathogenicity. *Microbiol Rev* 53: 210-230, 1989.
85. **Finlay BB and Falkow S.** *Salmonella* interactions with polarized human intestinal Caco-2 epithelial cells. *J Infect Dis* 162: 1096-1106, 1990.
86. **Finlay BB, Gumbiner B, and Falkow S.** Penetration of *Salmonella* through a polarized Madin-Darby canine kidney epithelial cell monolayer. *J Cell Biol* 107: 221-230, 1988.
87. **Fish SM, Proujansky R, and Reenstra WW.** Synergistic effects of interferon gamma and tumour necrosis factor alpha on T84 cell function. *Gut* 45: 191-198, 1999.
88. **Flegel WA, Muller F, Daubener W, Fischer HG, Hadding U, and Northoff H.** Cytokine response by human monocytes to *Clostridium difficile* toxin A and toxin B. *Infect Immun* 59: 3659-3666, 1991.
89. **Flores CA, Melvin JE, Figueroa CD, and Sepúlveda FV.** Abolition of Ca^{2+}-mediated intestinal anion secretion and increased stool dehydration in mice lacking the intermediate conductance Ca^{2+}-dependent K^+ channel Kcnn4. *The Journal of Physiology* 583: 705-717, 2007.
90. **Forstner JF and Forstner GG.** Effects of calcium on intestinal mucin: implications for cystic fibrosis. *Pediatr Res* 10: 609-613, 1976.
91. **Forte LR, Thorne PK, Eber SL, Krause WJ, Freeman RH, Francis SH, and Corbin JD.** Stimulation of intestinal Cl^- transport by heat-stable enterotoxin: activation of cAMP-dependent protein kinase by cGMP. *Am J Physiol* 263: C607-615, 1992.
92. **Freeman SL and MacNaughton WK.** Ionizing radiation induces iNOS-mediated epithelial dysfunction in the absence of an inflammatory response. *Am J Physiol Gastrointest Liver Physiol* 278: G243-250, 2000.
93. **Fullner KJ, Lencer WI, and Mekalanos JJ.** *Vibrio cholerae*-induced cellular responses of polarized T84 intestinal epithelial cells are dependent on production of cholera toxin and the RTX toxin. *Infect Immun* 69: 6310-6317, 2001.
94. **Fuss IJ, Neurath M, Boirivant M, Klein JS, de la Motte C, Strong SA, Fiocchi C, and Strober W.** Disparate CD4+ lamina propria (LP) lymphokine secretion profiles in inflammatory bowel disease.

Crohn's disease LP cells manifest increased secretion of IFN-gamma, whereas ulcerative colitis LP cells manifest increased secretion of IL-5. *J Immunol* 157: 1261-1270, 1996.
95. **Galietta LJ, Folli C, Marchetti C, Romano L, Carpani D, Conese M, and Zegarra-Moran O.** Modification of transepithelial ion transport in human cultured bronchial epithelial cells by interferon-gamma. *Am J Physiol Lung Cell Mol Physiol* 278: L1186-1194, 2000.
96. **Galietta LJ, Pagesy P, Folli C, Caci E, Romio L, Costes B, Nicolis E, Cabrini G, Goossens M, Ravazzolo R, and Zegarra-Moran O.** IL-4 is a potent modulator of ion transport in the human bronchial epithelium in vitro. *J Immunol* 168: 839-845, 2002.
97. **Gallois A, Klein JR, Allen LA, Jones BD, and Nauseef WM.** *Salmonella* pathogenicity island 2-encoded type III secretion system mediates exclusion of NADPH oxidase assembly from the phagosomal membrane. *J Immunol* 166: 5741-5748, 2001.
98. **Garcia MA, Yang N, and Quinton PM.** Normal mouse intestinal mucus release requires cystic fibrosis transmembrane regulator-dependent bicarbonate secretion. *J Clin Invest* 119: 2613-2622, 2009.
99. **Garty H and Palmer LG.** Epithelial sodium channels: function, structure, and regulation. *Physiol Rev* 77: 359-396, 1997.
100. **Gawenis LR, Stien X, Shull GE, Schultheis PJ, Woo AL, Walker NM, and Clarke LL.** Intestinal NaCl transport in NHE2 and NHE3 knockout mice. *Am J Physiol Gastrointest Liver Physiol* 282: G776-784, 2002.
101. **Gebbers JO, Ferguson DJ, Mason C, Crucioli V, and Jewell DP.** Local immune reaction in human intestinal spirochetosis. *Schweiz Med Wochenschr* 117: 1087-1091, 1987.
102. **Gebbers JO, Ferguson DJ, Mason C, Kelly P, and Jewell DP.** Spirochaetosis of the human rectum associated with an intraepithelial mast cell and IgE plasma cell response. *Gut* 28: 588-593, 1987.
103. **Gerbe F, van Es JH, Makrini L, Brulin B, Mellitzer G, Robine S, Romagnolo B, Shroyer NF, Bourgaux JF, Pignodel C, Clevers H, and Jay P.** Distinct ATOH1 and Neurog3 requirements define tuft cells as a new secretory cell type in the intestinal epithelium. *J Cell Biol* 192: 767-780, 2011.
104. **Gershon MD.** 5-Hydroxytryptamine (serotonin) in the gastrointestinal tract. *Curr Opin Endocrinol Diabetes Obes* 20: 14-21, 2013.
105. **Giannella RA, Gots RE, Charney AN, Greenough WB, 3rd, and Formal SB.** Pathogenesis of *Salmonella*-mediated intestinal fluid secretion. Activation of adenylate cyclase and inhibition by indomethacin. *Gastroenterology* 69: 1238-1245, 1975.
106. **Gill DM, Clements JD, Robertson DC, and Finkelstein RA.** Subunit number and arrangement in *Escherichia coli* heat-labile enterotoxin. *Infect Immun* 33: 677-682, 1981.
107. **Gill RK, Borthakur A, Hodges K, Turner JR, Clayburgh DR, Saksena S, Zaheer A, Ramaswamy K, Hecht G, and Dudeja PK.** Mechanism underlying inhibition of intestinal apical Cl/OH exchange following infection with enteropathogenic *E. coli*. *J Clin Invest* 117: 428-437, 2007.
108. **Golin-Bisello F, Bradbury N, and Ameen N.** STa and cGMP stimulate CFTR translocation to the surface of villus enterocytes in rat jejunum and is regulated by protein kinase G. *Am J Physiol Cell Physiol* 289: C708-716, 2005.
109. **Gopalakrishnan S, Pandey N, Tamiz AP, Vere J, Carrasco R, Somerville R, Tripathi A, Ginski M, Paterson BM, and Alkan SS.** Mechanism of action of ZOT-derived peptide AT-1002, a tight junction regulator and absorption enhancer. *Int J Pharm* 365: 121-130, 2009.
110. **Greger R.** Role of CFTR in the colon. *Annu Rev Physiol* 62: 467-491, 2000.
111. **Grubb BR and Gabriel SE.** Intestinal physiology and pathology in gene-targeted mouse models of cystic fibrosis. *Am J Physiol* 273: G258-266, 1997.
112. **Gruber AD, Elble RC, Ji HL, Schreur KD, Fuller CM, and Pauli BU.** Genomic cloning, molecular characterization, and functional analysis of human CLCA1, the first human member of the family of Ca^{2+}-activated Cl^- channel proteins. *Genomics* 54: 200-214, 1998.

113. **Gurney MA, Laubitz D, Ghishan FK, and Kiela PR.** Pathophysiology of Intestinal Na^+/H^+ exchange. *Cellular and molecular gastroenterology and hepatology* 3: 27-40, 2017.
114. **Gustafsson JK, Ermund A, Ambort D, Johansson ME, Nilsson HE, Thorell K, Hebert H, Sjovall H, and Hansson GC.** Bicarbonate and functional CFTR channel are required for proper mucin secretion and link cystic fibrosis with its mucus phenotype. *J Exp Med* 209: 1263-1272, 2012.
115. **Gustafsson JK, Navabi N, Rodriguez-Piñeiro AM, Alomran AHA, Premaratne P, Fernandez HR, Banerjee D, Sjövall H, Hansson GC, and Lindén SK.** Dynamic changes in mucus thickness and ion secretion during *Citrobacter rodentium* infection and clearance. *PLoS One* 8: e84430, 2013.
116. **Haas M.** The Na-K-Cl cotransporters. *Am J Physiol* 267: C869-885, 1994.
117. **Hampson DJ.** Brachyspiral colitis. *Diseases of swine* 10: 680-696, 2012.
118. **Hampson DJ and Ahmed N.** Spirochaetes as intestinal pathogens: lessons from a *Brachyspira* genome. *Gut Pathog* 1: 10-10, 2009.
119. **Hapfelmeier S, Ehrbar K, Stecher B, Barthel M, Kremer M, and Hardt WD.** Role of the *Salmonella* pathogenicity island 1 effector proteins SipA, SopB, SopE, and SopE2 in Salmonella enterica subspecies 1 serovar *typhimurium* colitis in streptomycin-pretreated mice. *Infect Immun* 72: 795-809, 2004.
120. **Hardt WD, Chen LM, Schuebel KE, Bustelo XR, and Galan JE.** *S. typhimurium* encodes an activator of Rho GTPases that induces membrane ruffling and nuclear responses in host cells. *Cell* 93: 815-826, 1998.
121. **Harris DL.** Swine dysentery I. Inoculation of pigs with *Treponema hyodysenteriae* (new species) and reproduction of the disease. *Vet Med Small Anim Clin* 67: 61-64, 1972.
122. **Harris H.** Swine Dysentery Too Costly to Live With. https://en.engormix.com/pig-industry/articles/swine-dysentery-t35518.htm, 2012.
123. **Harris M, Garcia-Caballero A, Stutts MJ, Firsov D, and Rossier BC.** Preferential assembly of epithelial sodium channel (ENaC) subunits in Xenopus oocytes: role of furin-mediated endogenous proteolysis. *J Biol Chem* 283: 7455-7463, 2008.
124. **Hartzell C, Putzier I, and Arreola J.** Calcium-activated chloride channels. *Annu Rev Physiol* 67: 719-758, 2005.
125. **Hayashi H, Szaszi K, Coady-Osberg N, Furuya W, Bretscher AP, Orlowski J, and Grinstein S.** Inhibition and redistribution of NHE3, the apical Na^+/H^+ exchanger, by *Clostridium difficile* toxin B. *J Gen Physiol* 123: 491-504, 2004.
126. **Hecht G, Hodges K, Gill RK, Kear F, Tyagi S, Malakooti J, Ramaswamy K, and Dudeja PK.** Differential regulation of Na^+/H^+ exchange isoform activities by enteropathogenic *E. coli* in human intestinal epithelial cells. *Am J Physiol Gastrointest Liver Physiol* 287: G370-378, 2004.
127. **Helbling R, Osterheld M-C, Vaudaux B, Jaton K, and Nydegger A.** Intestinal Spirochetosis mimicking inflammatory bowel disease in children. *BMC Pediatr* 12: 163-163, 2012.
128. **Hennequin C, Janoir C, Barc MC, Collignon A, and Karjalainen T.** Identification and characterization of a fibronectin-binding protein from Clostridium difficile. *Microbiology* 149: 2779-2787, 2003.
129. **Hermiston ML and Gordon JI.** Organization of the crypt-villus axis and evolution of its stem cell hierarchy during intestinal development. *Am J Physiol* 268: G813-822, 1995.
130. **Hillesheim J, Riederer B, Tuo B, Chen M, Manns M, Biber J, Yun C, Kocher O, and Seidler U.** Down regulation of small intestinal ion transport in PDZK1-(CAP70/NHERF3) deficient mice. *Pflugers Arch* 454: 575-586, 2007.
131. **Hinterleitner TA, Saada JI, Berschneider HM, Powell DW, and Valentich JD.** IL-1 stimulates intestinal myofibroblast COX gene expression and augments activation of Cl^- secretion in T84 cells. *Am J Physiol* 271: C1262-1268, 1996.

132. **Hiribarren A, Heyman M, L'Helgouac'h A, and Desjeux J.** Effect of cytokines on the epithelial function of the human colon carcinoma cell line HT29 cl 19A. *Gut* 34: 616-620, 1993.
133. **Hodges K and Gill R.** Infectious diarrhea: Cellular and molecular mechanisms. *Gut microbes* 1: 4-21, 2010.
134. **Holmgren J, Lonnroth I, Mansson J, and Svennerholm L.** Interaction of cholera toxin and membrane GM1 ganglioside of small intestine. *Proc Natl Acad Sci U S A* 72: 2520-2524, 1975.
135. **Hoogerwerf WA, Tsao SC, Devuyst O, Levine SA, Yun CH, Yip JW, Cohen ME, Wilson PD, Lazenby AJ, Tse CM, and Donowitz M.** NHE2 and NHE3 are human and rabbit intestinal brush-border proteins. *Am J Physiol* 270: G29-41, 1996.
136. **Hovind-Hougen K, Birch-Andersen A, Henrik-Nielsen R, Orholm M, Pedersen JO, Teglbjaerg PS, and Thaysen EH.** Intestinal spirochetosis: morphological characterization and cultivation of the spirochete *Brachyspira aalborgi* gen. nov., sp. nov. *J Clin Microbiol* 16: 1127-1136, 1982.
137. **Howe KL, Wang A, Hunter MM, Stanton BA, and McKay DM.** TGFbeta down-regulation of the CFTR: a means to limit epithelial chloride secretion. *Exp Cell Res* 298: 473-484, 2004.
138. **Hubel KA and Renquist KS.** Ion transport in normal and inflamed human jejunumin vitro. *Dig Dis Sci* 35: 815-820, 1990.
139. **Huffnagle GB and Dickson RP.** The bacterial microbiota in inflammatory lung diseases. *Clin Immunol* 159: 177-182, 2015.
140. **Hughes JM, Murad F, Chang B, and Guerrant RL.** Role of cyclic GMP in the action of heat-stable enterotoxin of *Escherichia coli*. *Nature* 271: 755, 1978.
141. **Hurd HS, Gailey JK, McKean JD, and Rostagno MH.** Rapid infection in market-weight swine following exposure to a *Salmonella typhimurium*-contaminated environment. *Am J Vet Res* 62: 1194-1197, 2001.
142. **In J, Foulke-Abel J, Zachos NC, Hansen A-M, Kaper JB, Bernstein HD, Halushka M, Blutt S, Estes MK, Donowitz M, and Kovbasnjuk O.** Enterohemorrhagic *Escherichia coli* reduces mucus and intermicrovillar bridges in human stem cell-derived colonoids. *Cell Mol Gastroenterol Hepatol* 2: 48-62.e43, 2016.
143. **In J, Foulke-Abel J, Zachos NC, Hansen AM, Kaper JB, Bernstein HD, Halushka M, Blutt S, Estes MK, Donowitz M, and Kovbasnjuk O.** Enterohemorrhagic *Escherichia coli* reduce mucus and intermicrovillar bridges in human stem cell-derived colonoids. *Cellular and molecular gastroenterology and hepatology* 2: 48-62.e43, 2016.
144. **Inglis SK, Corboz MR, Taylor AE, and Ballard ST.** Effect of anion transport inhibition on mucus secretion by airway submucosal glands. *Am J Physiol* 272: L372-377, 1997.
145. **Jia Y, Mathews CJ, and Hanrahan JW.** Phosphorylation by protein kinase C is required for acute activation of cystic fibrosis transmembrane conductance regulator by protein kinase A. *J Biol Chem* 272: 4978-4984, 1997.
146. **Joens LA and Kinyon JM.** Isolation of *Treponema hyodysenteriae* from wild rodents. *J Clin Microbiol* 15: 994-997, 1982.
147. **Johansson ME, Larsson JM, and Hansson GC.** The two mucus layers of colon are organized by the MUC2 mucin, whereas the outer layer is a legislator of host-microbial interactions. *Proc Natl Acad Sci U S A* 108 Suppl 1: 4659-4665, 2011.
148. **Johansson ME, Sjovall H, and Hansson GC.** The gastrointestinal mucus system in health and disease. *Nat Rev Gastroenterol Hepatol* 10: 352-361, 2013.
149. **Johansson MEV, Ambort D, Pelaseyed T, Schütte A, Gustafsson JK, Ermund A, Subramani DB, Holmén-Larsson JM, Thomsson KA, Bergström JH, van der Post S, Rodriguez-Piñeiro AM, Sjövall H, Bäckström M, and Hansson GC.** Composition and functional role of the mucus layers in the intestine. *Cell Mol Life Sci* 68: 3635, 2011.

150. **Johansson MEV, Phillipson M, Petersson J, Velcich A, Holm L, and Hansson GC.** The inner of the two Muc2 mucin-dependent mucus layers in colon is devoid of bacteria. *Proceedings of the National Academy of Sciences* 105: 15064, 2008.
151. **Joo NS, Krouse ME, Wu JV, Saenz Y, Jayaraman S, Verkman AS, and Wine JJ.** HCO_3^- transport in relation to mucus secretion from submucosal glands. *JOP* 2: 280-284, 2001.
152. **Kamosinska B, Radomski MW, Duszyk M, Radomski A, and Man SF.** Nitric oxide activates chloride currents in human lung epithelial cells. *Am J Physiol* 272: L1098-1104, 1997.
153. **Kanwar RK, Ganguly NK, Kanwar JR, Kumar L, and Walia BN.** Impairment of Na^+,K^+-ATPase activity following enterotoxigenic *Campylobacter jejuni* infection: changes in Na^+, Cl^- and 3-O-methyl-D-glucose transport in vitro, in rat ileum. *FEMS Microbiol Lett* 124: 381-385, 1994.
154. **Kaper JB, Nataro JP, and Mobley HL.** Pathogenic *Escherichia coli*. *Nat Rev Microbiol* 2: 123-140, 2004.
155. **Kaplan JH.** Biochemistry of Na, K-ATPase. *Annu Rev Biochem* 71: 511-535, 2002.
156. **Karpati F, Hjelte FL, and Wretlind B.** TNF-alpha and IL-8 in consecutive sputum samples from cystic fibrosis patients during antibiotic treatment. *Scand J Infect Dis* 32: 75-79, 2000.
157. **Kato A and Romero MF.** Regulation of electroneutral NaCl absorption by the small intestine. *Annu Rev Physiol* 73: 261-281, 2011.
158. **Keates AC, Castagliuolo I, Qiu B, Nikulasson S, Sengupta A, and Pothoulakis C.** CGRP upregulation in dorsal root ganglia and ileal mucosa during *Clostridium difficile* toxin A-induced enteritis. *Am J Physiol* 274: G196-202, 1998.
159. **Keller M, Ruegg A, Werner S, and Beer HD.** Active caspase-1 is a regulator of unconventional protein secretion. *Cell* 132: 818-831, 2008.
160. **Kelley TJ, Al-Nakkash L, and Drumm ML.** C-type natriuretic peptide increases chloride permeability in normal and cystic fibrosis airway cells. *Am J Respir Cell Mol Biol* 16: 464-470, 1997.
161. **Kennedy MJ and Yancey RJ.** Motility and chemotaxis in *Serpulina hyodysenteriae*. *Vet Microbiol* 49: 21-30, 1996.
162. **Kere J.** Overview of the SLC26 family and associated diseases. *Novartis Found Symp* 273: 2-11; discussion 11-18, 261-264, 2006.
163. **Kere J, Lohi H, and Hoglund P.** Genetic disorders of membrane transport III. Congenital chloride diarrhea. *Am J Physiol* 276: G7-g13, 1999.
164. **Khan I, Siddique I, Al-Awadi FM, and Mohan K.** Role of Na^+/H^+ exchanger isoform-1 in human inflammatory bowel disease. *Can J Gastroenterol* 17: 31-36, 2003.
165. **Khurana S, Ganguly NK, Khullar M, Panigrahi D, and Walia BN.** Studies on the mechanism of *Salmonella typhimurium* enterotoxin-induced diarrhoea. *Biochim Biophys Acta* 1097: 171-176, 1991.
166. **Killackey SA, Sorbara MT, and Girardin SE.** Cellular aspects of *Shigella* pathogenesis: Focus on the manipulation of host cell processes. *Frontiers in cellular and infection microbiology* 6: 38, 2016.
167. **Kim DW, Lenzen G, Page AL, Legrain P, Sansonetti PJ, and Parsot C.** The *Shigella flexneri* effector OspG interferes with innate immune responses by targeting ubiquitin-conjugating enzymes. *Proc Natl Acad Sci U S A* 102: 14046-14051, 2005.
168. **Kim JH, Lee-Kwon W, Park JB, Ryu SH, Yun CH, and Donowitz M.** Ca^{2+}-dependent inhibition of Na^+/H^+ exchanger 3 (NHE3) requires an NHE3-E3KARP-alpha-actinin-4 complex for oligomerization and endocytosis. *J Biol Chem* 277: 23714-23724, 2002.
169. **Kim YS and Ho SB.** Intestinal goblet cells and mucins in health and disease: recent insights and progress. *Current gastroenterology reports* 12: 319-330, 2010.
170. **Kirk KL, Halm DR, and Dawson DC.** Active sodium transport by turtle colon via an electrogenic Na-K exchange pump. *Nature* 287: 237-239, 1980.
171. **Kockerling A, Sorgenfrei D, and Fromm M.** Electrogenic Na^+ absorption of rat distal colon is confined to surface epithelium: a voltage-scanning study. *Am J Physiol* 264: C1285-1293, 1993.

172. **Kohler H, Sakaguchi T, Hurley BP, Kase BA, Reinecker HC, and McCormick BA.** *Salmonella enterica* serovar *typhimurium* regulates intercellular junction proteins and facilitates transepithelial neutrophil and bacterial passage. *Am J Physiol Gastrointest Liver Physiol* 293: G178-187, 2007.
173. **Kostman JR, Patel M, Catalano E, Camacho J, Hoffpauir J, and DiNubile MJ.** Invasive colitis and hepatitis due to previously uncharacterized spirochetes in patients with advanced human immunodeficiency virus infection. *Clin Infect Dis* 21: 1159-1165, 1995.
174. **Krasilnikov OV, Muratkhodjaev JN, and Zitzer AO.** The mode of action of *Vibrio cholerae* cytolysin. The influences on both erythrocytes and planar lipid bilayers. *Biochim Biophys Acta* 1111: 7-16, 1992.
175. **Kreindler JL, Bertrand CA, Lee RJ, Karasic T, Aujla S, Pilewski JM, Frizzell RA, and Kolls JK.** Interleukin-17A induces bicarbonate secretion in normal human bronchial epithelial cells. *American Journal of Physiology-Lung Cellular and Molecular Physiology* 296: L257-L266, 2009.
176. **Kruse R, Essén-Gustavsson B, Fossum C, and Jensen-Waern M.** Blood concentrations of the cytokines IL-1beta, IL-6, IL-10, TNF-alpha and IFN-gamma during experimentally induced swine dysentery. *Acta Vet Scand* 50: 32, 2008.
177. **Kudryashov DS, Cordero CL, Reisler E, and Satchell KJ.** Characterization of the enzymatic activity of the actin cross-linking domain from the *Vibrio cholerae* MARTX Vc toxin. *J Biol Chem* 283: 445-452, 2008.
178. **Kumar A, Gujral T, Gill RK, Coffing H, Anbazhagan AN, Borthakur A, Alrefai WA, and Dudeja PK.** Mo1746 TNF inhibits SLC26A3 expression via activation of NF-KappaB pathway. *Gastroenterology* 146: S-650, 2014.
179. **Kumar P, Kuhlmann FM, Bhullar K, Yang H, Vallance BA, Xia L, Luo Q, and Fleckenstein JM.** Dynamic interactions of a conserved enterotoxigenic *Escherichia coli* adhesin with intestinal mucins govern epithelium engagement and toxin delivery. *Infect Immun* 84: 3608-3617, 2016.
180. **Kumar P, Luo Q, Vickers TJ, Sheikh A, Lewis WG, and Fleckenstein JM.** EatA, an immunogenic protective antigen of enterotoxigenic *Escherichia coli* degrades intestinal mucin. *Infect Immun* 82: 500, 2014.
181. **Kunzelmann K and Mall M.** Electrolyte transport in the mammalian colon: mechanisms and implications for disease. *Physiol Rev* 82: 245-289, 2002.
182. **LaFrance ME, Farrow MA, Chandrasekaran R, Sheng J, Rubin DH, and Lacy DB.** Identification of an epithelial cell receptor responsible for *Clostridium difficile* TcdB-induced cytotoxicity. *Proc Natl Acad Sci U S A* 112: 7073-7078, 2015.
183. **Lamprecht G, Hsieh CJ, Lissner S, Nold L, Heil A, Gaco V, Schafer J, Turner JR, and Gregor M.** Intestinal anion exchanger down-regulated in adenoma (DRA) is inhibited by intracellular calcium. *J Biol Chem* 284: 19744-19753, 2009.
184. **Lebedev KA and Ponyakina ID.** Immunophysiology of epithelial cells and pattern-recognition receptors. *Hum Physiol* 32: 224-234, 2006.
185. **Leitch GJ.** Cholera enterotoxin-induced mucus secretion and increase in the mucus blanket of the rabbit ileum in vivo. *Infect Immun* 56: 2871-2875, 1988.
186. **Lenzen H, Lünnemann M, Bleich A, Manns MP, Seidler U, and Jörns A.** Downregulation of the NHE3-binding PDZ-adaptor protein PDZK1 expression during cytokine-induced inflammation in interleukin-10–deficient mice. *PLoS One* 7: e40657, 2012.
187. **Li H, Xu H, Zhou Y, Zhang J, Long C, Li S, Chen S, Zhou JM, and Shao F.** The phosphothreonine lyase activity of a bacterial type III effector family. *Science* 315: 1000-1003, 2007.
188. **Li Z and Langhans SA.** Transcriptional regulators of Na,K-ATPase subunits. *Front Cell Dev Biol* 3: 66, 2015.

189. **Liao AP, Petrof EO, Kuppireddi S, Zhao Y, Xia Y, Claud EC, and Sun J.** *Salmonella* type III effector AvrA stabilizes cell tight junctions to inhibit inflammation in intestinal epithelial cells. *PLoS One* 3: e2369, 2008.
190. **Lima AA, Lyerly DM, Wilkins TD, Innes DJ, and Guerrant RL.** Effects of *Clostridium difficile* toxins A and B in rabbit small and large intestine in vivo and on cultured cells in vitro. *Infect Immun* 56: 582-588, 1988.
191. **Livio S, Strockbine NA, Panchalingam S, Tennant SM, Barry EM, Marohn ME, Antonio M, Hossain A, Mandomando I, Ochieng JB, Oundo JO, Qureshi S, Ramamurthy T, Tamboura B, Adegbola RA, Hossain MJ, Saha D, Sen S, Faruque AS, Alonso PL, Breiman RF, Zaidi AK, Sur D, Sow SO, Berkeley LY, O'Reilly CE, Mintz ED, Biswas K, Cohen D, Farag TH, Nasrin D, Wu Y, Blackwelder WC, Kotloff KL, Nataro JP, and Levine MM.** *Shigella* isolates from the global enteric multicenter study inform vaccine development. *Clin Infect Dis* 59: 933-941, 2014.
192. **Loewen ME, Gabriel SE, and Forsyth GW.** The calcium-dependent chloride conductance mediator pCLCA1. *Am J Physiol Cell Physiol* 283: C412, 2002.
193. **Loo DD and Kaunitz JD.** Ca^{2+} and cAMP activate K^+ channels in the basolateral membrane of crypt cells isolated from rabbit distal colon. *J Membr Biol* 110: 19-28, 1989.
194. **Luo M, Yeruva S, Liu Y, Chodisetti G, Riederer B, Menon MB, Tachibana K, Doi T, and Seidler UE.** IL-1β-induced downregulation of the multifunctional PDZ adaptor PDZK1 is attenuated by ERK inhibition, RXRα, or PPARα stimulation in enterocytes. *Front Physiol* 8, 2017.
195. **Luo Q, Kumar P, Vickers TJ, Sheikh A, Lewis WG, Rasko DA, Sistrunk J, and Fleckenstein JM.** Enterotoxigenic *Escherichia coli* secretes a highly conserved mucin-degrading metalloprotease to effectively engage intestinal epithelial cells. *Infect Immun* 82: 509-521, 2014.
196. **Luppi A.** Swine enteric colibacillosis: diagnosis, therapy and antimicrobial resistance. *Porcine health management* 3: 16, 2017.
197. **MacNaughton WK, Lowe SS, and Cushing K.** Role of nitric oxide in inflammation-induced suppression of secretion in a mouse model of acute colitis. *Am J Physiol Gastrointest Liver Physiol* 275: G1353, 1998.
198. **Mahu M, de Jong E, De Pauw N, Vande Maele L, Vandenbroucke V, Vandersmissen T, Miry C, Pasmans F, Haesebrouck F, Martel A, and Boyen F.** First isolation of "*Brachyspira hampsonii*" from pigs in Europe. *Vet Rec* 174: 47, 2014.
199. **Makela S, Kere J, Holmberg C, and Hoglund P.** SLC26A3 mutations in congenital chloride diarrhea. *Hum Mutat* 20: 425-438, 2002.
200. **Masereel B, Pochet L, and Laeckmann D.** An overview of inhibitors of Na^+/H^+ exchanger. *Eur J Med Chem* 38: 547-554, 2003.
201. **Mason RW, Simpson-Small T, and Hopp L.** Regulation of 86Rb+ ion transport across polarized human colonocytes by bis-phenolic compounds. *Clin Exp Pharmacol Physiol* 30: 623-626, 2003.
202. **Matsuzawa T, Kuwae A, Yoshida S, Sasakawa C, and Abe A.** Enteropathogenic *Escherichia coli* activates the RhoA signaling pathway via the stimulation of GEF-H1. *EMBO J* 23: 3570-3582, 2004.
203. **Mawe GM and Hoffman JM.** Serotonin signalling in the gut--functions, dysfunctions and therapeutic targets. *Nat Rev Gastroenterol Hepatol* 10: 473-486, 2013.
204. **McAlindon ME, Hawkey CJ, and Mahida YR.** Expression of interleukin 1 beta and interleukin 1 beta converting enzyme by intestinal macrophages in health and inflammatory bowel disease. *Gut* 42: 214-219, 1998.
205. **McGuckin MA, Linden SK, Sutton P, and Florin TH.** Mucin dynamics and enteric pathogens. *Nat Rev Microbiol* 9: 265-278, 2011.
206. **Mikosza ASJ, Hampson DJ, Koopmans MPG, and van Duynhoven YTHP.** Presence of *Brachyspira aalborgi* and *B. pilosicoli* in feces of patients with diarrhea. *J Clin Microbiol* 41: 4492-4492, 2003.

207. **Milner JA and Sellwood R.** Chemotactic response to mucin by *Serpulina hyodysenteriae* and other porcine spirochetes: potential role in intestinal colonization. *Infect Immun* 62: 4095-4099, 1994.
208. **Mirajkar NS, Bekele AZ, Chander YY, and Gebhart CJ.** Molecular epidemiology of novel pathogen "*Brachyspira hampsonii*" reveals relationships between diverse genetic groups, regions, host species, and other pathogenic and commensal *Brachyspira* species. *J Clin Microbiol* 53: 2908-2918, 2015.
209. **Mirajkar NS and Gebhart CJ.** Understanding the molecular epidemiology and global relationships of *Brachyspira hyodysenteriae* from swine herds in the United States: a multi-locus sequence typing approach. *PLoS One* 9: e107176, 2014.
210. **Mitola S, Sorbello V, Ponte E, Copreni E, Mascia C, Bardessono M, Goia M, Biasi F, Conese M, Poli G, Bussolino F, and De Rose V.** Tumor necrosis factor-alpha in airway secretions from cystic fibrosis patients upregulate endothelial adhesion molecules and induce airway epithelial cell apoptosis: implications for cystic fibrosis lung disease. *Int J Immunopathol Pharmacol* 21: 851-865, 2008.
211. **Mogensen TH.** Pathogen recognition and inflammatory signaling in innate immune defenses. *Clin Microbiol Rev* 22: 240-273, 2009.
212. **Moore R, Pothoulakis C, LaMont JT, Carlson S, and Madara JL.** *C. difficile* toxin A increases intestinal permeability and induces Cl^- secretion. *Am J Physiol* 259: G165-172, 1990.
213. **Moss J, Osborne JC, Jr., Fishman PH, Nakaya S, and Robertson DC.** *Escherichia coli* heat-labile enterotoxin. Ganglioside specificity and ADP-ribosyltransferase activity. *J Biol Chem* 256: 12861-12865, 1981.
214. **Muller AJ, Hoffmann C, Galle M, Van Den Broeke A, Heikenwalder M, Falter L, Misselwitz B, Kremer M, Beyaert R, and Hardt WD.** The *S. Typhimurium* effector SopE induces caspase-1 activation in stromal cells to initiate gut inflammation. *Cell host & microbe* 6: 125-136, 2009.
215. **Muzes G, Molnar B, Tulassay Z, and Sipos F.** Changes of the cytokine profile in inflammatory bowel diseases. *World J Gastroenterol* 18: 5848-5861, 2012.
216. **Myers LL, Shoop DS, and Collins JE.** Rabbit model to evaluate enterovirulence of *Bacteroides fragilis*. *J Clin Microbiol* 28: 1658-1660, 1990.
217. **Myers LL, Shoop DS, Stackhouse LL, Newman FS, Flaherty RJ, Letson GW, and Sack RB.** Isolation of enterotoxigenic *Bacteroides fragilis* from humans with diarrhea. *J Clin Microbiol* 25: 2330-2333, 1987.
218. **Na X, Kim H, Moyer MP, Pothoulakis C, and LaMont JT.** gp96 is a human colonocyte plasma membrane binding protein for *Clostridium difficile* toxin A. *Infect Immun* 76: 2862-2871, 2008.
219. **Nadjsombati MS, McGinty JW, Lyons-Cohen MR, Jaffe JB, DiPeso L, Schneider C, Miller CN, Pollack JL, Nagana Gowda GA, Fontana MF, Erle DJ, Anderson MS, Locksley RM, Raftery D, and von Moltke J.** Detection of succinate by intestinal tuft cells triggers a type 2 innate immune circuit. *Immunity* 49: 33-41.e37, 2018.
220. **Nakamura H, Yoshimura K, Bajocchi G, Trapnell BC, Pavirani A, and Crystal RG.** Tumor necrosis factor modulation of expression of the cystic fibrosis transmembrane conductance regulator gene. *FEBS Lett* 314: 366-370, 1992.
221. **Nakamura H, Yoshimura K, McElvaney NG, and Crystal RG.** Neutrophil elastase in respiratory epithelial lining fluid of individuals with cystic fibrosis induces interleukin-8 gene expression in a human bronchial epithelial cell line. *J Clin Invest* 89: 1478-1484, 1992.
222. **Namkung W, Phuan PW, and Verkman AS.** TMEM16A inhibitors reveal TMEM16A as a minor component of calcium-activated chloride channel conductance in airway and intestinal epithelial cells. *J Biol Chem* 286: 2365-2374, 2011.
223. **Naresh R and Hampson DJ.** Attraction of *Brachyspira pilosicoli* to mucin. *Microbiol* 156: 191-197, 2010.
224. **Naresh R, Song Y, and Hampson DJ.** The intestinal spirochete *Brachyspira pilosicoli* attaches to cultured Caco-2 cells and induces pathological changes. *PLoS One* 4: e8352, 2009.

225. **Navabi N, Johansson ME, Raghavan S, and Linden SK.** *Helicobacter pylori* infection impairs the mucin production rate and turnover in the murine gastric mucosa. *Infect Immun* 81: 829-837, 2013.
226. **Niyogi SK.** Shigellosis. *J Microbiol* 43: 133-143, 2005.
227. **Njoku OO and Leitch GJ.** Separation of cholera enterotoxin-induced mucus secretion from electrolyte secretion in rabbit ileum by acetazolamide, colchicine, cycloheximide, cytochalasin B and indomethacin. *Digestion* 27: 174-184, 1983.
228. **Nobles M, Diener M, Mestres P, and Rummel W.** Segmental heterogeneity of the rat colon in the response to activators of secretion on the cAMP-, the cGMP- and the Ca^{2+}-pathway. *Acta Physiol Scand* 142: 375-386, 1991.
229. **Nordman H, Davies JR, Lindell G, de Bolos C, Real F, and Carlstedt I.** Gastric MUC5AC and MUC6 are large oligomeric mucins that differ in size, glycosylation and tissue distribution. *Biochem J* 364: 191-200, 2002.
230. **Norlander AE, Saleh MA, Kamat NV, Ko B, Gnecco J, Zhu L, Dale BL, Iwakura Y, Hoover RS, McDonough AA, and Madhur MS.** Interleukin-17A regulates renal sodium transporters and renal injury in angiotensin II-induced hypertension. *Hypertension* 68: 167-174, 2016.
231. **Nusrat A, von Eichel-Streiber C, Turner JR, Verkade P, Madara JL, and Parkos CA.** *Clostridium difficile* toxins disrupt epithelial barrier function by altering membrane microdomain localization of tight junction proteins. *Infect Immun* 69: 1329-1336, 2001.
232. **O'Loughlin EV, Hunt DM, Gaskin KJ, Stiel D, Bruzuszcak IM, Martin HC, Bambach C, and Smith R.** Abnormal epithelial transport in cystic fibrosis jejunum. *Am J Physiol* 260: G758-763, 1991.
233. **Ochiai S, Adachi Y, and Mori K.** Unification of the genera *Serpulina* and *Brachyspira*, and proposals of *Brachyspira hyodysenteriae* Comb. Nov., *Brachyspira innocens* Comb. Nov. and *Brachyspira pilosicoli* Comb. Nov. *Microbiol Immunol* 41: 445-452, 1997.
234. **Onyiah JC and Colgan SP.** Cytokine responses and epithelial function in the intestinal mucosa. *Cell Mol Life Sci* 73: 4203-4212, 2016.
235. **Ousingsawat J, Martins JR, Schreiber R, Rock JR, Harfe BD, and Kunzelmann K.** Loss of TMEM16A causes a defect in epithelial Ca^{2+}-dependent chloride transport. *J Biol Chem* 284: 28698-28703, 2009.
236. **Ousingsawat J, Mirza M, Tian Y, Roussa E, Schreiber R, Cook DI, and Kunzelmann K.** Rotavirus toxin NSP4 induces diarrhea by activation of TMEM16A and inhibition of Na^+ absorption. *Pflugers Arch* 461: 579-589, 2011.
237. **Park JH, Rhee P-L, Lee JH, Kim JJ, Rhee JC, Kim SJ, and Lee J.** Segmental heterogeneity of electrogenic secretions in human ascending colon and rectum. *Int J Colorectal Dis* 21: 357, 2005.
238. **Pawlotsky JM, Ruszniewski P, Reyl-Desmars F, Bourgeois M, and Lewin MJ.** Effects of PGE2, misoprostol, and enprostil on guinea pig enterocyte adenylate cyclase. Clinical implications. *Dig Dis Sci* 38: 316-320, 1993.
239. **Pedersen SF, King SA, Nygaard EB, Rigor RR, and Cala PM.** NHE1 inhibition by amiloride- and benzoylguanidine-type compounds. Inhibitor binding loci deduced from chimeras of NHE1 homologues with endogenous differences in inhibitor sensitivity. *J Biol Chem* 282: 19716-19727, 2007.
240. **Perelle S, Gibert M, Bourlioux P, Corthier G, and Popoff MR.** Production of a complete binary toxin (actin-specific ADP-ribosyltransferase) by *Clostridium difficile* CD196. *Infect Immun* 65: 1402-1407, 1997.
241. **Perez-Lopez A, Behnsen J, Nuccio S-P, and Raffatellu M.** Mucosal immunity to pathogenic intestinal bacteria. *Nature Reviews Immunology* 16: 135, 2016.
242. **Perkins C, Wills-Karp M, and Finkelman FD.** IL-4 induces IL-13-independent allergic airway inflammation. *J Allergy Clin Immunol* 118: 410-419, 2006.
243. **Phalipon A and Sansonetti PJ.** *Shigella's* ways of manipulating the host intestinal innate and adaptive immune system: a tool box for survival? *Immunol Cell Biol* 85: 119-129, 2007.

244. **Picciotto MR, Cohn JA, Bertuzzi G, Greengard P, and Nairn AC.** Phosphorylation of the cystic fibrosis transmembrane conductance regulator. *J Biol Chem* 267: 12742-12752, 1992.
245. **Pothoulakis C, Castagliuolo I, Leeman SE, Wang CC, Li H, Hoffman BJ, and Mezey E.** Substance P receptor expression in intestinal epithelium in *Clostridium difficile* toxin A enteritis in rats. *Am J Physiol* 275: G68-75, 1998.
246. **Potter GD and Burlingame SM.** Ion transport by neonatal rabbit distal colon. *Am J Physiol* 250: G754-759, 1986.
247. **Prevost MC, Lesourd M, Arpin M, Vernel F, Mounier J, Hellio R, and Sansonetti PJ.** Unipolar reorganization of F-actin layer at bacterial division and bundling of actin filaments by plastin correlate with movement of *Shigella flexneri* within HeLa cells. *Infect Immun* 60: 4088-4099, 1992.
248. **Priyamvada S, Gomes R, Gill RK, Saksena S, Alrefai WA, and Dudeja PK.** Mechanisms underlying dysregulation of electrolyte absorption in inflammatory bowel disease-associated diarrhea. *Inflamm Bowel Dis* 21: 2926-2935, 2015.
249. **Qu Z and Hartzell HC.** Bestrophin Cl^- channels are highly permeable to HCO_3^-. *Am J Physiol Cell Physiol* 294: C1371-C1377, 2008.
250. **Quinn RA, Lim YW, Maughan H, Conrad D, Rohwer F, and Whiteson KL.** Biogeochemical forces shape the composition and physiology of polymicrobial communities in the cystic fibrosis lung. *mBio* 5: e00956-00913, 2014.
251. **Quintana-Hayashi MP, Mahu M, De Pauw N, Boyen F, Pasmans F, Martel A, Premaratne P, Fernandez HR, Teymournejad O, Vande Maele L, Haesebrouck F, and Linden SK.** The levels of *Brachyspira hyodysenteriae* binding to porcine colonic mucins differ between individuals, and binding is increased to mucins from infected pigs with de novo MUC5AC synthesis. *Infect Immun* 83: 1610-1619, 2015.
252. **Quintana-Hayashi MP, Navabi N, Mahu M, Venkatakrishnan V, Fernandez HR, Haesebrouck F, Pasmans F, and Linden SK.** Neutrophil elastase and IL17 expressed in the pig colon during *Brachyspira hyodysenteriae* infection synergistically with the pathogen induce increased mucus transport speed and production via MAPK3. *Infect Immun*, 2017.
253. **Quinton PM.** Role of epithelial HCO_3^- transport in mucin secretion: lessons from cystic fibrosis. *Am J Physiol Cell Physiol* 299: C1222-1233, 2010.
254. **Rajkumar R, Devaraj H, and Niranjali S.** Binding of *Shigella* to rat and human intestinal mucin. *Mol Cell Biochem* 178: 261-268, 1998.
255. **Rask-Madsen J and Hjelt K.** Effect of amiloride on electrical activity and electrolyte transport in human colon. *Scand J Gastroenterol* 12: 1-6, 1977.
256. **Read LT, Hahn RW, Thompson CC, Bauer DL, Norton EB, and Clements JD.** Simultaneous exposure to *Escherichia coli* heat-labile and heat-stable enterotoxins increases fluid secretion and alters cyclic nucleotide and cytokine production by intestinal epithelial cells. *Infect Immun* 82: 5308-5316, 2014.
257. **Resta-Lenert S and Barrett KE.** Enteroinvasive bacteria alter barrier and transport properties of human intestinal epithelium: role of iNOS and COX-2. *Gastroenterology* 122: 1070-1087, 2002.
258. **Resta-Lenert S and Barrett KE.** Probiotics and commensals reverse TNF-alpha- and IFN-gamma-induced dysfunction in human intestinal epithelial cells. *Gastroenterology* 130: 731-746, 2006.
259. **Ristimaki A, Garfinkel S, Wessendorf J, Maciag T, and Hla T.** Induction of cyclooxygenase-2 by interleukin-1 alpha. Evidence for post-transcriptional regulation. *J Biol Chem* 269: 11769-11775, 1994.
260. **Rocha F, Musch MW, Lishanskiy L, Bookstein C, Sugi K, Xie Y, and Chang EB.** IFN-γ downregulates expression of Na^+/H^+ exchangers NHE2 and NHE3 in rat intestine and human Caco-2/bbe cells. *Am J Physiol Cell Physiol* 280: C1224-C1232, 2001.
261. **Rodgers FG, Rodgers C, Shelton AP, and Hawkey CJ.** Proposed pathogenic mechanism for the diarrhea associated with human intestinal spirochetes. *Am J Clin Pathol* 86: 679-682, 1986.

262. **Rohde J, Habighorst-Blome K, and Seehusen F.** "*Brachyspira hampsonii*" clade I isolated from Belgian pigs imported to Germany. *Vet Microbiol* 168: 432-435, 2014.
263. **Rohde J, Rothkamp A, and Gerlach GF.** Differentiation of porcine *Brachyspira* species by a novel nox PCR-based restriction fragment length polymorphism analysis. *J Clin Microbiol* 40: 2598-2600, 2002.
264. **Rohde JR, Breitkreutz A, Chenal A, Sansonetti PJ, and Parsot C.** Type III secretion effectors of the IpaH family are E3 ubiquitin ligases. *Cell host & microbe* 1: 77-83, 2007.
265. **Roux J, McNicholas CM, Carles M, Goolaerts A, Houseman BT, Dickinson DA, Iles KE, Ware LB, Matthay MA, and Pittet J-F.** IL-8 inhibits cAMP-stimulated alveolar epithelial fluid transport via a GRK2/PI3K-dependent mechanism. *The FASEB Journal* 27: 1095-1106, 2012.
266. **Rubin JE, Costa MO, Hill JE, Kittrell HE, Fernando C, Huang Y, O'Connor B, and Harding JC.** Reproduction of mucohaemorrhagic diarrhea and colitis indistinguishable from swine dysentery following experimental inoculation with *"Brachyspira hampsonii"* strain 30446. *PLoS One* 8: e57146, 2013.
267. **Sakaguchi T, Kohler H, Gu X, McCormick BA, and Reinecker HC.** *Shigella flexneri* regulates tight junction-associated proteins in human intestinal epithelial cells. *Cell Microbiol* 4: 367-381, 2002.
268. **Saksena S, Singla A, Goyal S, Katyal S, Bansal N, Gill RK, Alrefai WA, Ramaswamy K, and Dudeja PK.** Mechanisms of transcriptional modulation of the human anion exchanger SLC26A3 gene expression by IFN-gamma. *Am J Physiol Gastrointest Liver Physiol* 298: G159-166, 2010.
269. **Sala-Rabanal M, Yurtsever Z, Nichols CG, and Brett TJ.** Secreted CLCA1 modulates TMEM16A to activate Ca^{2+}-dependent chloride currents in human cells. *eLife* 4: e05875, 2015.
270. **Sandle G.** Salt and water absorption in the human colon: a modern appraisal. *Gut* 43: 294-299, 1998.
271. **Sandle GI, Higgs N, Crowe P, Marsh MN, Venkatesan S, and Peters TJ.** Cellular basis for defective electrolyte transport in inflamed human colon. *Gastroenterology* 99: 97-105, 1990.
272. **Sandle GI and Hunter M.** Apical potassium (BK) channels and enhanced potassium secretion in human colon. *QJM* 103: 85-89, 2010.
273. **Sandle GI, McNicholas CM, and Lomax RB.** Potassium channels in colonic crypts. *Lancet* 343: 23-25, 1994.
274. **Sandle GI, Wills NK, Alles W, and Binder HJ.** Electrophysiology of the human colon: evidence of segmental heterogeneity. *Gut* 27: 999-1005, 1986.
275. **Sansonetti PJ, Phalipon A, Arondel J, Thirumalai K, Banerjee S, Akira S, Takeda K, and Zychlinsky A.** Caspase-1 activation of IL-1beta and IL-18 are essential for *Shigella flexneri*-induced inflammation. *Immunity* 12: 581-590, 2000.
276. **Schild L, Schneeberger E, Gautschi I, and Firsov D.** Identification of amino acid residues in the α, β, and γ subunits of the epithelial sodium channel (ENaC) involved in amiloride block and ion permeation. *J Gen Physiol* 109: 15-26, 1997.
277. **Schmall LM, Argenzio RA, and Whipp SC.** Pathophysiologic features of swine dysentery: cyclic nucleotide-independent production of diarrhea. *Am J Vet Res* 44: 1309-1316, 1983.
278. **Schroeder BC, Waldegger S, Fehr S, Bleich M, Warth R, Greger R, and Jentsch TJ.** A constitutively open potassium channel formed by KCNQ1 and KCNE3. *Nature* 403: 196-199, 2000.
279. **Schultheis PJ, Clarke LL, Meneton P, Harline M, Boivin GP, Stemmermann G, Duffy JJ, Doetschman T, Miller ML, and Shull GE.** Targeted disruption of the murine Na^+/H^+ exchanger isoform 2 gene causes reduced viability of gastric parietal cells and loss of net acid secretion. *J Clin Invest* 101: 1243-1253, 1998.
280. **Schultheis PJ, Clarke LL, Meneton P, Miller ML, Soleimani M, Gawenis LR, Riddle TM, Duffy JJ, Doetschman T, Wang T, Giebisch G, Aronson PS, Lorenz JN, and Shull GE.** Renal and intestinal absorptive defects in mice lacking the NHE3 Na^+/H^+ exchanger. *Nat Genet* 19: 282-285, 1998.

281. **Schultz SG and Zalusky R.** Ion transport in isolated rabbit ileum. I. Short-circuit current and Na fluxes. *J Gen Physiol* 47: 567-584, 1964.
282. **Schweinfest CW, Spyropoulos DD, Henderson KW, Kim JH, Chapman JM, Barone S, Worrell RT, Wang Z, and Soleimani M.** SLC26a3 (dra)-deficient mice display chloride-losing diarrhea, enhanced colonic proliferation, and distinct up-regulation of ion transporters in the colon. *J Biol Chem* 281: 37962-37971, 2006.
283. **Simonovic I, Rosenberg J, Koutsouris A, and Hecht G.** Enteropathogenic *Escherichia coli* dephosphorylates and dissociates occludin from intestinal epithelial tight junctions. *Cell Microbiol* 2: 305-315, 2000.
284. **Sixma TK, Pronk SE, Kalk KH, Wartna ES, van Zanten BA, Witholt B, and Hol WG.** Crystal structure of a cholera toxin-related heat-labile enterotoxin from *E. coli*. *Nature* 351: 371-377, 1991.
285. **Smith HW and Halls S.** The simultaneous oral administration of *Salmonella dublin*, *S. typhimurium* and *S. choleraesuis* to calves and other animals. *J Med Microbiol* 1: 203-209, 1968.
286. **Sommer D, Bogdan R, Berger J, Peters DM, Morty RE, Clauss WG, and Fronius M.** CFTR-dependent Cl- secretion in *Xenopus laevis* lung epithelium. *Respir Physiol Neurobiol* 158: 97-106, 2007.
287. **Specian RD and Oliver MG.** Functional biology of intestinal goblet cells. *Am J Physiol* 260: C183-193, 1991.
288. **Sperandio B, Fischer N, Joncquel Chevalier-Curt M, Rossez Y, Roux P, Robbe Masselot C, and Sansonetti PJ.** Virulent *Shigella flexneri* affects secretion, expression, and glycosylation of gel-forming mucins in mucus-producing cells. *Infect Immun* 81: 3632-3643, 2013.
289. **Stanton TB.** Proposal to change the genus designation *Serpula* to *Serpulina* gen. nov. containing the species *Serpulina hyodysenteriae* comb. nov. and *Serpulina innocens* comb. nov. *Int J Syst Bacteriol* 42: 189-190, 1992.
290. **Stanton TB, Fournie-Amazouz E, Postic D, Trott DJ, Grimont PA, Baranton G, Hampson DJ, and Saint Girons I.** Recognition of two new species of intestinal spirochetes: *Serpulina intermedia* sp. nov. and *Serpulina murdochii* sp. nov. *Int J Syst Bacteriol* 47: 1007-1012, 1997.
291. **Stanton TB, Jensen NS, Casey TA, Tordoff LA, Dewhirst FE, and Paster BJ.** Reclassification of *Treponema hyodysenteriae* and *Treponema innocens* in a new genus, *Serpula* gen. nov., as *Serpula hyodysenteriae* comb. nov. and *Serpula innocens* comb. nov. *Int J Syst Bacteriol* 41: 50-58, 1991.
292. **Subramanya SB, Rajendran VM, Srinivasan P, Nanda Kumar NS, Ramakrishna BS, and Binder HJ.** Differential regulation of cholera toxin-inhibited Na-H exchange isoforms by butyrate in rat ileum. *Am J Physiol Gastrointest Liver Physiol* 293: G857-863, 2007.
293. **Sun H, Harris WT, Kortyka S, Kotha K, Ostmann AJ, Rezayat A, Sridharan A, Sanders Y, Naren AP, and Clancy JP.** TGF-beta downregulation of distinct chloride channels in cystic fibrosis-affected epithelia. *PLoS One* 9: e106842, 2014.
294. **Surawicz CM, Roberts PL, Rompalo A, Quinn TC, Holmes KK, and Stamm WE.** Intestinal spirochetosis in homosexual men. *Am J Med* 82: 587-592, 1987.
295. **Tabcharani JA, Chang XB, Riordan JR, and Hanrahan JW.** Phosphorylation-regulated Cl^- channel in CHO cells stably expressing the cystic fibrosis gene. *Nature* 352: 628-631, 1991.
296. **Tafazoli F, Magnusson KE, and Zheng L.** Disruption of epithelial barrier integrity by *Salmonella enterica* serovar *typhimurium* requires geranylgeranylated proteins. *Infect Immun* 71: 872-881, 2003.
297. **Takafuji V, Cosme R, Lublin D, Lynch K, and Roche JK.** Prostanoid receptors in intestinal epithelium: selective expression, function, and change with inflammation. *Prostaglandins, Leukotrienes and Essential Fatty Acids (PLEFA)* 63: 223-235, 2000.
298. **Tang A, Sharma A, Jen R, Hirschfeld AF, Chilvers MA, Lavoie PM, and Turvey SE.** Inflammasome-mediated IL-1β production in humans with cystic fibrosis. *PLoS One* 7: e37689, 2012.
299. **Tang L, Fatehi M, and Linsdell P.** Mechanism of direct bicarbonate transport by the CFTR anion channel. *J Cyst Fibros* 8: 115-121, 2009.

300. **Taxt A, Aasland R, Sommerfelt H, Nataro J, and Puntervoll P.** Heat-stable enterotoxin of enterotoxigenic *Escherichia coli* as a vaccine target. *Infect Immun* 78: 1824-1831, 2010.
301. **Thai P, Loukoianov A, Wachi S, and Wu R.** Regulation of airway mucin gene expression. *Annu Rev Physiol* 70: 405-429, 2008.
302. **Thelestam M.** Bacterial protein toxins--general conclusions. *Int J Med Microbiol* 290: 503-506, 2000.
303. **Tomson FL, Viswanathan VK, Kanack KJ, Kanteti RP, Straub KV, Menet M, Kaper JB, and Hecht G.** Enteropathogenic *Escherichia coli* EspG disrupts microtubules and in conjunction with Orf3 enhances perturbation of the tight junction barrier. *Mol Microbiol* 56: 447-464, 2005.
304. **Trott DJ, Stanton TB, Jensen NS, and Hampson DJ.** Phenotypic characteristics of *Serpulina pilosicoli* the agent of intestinal spirochaetosis. *FEMS Microbiol Lett* 142: 209-214, 1996.
305. **Trout L, Gatzy JT, and Ballard ST.** Acetylcholine-induced liquid secretion by bronchial epithelium: role of Cl- and HCO3- transport. *Am J Physiol* 275: L1095-1099, 1998.
306. **Trucksis M, Conn TL, Wasserman SS, and Sears CL.** *Vibrio cholerae* ACE stimulates Ca^{2+}-dependent Cl^-/HCO_3^- secretion in T84 cells in vitro. *Am J Physiol Cell Physiol* 279: C567-577, 2000.
307. **Tsinganou E and Gebbers J-O.** Human intestinal spirochetosis – a review. *Germ Med Sci* 8: Doc01, 2010.
308. **Uchiya K, Barbieri MA, Funato K, Shah AH, Stahl PD, and Groisman EA.** A *Salmonella* virulence protein that inhibits cellular trafficking. *EMBO J* 18: 3924-3933, 1999.
309. **Uzzau S, Cappuccinelli P, and Fasano A.** Expression of *Vibrio cholerae* zonula occludens toxin and analysis of its subcellular localization. *Microb Pathog* 27: 377-385, 1999.
310. **Vaandrager AB, Bot AG, and De Jonge HR.** Guanosine 3',5'-cyclic monophosphate-dependent protein kinase II mediates heat-stable enterotoxin-provoked chloride secretion in rat intestine. *Gastroenterology* 112: 437-443, 1997.
311. **Vazquez-Torres A, Xu Y, Jones-Carson J, Holden DW, Lucia SM, Dinauer MC, Mastroeni P, and Fang FC.** *Salmonella* pathogenicity island 2-dependent evasion of the phagocyte NADPH oxidase. *Science* 287: 1655-1658, 2000.
312. **Veenendaal AK, Hodgkinson JL, Schwarzer L, Stabat D, Zenk SF, and Blocker AJ.** The type III secretion system needle tip complex mediates host cell sensing and translocon insertion. *Mol Microbiol* 63: 1719-1730, 2007.
313. **Velge P, Wiedemann A, Rosselin M, Abed N, Boumart Z, Chausse AM, Grepinet O, Namdari F, Roche SM, Rossignol A, and Virlogeux-Payant I.** Multiplicity of *Salmonella* entry mechanisms, a new paradigm for *Salmonella* pathogenesis. *MicrobiologyOpen* 1: 243-258, 2012.
314. **Vimal D, Khullar M, Gupta S, and Ganguly N.** Intestinal mucins: the binding sites forsalmonella typhimurium. *Mol Cell Biochem* 204: 107-117, 2000.
315. **Viswanathan VK, Mallozzi MJ, and Vedantam G.** *Clostridium difficile* infection: An overview of the disease and its pathogenesis, epidemiology and interventions. *Gut microbes* 1: 234-242, 2010.
316. **Visweswariah SS, Shanthi G, and Balganesh TS.** Interaction of heat-stable enterotoxins with human colonic (T84) cells: modulation of the activation of guanylyl cyclase. *Microb Pathog* 12: 209-218, 1992.
317. **Wagner JA, Cozens AL, Schulman H, Gruenert DC, Stryer L, and Gardner P.** Activation of chloride channels in normal and cystic fibrosis airway epithelial cells by multifunctional calcium/calmodulin-dependent protein kinase. *Nature* 349: 793-796, 1991.
318. **Walker NM, Simpson JE, Yen PF, Gill RK, Rigsby EV, Brazill JM, Dudeja PK, Schweinfest CW, and Clarke LL.** Down-regulated in adenoma Cl/HCO3 exchanger couples with Na/H exchanger 3 for NaCl absorption in murine small intestine. *Gastroenterology* 135: 1645-1653.e1643, 2008.
319. **Wang W, Uzzau S, Goldblum SE, and Fasano A.** Human zonulin, a potential modulator of intestinal tight junctions. *J Cell Sci* 113 Pt 24: 4435-4440, 2000.

320. **Wang Z, Petrovic S, Mann E, and Soleimani M.** Identification of an apical Cl^-/HCO_3^- exchanger in the small intestine. *Am J Physiol Gastrointest Liver Physiol* 282: G573-579, 2002.
321. **Wedenoja S, Hoglund P, and Holmberg C.** Review article: the clinical management of congenital chloride diarrhoea. *Aliment Pharmacol Ther* 31: 477-485, 2010.
322. **Welle T, Hoekstra AT, Daemen I, Berkers CR, and Costa MO.** Metabolic response of porcine colon explants to in vitro infection by *Brachyspira hyodysenteriae*: a leap into disease pathophysiology. *Metabolomics* 13: 83, 2017.
323. **Wilberts BL, Arruda PH, Kinyon JM, Madson DM, Frana TS, and Burrough ER.** Comparison of lesion severity, distribution, and colonic mucin expression in pigs with acute swine dysentery following oral inoculation with "*Brachyspira hampsonii*" or *Brachyspira hyodysenteriae*. *Vet Pathol* 51: 1096-1108, 2014.
324. **Will PC, Lebowitz JL, and Hopfer U.** Induction of amiloride-sensitive sodium transport in the rat colon by mineralocorticoids. *Am J Physiol Renal Physiol* 239: F618-F618, 1980.
325. **Wu Z, Milton D, Nybom P, Sjo A, and Magnusson KE.** *Vibrio cholerae* hemagglutinin/protease (HA/protease) causes morphological changes in cultured epithelial cells and perturbs their paracellular barrier function. *Microb Pathog* 21: 111-123, 1996.
326. **Wu Z, Nybom P, and Magnusson KE.** Distinct effects of *Vibrio cholerae* haemagglutinin/protease on the structure and localization of the tight junction-associated proteins occludin and ZO-1. *Cell Microbiol* 2: 11-17, 2000.
327. **Xiao F, Yu Q, Li J, Johansson ME, Singh AK, Xia W, Riederer B, Engelhardt R, Montrose M, Soleimani M, Tian DA, Xu G, Hansson GC, and Seidler U.** SLC26A3 deficiency is associated with loss of colonic HCO_3^- secretion, absence of a firm mucus layer and barrier impairment in mice. *Acta Physiol (Oxf)* 211: 161-175, 2014.
328. **Yang H, Jiang W, Furth EE, Wen X, Katz JP, Sellon RK, Silberg DG, Antalis TM, Schweinfest CW, and Wu GD.** Intestinal inflammation reduces expression of DRA, a transporter responsible for congenital chloride diarrhea. *Am J Physiol* 275: G1445-1453, 1998.
329. **Yee RB and Buffenmyer CL.** Infection of cultured mouse macrophages with *Shigella flexneri*. *Infect Immun* 1: 459-463, 1970.
330. **Yeruva S, Chodisetti G, Luo M, Chen M, Cinar A, Ludolph L, Lünnemann M, Goldstein J, Singh AK, and Riederer B.** Evidence for a causal link between adaptor protein PDZK1 downregulation and Na^+/H^+ exchanger NHE3 dysfunction in human and murine colitis. *Pflugers Arch* 467: 1795-1807, 2015.
331. **Yu H, Chen K, Sun Y, Carter M, Garey KW, Savidge TC, Devaraj S, Tessier ME, von Rosenvinge EC, Kelly CP, Pasetti MF, and Feng H.** Cytokines are markers of the *Clostridium difficile*-induced inflammatory response and predict disease severity. *Clin Vaccine Immunol* 24, 2017.
332. **Yu K, Lujan R, Marmorstein A, Gabriel S, and Hartzell HC.** Bestrophin-2 mediates bicarbonate transport by goblet cells in mouse colon. *J Clin Invest* 120: 1722-1735, 2010.
333. **Yuan P, Zhang H, Cai C, Zhu S, Zhou Y, Yang X, He R, Li C, Guo S, Li S, Huang T, Perez-Cordon G, Feng H, and Wei W.** Chondroitin sulfate proteoglycan 4 functions as the cellular receptor for *Clostridium difficile* toxin B. *Cell Res* 25: 157-168, 2015.
334. **Yurtsever Z, Sala-Rabanal M, Randolph DT, Scheaffer SM, Roswit WT, Alevy YG, Patel AC, Heier RF, Romero AG, Nichols CG, Holtzman MJ, and Brett TJ.** Self-cleavage of human CLCA1 protein by a novel internal metalloprotease domain controls calcium-activated chloride channel activation. *J Biol Chem* 287: 42138-42149, 2012.
335. **Zachos NC, Tse M, and Donowitz M.** Molecular physiology of intestinal Na^+/H^+ exchange. *Annu Rev Physiol* 67: 411-443, 2005.
336. **Zarepour M, Bhullar K, Montero M, Ma C, Huang T, Velcich A, Xia L, and Vallance BA.** The mucin Muc2 limits pathogen burdens and epithelial barrier dysfunction during *Salmonella enterica* serovar Typhimurium colitis. *Infect Immun* 81: 3672-3683, 2013.

337. **Zeissig S, Bergann T, Fromm A, Bojarski C, Heller F, Guenther U, Zeitz M, Fromm M, and Schulzke JD.** Altered ENaC expression leads to impaired sodium absorption in the noninflamed intestine in Crohn's disease. *Gastroenterology* 134: 1436-1447, 2008.
338. **Zhang S, Santos RL, Tsolis RM, Stender S, Hardt WD, Baumler AJ, and Adams LG.** The *Salmonella enterica* serotype *typhimurium* effector proteins SipA, SopA, SopB, SopD, and SopE2 act in concert to induce diarrhea in calves. *Infect Immun* 70: 3843-3855, 2002.
339. **Zhao H, Wiederkehr MR, Fan L, Collazo RL, Crowder LA, and Moe OW.** Acute inhibition of Na/H exchanger NHE-3 by cAMP. Role of protein kinase a and NHE-3 phosphoserines 552 and 605. *J Biol Chem* 274: 3978-3987, 1999.
340. **Zizak M, Lamprecht G, Steplock D, Tariq N, Shenolikar S, Donowitz M, Yun CH, and Weinman EJ.** cAMP-induced phosphorylation and inhibition of Na^+/H^+ exchanger 3 (NHE3) are dependent on the presence but not the phosphorylation of NHE regulatory factor. *J Biol Chem* 274: 24753-24758, 1999.